IDENTIFICATION AND MECHANISMS OF ALLELOCHEMICALS REGULATING ROOT-KNOT NEMATODE PARASITISM

KIHIKA RUTH MUTHONI (M.Sc.)
I84/39349/2017

A THESIS SUBMITTED IN FULFILLMENT OF THE REQUIREMENTS FOR THE AWARD OF THE DEGREE OF DOCTOR OF PHILOSOPHY IN CHEMISTRY IN THE SCHOOL OF PURE AND APPLIED SCIENCES OF KENYATTA UNIVERSITY

OCTOBER 2023

DECLARATION

I hereby declare that this is my original work and has not been presented for degree or other awards in any other university.

Signature..... **Date** 25.10.2023

Ruth Muthoni Kihika
Department of Chemistry,
Kenyatta University

SUPERVISORS

We confirm that the work reported in this thesis was carried out by the candidate under our supervision.

Signature..... **Date** 25/10/23

Dr. Margaret M. Ng'ang'a
Department of Chemistry
Kenyatta University

Signature..... **Date**.....25/10/2023.....

Dr. David P. Tchouassi
Behavioral and Chemical Ecology Unit,
International Centre of Insect Physiology and Ecology

Signature..... **Date** 25th Oct 2023

Prof. Baldwyn Torto
Behavioral and Chemical Ecology Unit,
International Centre of Insect Physiology and Ecology

DEDICATION

It is with deep gratitude that I dedicate this thesis to my husband Joseph and our sons, Ryan and William for their great support that has been my greatest inspiration throughout my pursuit for this degree. I dedicate also to my sister, Emma and my father, Kenneth Kihika for their encouragement.

ACKNOWLEDGEMENTS

First, I thank the Almighty God for the wisdom, strength, good health and grace to reach this level in my academic journey. I am grateful to my supervisors; Dr. Margaret Ng'ang'a of Kenyatta University, Prof. Baldwyn Torto and Dr. David P. Tchouassi of the International Centre of Insect Physiology and Ecology (*icipe*) for their mentorship, guidance, support and this great opportunity for my career development. I sincerely thank Dr. John J. Beck of the United States Department of Agriculture/Agriculture Research Service – Centre for Medical, Agricultural and Veterinary Entomology for his immense contribution and valuable advice during my research.

I gratefully acknowledge the financial support for this research by the following organizations and agencies: German Academic Exchange Service (DAAD) (Grant number 91672644, through a PhD scholarship tenable through the African Regional Postgraduate Program in Insect Science (ARPPIS)-In-Region programme Scholarship at *icipe*); United States Department of Agriculture, Agricultural Research Service, Agreement No. 58-6615-3-011F; Norwegian Agency for Development Cooperation, the Section for research, innovation, and higher education grant number RAF-3058 KEN-18/0005 (CAP-Africa). I thank the L'Oreal-UNESCO for Women in Science for the grant of the sub-Saharan Africa Young Talents award and the Mawazo Institute for the Mawazo Learning Exchange fellowship.

My gratitude also goes to Dr. Robert Skilton, the former head of Capacity Building and Institutional Development Program at *icipe*, Ms. Vivian Otieno (Capacity Building Officer), Ms. Esther Ndung'u (Capacity Building Assistant) and Ms. Margaret Ochanda (Office Assistant) for their support in trainings and administrative matters. I thank Ms. Charity Mwangi, the

Administrative Assistant at the Behavioral and Chemical Ecology unit (BCEU), for the invaluable administrative and moral support she has accorded me during my studies.

I am grateful to my fellow colleagues at the Behavioral and Chemical Ecology Unit, *icipe*; Hillary Kirwa, Onesmus Wanyama, and Paul Odondi for various technical support throughout this study. I also thank Kenyatta University for granting me an opportunity to pursue the PhD program and the entire staff at the Chemistry Department for their support during my research. My utmost gratitude to my family for every support as I pursue my educational goals. I particularly thank my husband Joseph and sons, Ryan and William for their endurance and understanding in supporting me to complete this work.

TABLE OF CONTENTS

LIST OF TABLES

LIST OF FIGURES

LIST OF PLATES

ABBREVIATIONS AND ACRONYMS

ANOSIM	Analysis of similarities
ANOVA	Analysis of Variance
CABI	Centre for Agriculture and Bioscience International
DAMPs	Damage Associated Molecular Patterns
DPI	Day Post Infection
EPNs	Entomopathogenic nematodes
ET	Ethylene
ESI	Electrospray Ionization
ETI	Effector Triggered Immunity
GC/MS	Gas Chromatography coupled to Mass Spectrometry
GLM	Generalized Linear Model
icipe	International Centre of Insect Physiology and Ecology
JA	Jasmonic Acid
J1	First stage juvenile
J2	Second stage juvenile
J3	Third stage juvenile
J4	Fourth stage juvenile
LC	Lethal Concentration
LC-QQQ-MS	Liquid Chromatography coupled to triple quadrupole tandem mass spectrometry
MeDiJA	Methyl dihydrojasmonate
MeSA	Methyl salicylate
NAMPs	Nematode Associated Molecular Patterns
NMDS	Non-metric multidimensional scaling
PCoA	Principal co-ordinate analysis
PDMS/DVB	Polydimethylsiloxane/Divinylbenzene
PPNs	Plant Parasitic Nematodes
PTI	Pathogen Associated Molecular Pattern Triggered Immunity
RI	Retention Indices
RKNs	Root- Knot Nematodes
SA	Salicylic Acid
SIMPER	Similarity Percentages
SNK	Student-Neuman-Kuels
SPME	Solid Phase Microextraction
VOCs	Volatile Organic Compounds
UPLC	Ultra-Performance Liquid Chromatography
USD	United States Dollars

ABSTRACT

Global crop production is hampered by numerous pests and parasites including plant parasitic nematodes (PPNs). Root-knot nematodes (RKNs; *Meloidogyne spp.)* are among the most pervasive economically important PPNs accounting for crop losses of over USD 100 billion globally, thus posing a severe risk to food security. Despite the current measures deployed in the management of RKNs, their damage still persists, necessitating more effective approaches. Recent studies identified constitutive plant compounds that influence the host seeking behavior of RKNs. The current study sought to elucidate the chemical dialogue between host plants and RKNs during parasitism and investigate the chemical mechanisms of non-host plants in reducing nematode infestation. The influence of the infective stage juveniles (J2) of RKNs in inducing tomato (*Solanum lycopersicum*) root and leaf volatiles, and chemotactic effects on conspecifics was investigated. The hypothesis that the non-host Asteraceae plant vegetable black-jack (*Bidens pilosa*) suppresses infection of the PPN *Meloidogyne incognita,* in two susceptible Solanaceae host plants; tomato (*Solanum lycopersicum*) and black nightshade (*S. nigrum*) was also tested. In behavioral olfactometer assays, J2 avoided roots of 2-day infected plants but preferred 7-day infected tomato compared to healthy plants. Coupled gas chromatography-mass spectrometry (GC/MS) was used to identify root and leaf volatiles from healthy and RKN-infected tomato at two and seven-days post infection. Chemical analysis showed a two- to seven-fold increase in the amounts of monoterpenes emitted from tomato roots infected with *M. javanica* relative to healthy roots. Additionally, infected plants released ~4 to 225-fold quantitatively more leaf volatiles, and were compositionally richer than the healthy plants. Analysis of similarities (ANOSIM) and non-metric multidimensional scaling (NMDS) of the leaf volatile organic compounds (VOCs) showed that five terpenes, 2-δ-carene (**25**), β-phellandrene (**29**), δ-caryophyllene (**13**), elemene (**58**), and α- humulene (**66**) contributed to the dissimilarity trends between healthy and infected tomato irrespective of the nematode species. In further bioassays, the monoterpenes β-pinene (**24**), 2-δ-carene (**25**), α-phellandrene (**26**), and β-phellandrene (**29**) differentially attracted (51-87%) J2 relative to control. Concurrent reduction and increase in the levels of methyl salicylate (**3**) and (*Z*)-methyl dihydrojasmonate (**45**), respectively, in the root volatiles reduced J2 responses. Screenhouse pot experiments combined with laboratory *in vitro* hatching and mortality assays and chemical analysis to test the effect of non-host plant in growth and development of RKNs in susceptible host plants were used. In intercrop and drip pot experiments, blackjack significantly reduced the number of galls and egg masses in RKN-susceptible host plants by 3-9-fold compared to controls (susceptible plants). LC-QQQ-MS analysis of the most bioactive fraction from the root exudates of blackjack identified several classes of compounds, including aromatic acids, a dicarboxylic acid, vitamins, amino acids, and a flavonoid. In *in vitro* assays, the vitamins, ascorbic acid (**86**) and nicotinic acid (**88**) and the aromatic acids, *p*-coumaric acid (**92**) and 2-hydroxybenzoic acid (**13**) caused the highest inhibition in egg hatching, whereas ascorbic acid (**86**) (vitamin) and 2-hydroxybenzoic acid (**13**) (aromatic acid) elicited strong nematicidal activity against *M. incognita*, with $LC_{50/48\ h}$ values of 12 and 300 ng μl^{-1}, respectively. These results demonstrate that RKN infection induces chemical changes both locally and systemically in the host plant. Additionally, the host plant can alter its root volatile composition to inhibit PPN attack. The observed plant-produced inhibition of J2 warrants further investigation as a potential management tool for growers. The findings also provide insights into how certain non-host plants can be used as companion crops to disrupt PPN infestation.

CHAPTER ONE

INTRODUCTION

1.1 Background

Root-knot nematodes (RKNs) of the genus *Meloidogyne* are globally distributed plant worms that are sedentary and endoparasitic. They are highly polyphagous, as they parasitize numerous crop species for the nematodes growth and reproduction (Luc *et al.*, 2005). The root structure is changed when the nematodes invade the roots and migrate to the feeding sites (Figure 1.1) and this affects the uptake of nutrients and water, eventually diminishing the crop yields (Curtis, 2007).

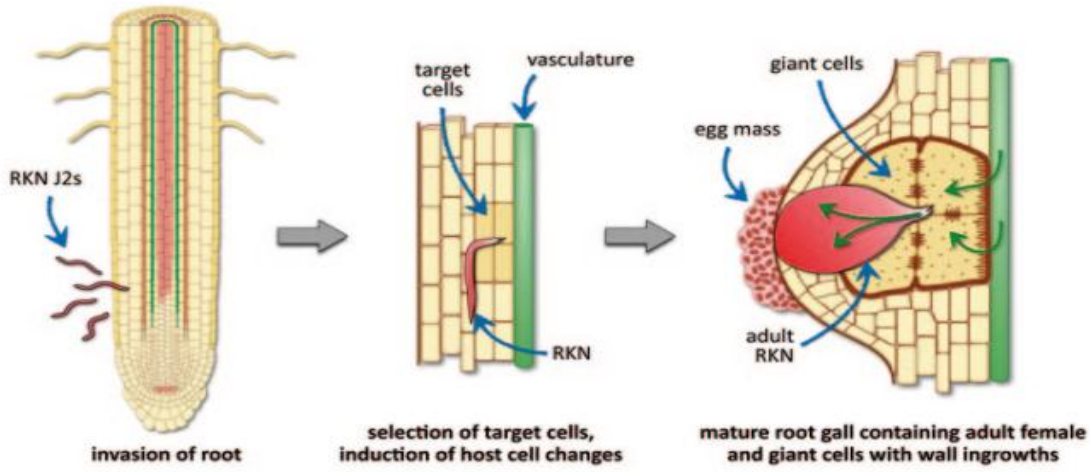

Figure 1.1: Schematic representation of the root knot nematode life cycle (Jones *et al.*, 2011).

The early pointer of RKN infection in farmers' fields are patches of unevenly growing crops in an otherwise healthy crop. Their infestation on plants may not be obvious because the symptoms observed on plant shoots resemble those of a plant lacking nutrients or a damaged root system. These comprise of foliage discoloration, wilting, stunting, and distorted shoots (Khan, 1993; Nicol *et al.*, 2011). When the environmental conditions are favorable, there is fast growth rate

and reproduction leading to several generations in one cropping period which increases the severity of crop damage (Perry *et al.*, 2009).

Geographically, the distribution of the diverse RKN species depends on temperature, cropping history, and soil type (Khan, 1993; Karssen and Moens, 2006). Some are classified as major species based on their global dispersal and wide host range, and these include *M. incognita*, *M. arenaria M. javanica*, largely reported in the tropics and are responsible for substantial economic losses (Taylor and Sasser, 1978; Jones *et al.* 2011). *Meloidogyne halpa*, also known as the northern RKN, is a key temperate species (Luc *et al.*, 2005). On the other hand, RKNs that have a restricted host range and distribution are referred to as minor pest species. These include *M. minor* found in golf courses and sports fields (Wesemael *et al.*, 2014), *M. graminicola*, the rice RKN (Karssen and Moens, 2006) and *M. chitiwoodi* (Luc *et al.*, 2005; Nicol *et al.*, 2011). Importantly, a highly virulent species known as *M. enterolobii* can parasitize and reproduce on cultivars that are resistant to other RKN species (Fargette, 1987; Fargette *et al.*, 1994). Figure 1.2 shows the global distribution of *M. incognita*, a major RKN species globally.

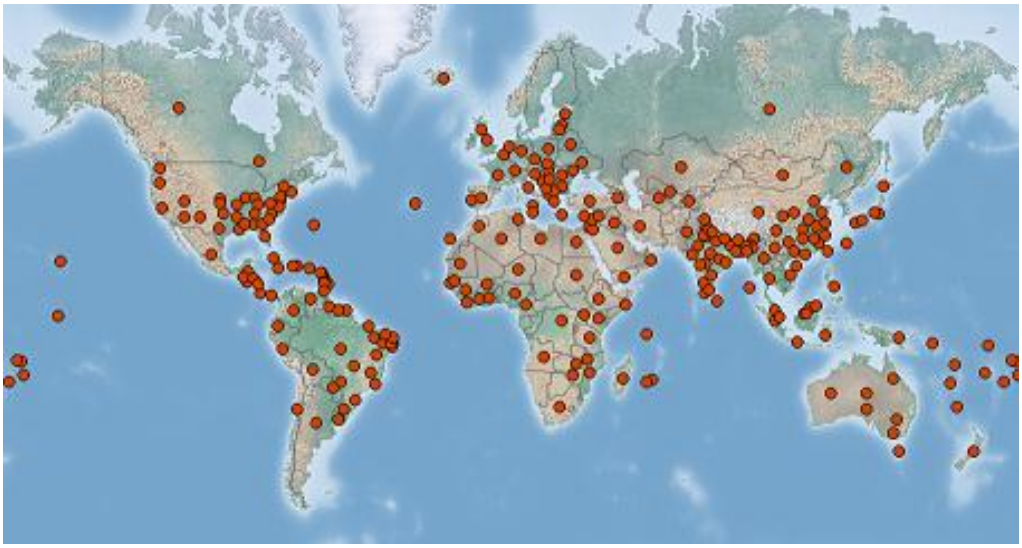

Figure 1.2: Global distribution of *Meloidogyne incognita* (represented by the red dots in countries where it has been reported) (***https://www.cabi.org/isc/datasheet/33245***)

In Africa, *M. javanica, M. incognita,* and *M. arenaria* are the most predominant species and have previously been reported in 26, 37, and 26 countries, respectively (IITA, 1981; De Waele and Elsen, 2007). Jointly, the three key species are known to infect important food crops in all agroecological zones. Additionally, *M. enterolobii* was identified in root tubers such as potatoes in Southern Africa (Onkendi and Moleleki, 2013) and vegetables such as African nightshades in Kenya (Chitambo *et al*, 2016).

Economically, RKNs are projected to cause yearly losses of over USD 100 billion (Abad *et al*, 2008) and in Kenya, over 80% of production losses are encountered in tomatoes (Birithia *et al.*, 2012). The impact of *Meloidogyne* spp. is largely underestimated especially in Africa, due to insufficient data on their effect on food production (Coyne *et al*., 2018) even though losses can range between 40-100%. However, there is an increasing awareness of the devastating effects of these parasitic nematodes in crop production among smallholder farmers in developing countries. The existing strategies used in the control and management of these polyphagous plant parasitic nematodes (PPNs) have proven inadequate demanding supplementary approaches such as the use of semiochemicals.

Previous studies that investigated various host plants of RKNs identified root compounds that influence the response of RKN infective stage (J2s) (Kihika *et al*., 2017; Murungi *et al.*, 2018; Kirwa *et al*., 2018). These include the volatiles, α-pinene (**1**), limonene (**2**), methyl salicylate (**3**), 2-isopropyl-3-methoxypyrazine (**4**), tridecane (**5**), and thymol (**6**) from tomato (*Solanum lycopersicum L.*) and pepper (*Capsicum annum*) (Kihika *et al*., 2017; Murungi *et al.*, 2018). Additionally, the non-volatiles, zeatin (**7**) and quercetin (**8**) were identified in tomato roots as important kairomonal signals of the J2 (Kirwa *et al*., 2018).

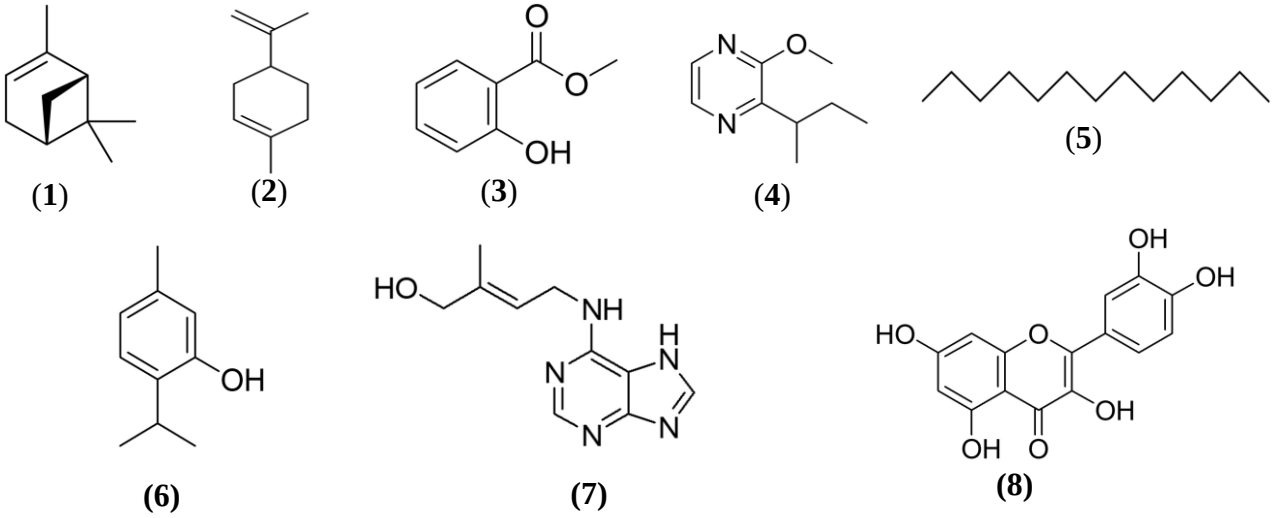

(**1**) (**2**) (**3**) (**4**) (**5**)

(**6**) (**7**) (**8**)

In another study, non-host plants of the Asteraceae family produced root volatiles such as camphor (**9**), I,8-cineole (**10**), and (*E*)-β-farnesene (**11**) that modulate the host seeking behavior of the J2 (Mwamba *et al.*, 2021). However, efforts to elucidate the chemical mechanisms of RKNs parasitism remains poorly studied yet this would provide an avenue for the development of alternative control strategies.

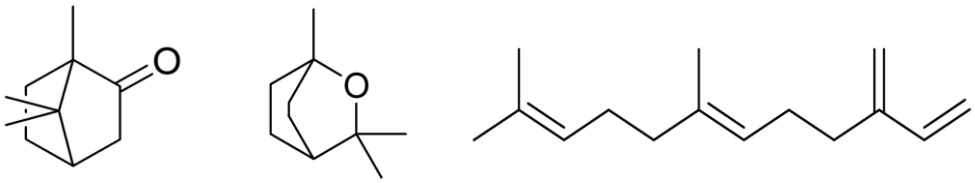

(**9**) (**10**) (**11**)

Nematodes are known to secrete effector proteins that are thought to be influential in manipulating the development and defense signaling pathways of host cells (Perry *et al.*, 2009). Currently, knowledge of the chemical dialogue between RKNs and plants during parasitism has largely been understudied. Additionally, the mechanisms of non-host plants in reducing the nematode population are not fully investigated.

1.2 Statement of the problem

RKNs are polyphagous phytoparasitic nematodes that pose an increasing threat to agricultural crop production (Abad *et al.*, 2008). Damages caused by RKN are rarely visible but lead to diminished yields and quality of crops with significant economic losses (Coyne *et al*., 2018). Their infection suppresses host plant defenses leading to increased vulnerability of the plant to opportunistic pathogens that further reduce yield and increase losses (Haegeman *et al.*, 2012; Leelarasamee *et al*., 2018). Additionally, the high cost of control and management impacts negatively on farmers' income (Coyne *et al*., 2018). The conventional chemical, biological and cultural control approaches are insufficient to curb these PPNs in addition to being labor intensive or expensive. Further, the use of nematicides, which are the most effective, have detrimental environmental consequences and can be toxic to humans and beneficial microbes (Sikora *et al.*, 2018). The underscored challenges necessitate the investigation of alternative eco-friendly methods that can be integrated into the management of RKNs. Semiochemicals that mediate plant-RKN interactions could offer complimentary strategies for enhanced integrated management strategies.

1.3 Justification

RKNs have developed sophisticated strategies for exploiting host plants, their developmental process, and defense mechanisms. They either suppress host defense mechanisms during infestation or can avoid detection altogether, which accounts for their success as parasites (Haegeman *et al.*, 2012). The development of sustainable, ecologically responsive, and effective strategies to control RKNs can be achieved by understanding the semiochemical basis of this unique parasitic behavior. Semiochemicals can complement and be part of an improved IPM package. Previously, using *Capsicum annum* cultivars, tomato, and spinach, host plant chemical

signals were reported to influence J2 host selection and discrimination (Kihika *et al.*, 2017; Murungi *et al.*, 2018). The root volatiles of susceptible host plants attract the infective juveniles while resistant plants produce compounds that disrupt the chemotactic host-finding signals (Čepulytė et al., 2018; Murungi *et al.*, 2018; Mwamba *et al.*, 2021). Whereas numerous studies have elucidated the molecular basis of RKN parasitism (Ali *et al.*, 2017; Shukla *et al.*, 2018), the chemical dialogue in plant-RKN interactions during parasitism has not been well studied. This study, therefore, sought to investigate the local and systemic responses of plants to nematode attack and determine how the compounds associated with RKN infection influence J2 behavior. Further, we evaluated the chemical mechanisms of non-host plants in reducing RKN infection.

1.4 Hypotheses

i. RKN infection induces changes in the tomato (*Solanum lycopersicum L.*) root volatile chemistry and influences J2 host location.
ii. Root infection by RKN modifies the plant shoot chemistry of tomato plants.
iii. The root exudates of the Asteraceae plant, blackjack (*Bidens pilosa*), suppress the growth and development of RKN in susceptible crops, tomato and black nightshade (*Solanum nigrum Linn*).
iv. The bioactive fraction of blackjack root exudates contains compounds that influence the hatching and mortality of J2.

1.5 Objectives

1.5.1 General Objective

To investigate plant allelochemical responses to root-knot nematode parasitism associated with penetration of host plants

1.5.2 Specific Objectives

i. To determine the influence of RKN infection on the J2 host-seeking behavior of tomato.

ii. To identify the changes in tomato shoot chemistry following root infection by RKN.

iii. To evaluate the effect of blackjack root exudates on the development of RKN in susceptible crops.

iv. To identify compounds in the bioactive fractions of blackjack root exudates and determine their effects on nematode behavior.

1.6 Significance of the study

The study sought to determine the underlying chemical mechanisms that mediate the parasitism of RKN in susceptible host plants and identify specific compounds in the root exudates of a non-host plant that contribute to suppressed growth and reproduction of RKN. This will offer semiochemical-based alternatives that can be developed for the management of RKNs.

1.7 Scope and limitations of the study

The study evaluated the chemical interactions between one susceptible tomato cultivar, namely 'Cal J', and two RKN species, *Meloidogyne incognita* and *M. javanica* which are among the most prevalent in Kenya and Africa (Coyne *et al*., 2018). Additionally, only one non-host Asteraceae plant, blackjack, was used to investigate the RKN suppression effects of their root exudates in susceptible tomato and black nightshade in laboratory and semi-field experiments.

CHAPTER TWO

LITERATURE REVIEW

2.1 The biology of root knot nematodes

Morphologically, the body wall of RKN is made of the three major layers which are the cuticle, the hypodermis and the somatic muscles (Figure. 2.1). In the J2 and males, the body wall allows them to move through the soil and in the plant tissue while the females are protected from the external environment (Perry *et al.,* 2009). The cuticle is secreted by the hypodermis that covers the entire body including all the openings (Perry *et al.,* 2009) and it acts as the boundary between the organism and the harsh soil environment protecting the J2 and males from chemical, biological, and physical hazards. Its structure controls the diffusion of liquids through the body wall (Luc *et al.,* 2005).

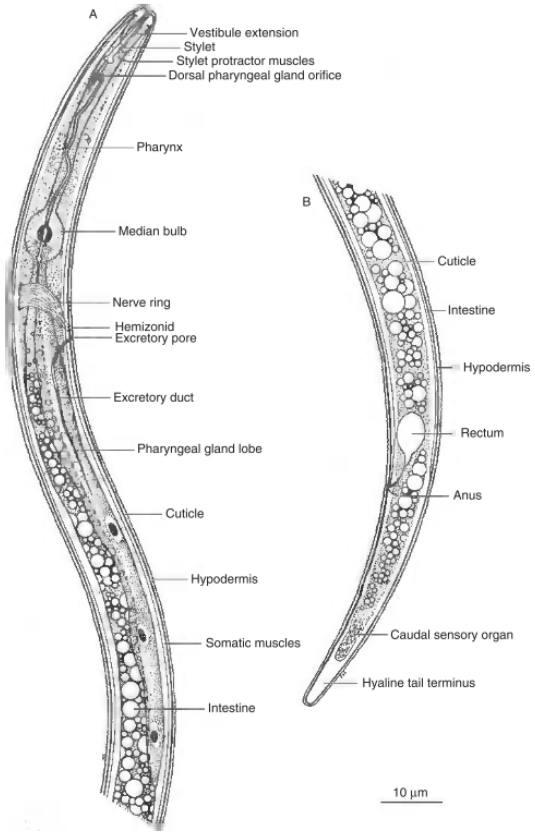

Figure 2.1: Drawings of a second-stage juvenile root knot nematode. A: anterior region and B: posterior region (Eisenback, 1985; Perry *et al*., 2009).

The digestive, reproductive, and excretory systems are suspended within the central cavity, pseudocoelom. (Karssen and Moens, 2006). The J2 have a delicate stylet (9 – 16 µm long), are vermiform, annulated, and 250 to 650 µm long. The J3 and J4 do not have a stylet and mature while inside the J2 cuticle; they are normally swollen and sedentary inside the root (Karssen and Moens, 2006). The females have a protruding neck, are white in color, pear-shaped and sedentary (Perry and Moens, 2006). Males are 600 to 2500 µm long, migratory, worm-like and annulated (Figure 2.2).

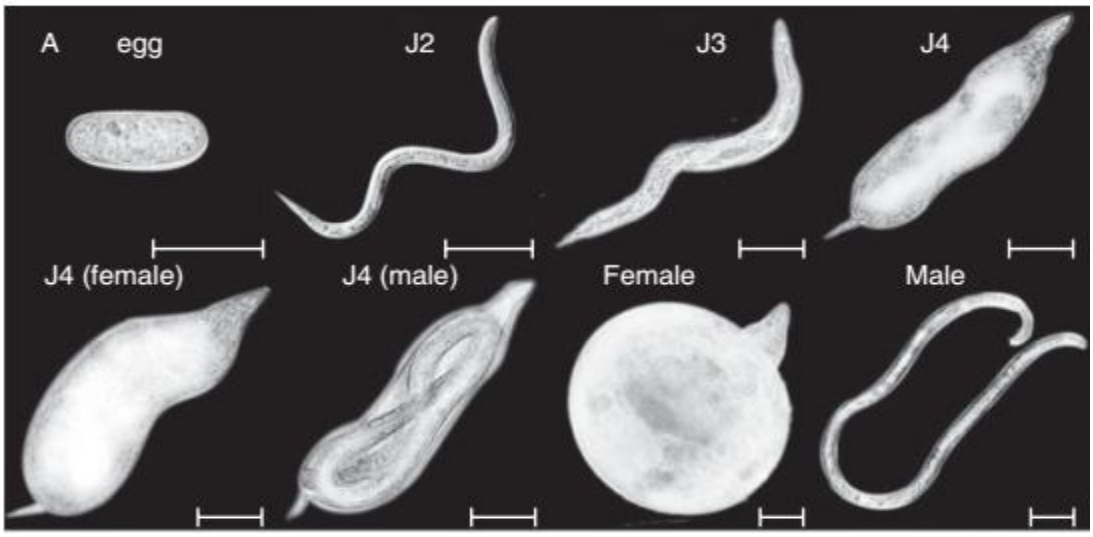

Figure 2.2: Developmental stages of root knot nematodes from egg to adult nematodes (Perry *et al.*, 2009). Scale bars, 40 µm

The RKNs feed and reproduce on altered cells within plant roots, forming galls of different sizes (Karssen and Moens, 2006). The second-stage infective juvenile (J2) locates the zone of elongation and enters a root then migrates between the cortical cells causing negligible damage. The J2s become sedentary and begin forming nutrient sinks in the pericycle and vascular tissue where they induce karyokinesis without cytokinesis (Perry *et al.*, 2009; Jones *et al.*, 2011). A gall is formed by redifferentiation of some root cells due to hypertrophy and hyperplasia (Karssen and Moens, 2006; Coyne *et al.*, 2007).

2.2 The life cycle of root knot nematodes

The life cycle of RKNs consists of an egg, a distinctive free-living pre-parasitic stage in the soil, and parasitic stages inside the root tissue. The females lay the eggs in a gelatinous sac and they are deposited inside the galled root tissue or on the surface of the root. Embryonic development results in the J1 which molts into the J2 that emerges from the egg. The emergence of J2 is highly dependent on temperature and soil moisture, but the root diffusates and generation can modify the hatching response so that it happens when conditions are suitable for motility and host location (Perry and Moens, 2006; Perry *et al.*, 2009). When the pre-parasitic J2 establish their feeding sites, the parasitic phase of the J2 molts two times into J3 and J4 and finally becomes an adult (Figure 2.3).

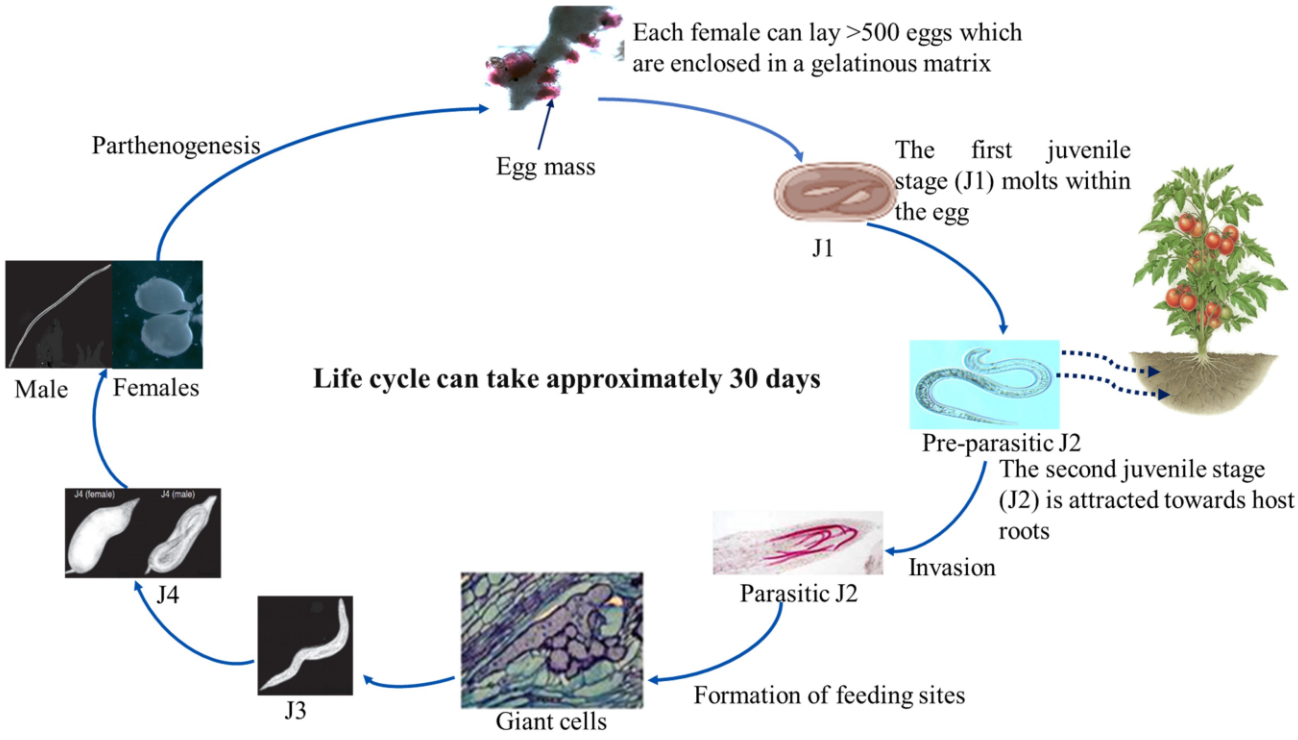

Figure 2.3: The life cycle of root knot nematodes. Modified from (Abad *et al.*, 2009)

2.3 Root knot nematode management strategies

Root-knot nematodes are controlled using various methods that include cultural, biological, chemical, and the use of resistant varieties. These are aimed at reducing pest population in the soil, reducing disease incidence in plants, protecting the plant from nematode invasion, or where the plant defense system prevents the development of nematode when parasitic J2 locates a feeding site.

Cultural control employs measures such as crop rotation where non-hosts or nematode antagonistic plants are alternated with susceptible hosts (Chen *et al.*, 2004). Cover crops such as marigold have been found to produce chemicals that are toxic to nematodes (Krueger *et al.*, 2007; Hooks *et al.*, 2010; Faizi *et al*., 2011; Kalaiselvam and Devaraj, 2011). However, these compounds had limited nematicidal activity when applied in soil and only the intact plant growing for about 3-4 months was effective (Hooks *et al.*, 2007). For instance, α-terthienyl (**12**) identified in marigold failed to reduce nematode population when incorporated in soil (Hooks *et al.*, 2007).

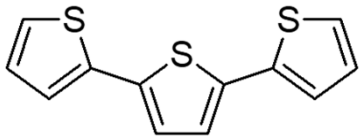

(**12**)

Cover crops have an added benefit of stabilizing topsoil and improving soil quality. Flooding and solarization have also been used to suppress nematode populations before planting season, but this method is not very practical in smallholder farming systems. Additionally, organic soil amendment is practiced where poultry or livestock manure as well as plant-based products with nematicidal activity are mixed with soil before planting. This has the advantage of improving

soil fertility even though large quantities are required to work effectively (Riegel and Noe 2000; Tsay *et al.*, 2004; Mateille *et al.*, 2007; Perry *et al.*, 2009).

Biological agents such as fungi and bacteria are used for controlling nematodes. Some fungi infect the nematodes by sticking their spores to their cuticle, germinating and forming tubes that penetrate the body (Webster, 1972; Lamovseki *et al.,* 2013) while others are parasitic to the eggs and the RKN females such as *Pochonia chlamydosporia and Paecilomyces lilacinus* (Collange *et al.*, 2011; Qureshi *et al.*, 2012). In a previous study, the application of *Trichoderma sp*. MK4, *T. asperellum* M2RT4, and *P. lilacinum* led to endophytic colonization of pineapple root causing a substantial reduction in root-knot disease incidence and an increase in plant root mass (Kiriga *et al.*, 2018). The inability to economically produce massive amounts of biological material to be utilized over large areas is a significant drawback to the effective use of biological control.

Conventional nematicides are normally applied before planting to diminish the nematode population, however, they must penetrate large soil volumes to be effective (Mitkowski and Abawi, 2003). A very active pre-plant treatment, methyl bromide, was phased out following environmental concerns of ozone depletion (Schneider *et al*., 2003; Schneider *et al.,* 2006; Schneider and Hanson, 2009). Additionally, other nematicides had toxic effects, poor target specificity, and were harmful to human or environmental safety, such as groundwater contamination (Taylor and Sasser, 1978; Chitwood, 2002). Organophosphates and carbamates are the current viable methods for controlling RKNs because they are not toxic to plants. However, they are acutely neurotoxic to humans (Perry *et al.*, 2009; Jones *et al.*, 2011).

Resistant cultivars are effective in controlling nematodes using resistant genes and they have actual economic benefits (Lilley *et al.,* 2011). In tomatoes, resistance is conferred by the Mi-1.2 gene which was successfully obtained from a wild cultivar, *Lycopersicon peruvianum* (Starr *et al*., 2002) but the resistant gene is unstable at high temperatures posing a major problem in plant breeding (Luc *et al.,* 2005). The resistant genes Me1 and Me3 (Djian-Caporalino *et al.,* 2007) confer resistance to the pepper cultivars, Charlestone belle and Carolina wonder, respectively (Thies *et al*., 2008). The association of some undesirable characteristics with resistant traits has limited their applicability (Jones *et al.,* 2011).

2.4 Chemical communication in plant-nematode interactions

The soil contains a composite mixture of air, water and numerous living organisms that influence various interactions in the subterranean environment. Complex biological and ecological processes occur in the rhizosphere where plant roots exude a range of compounds that mediate below ground interactions with both beneficial and pathogenic organisms (Curtis, 2008). Carbon dioxide (CO_2) is the simplest and most ubiquitous signal produced by respiring roots and other biotic sources. More than 20 studies were listed by Johnson & Gregory (2006) showing that CO_2 was a major attractant for root feeding arthropods. However, since it's such a general signal, Turlings *et al.*, (2012) suggested that it is more likely to be a response enhancer that leads the organisms towards the general root area and other more specific cues are required for host location.

For beneficial nematodes, also known as entomopathogenic nematodes (EPNs), root-produced volatiles act as foraging cues where the infective third larval instar has to seek a host in the physically and chemically complex soil matrix (Turlings *et al.,* 2012). EPNs will display cruising

(moving actively in search of a host) or ambushing (waiting at one place for an arthropod pest to pass by) foraging behavior (Wilson *et al.*, 2012), but more significantly, chemical signals are important host detection cues (van Tol *et al.*, 2001). Numerous studies have demonstrated that EPNs rely on herbivore induced plant volatiles (Rasmann *et al*., 2005; Ali *et al.*, 2010; Ali *et al.*, 2011; Turlings et al., 2012; Laznik & Trdan, 2013) to locate a host. For example, the terpenoid (*E*)-β-caryophyllene (**13**) released by maize (*Zea* mays) roots damaged by the Western corn rootworms (*Diabrotica virgifera virgifera*), is a specific recruitment signal for the EPN *Heterorhabditis megidis* (Rasmann *et al*., 2005). Equally, root stocks of citrus (*Citrus paradisi* Macf. × *Poncirus trifoliata* L. Raf.) infested with the weevil *Diaprepes abbreviates* larvae release giejerenes, which are C_{12} terpenes that attract the EPN, *Steinernema diaprepesi* (Ali *et al.*, 2010).

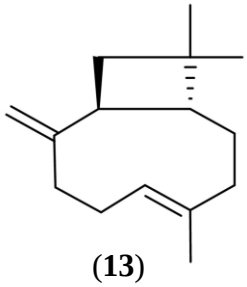

(**13**)

The plant produced volatiles also modulate EPNs inter-specific social behavioral plasticity, learning, and memory (Willet *et al.*, 2015). In addition, root cap exudates of different green pea varieties induced reversible quiescence in various EPN species and lower concentrations increased their activity and infectiousness compared to higher concentrations (Hiltpold *et al.*, 2015).

In plant parasitic nematodes (PPNs), chemical signals are crucial at various phases in the life cycle, for instance, in one study, weevil infested citrus roots was shown to attract the citrus

sedentary root nematode, *Tylenchulus semipenetrans* Cobb, when compared to non-infested plants suggesting that the PPNs can take advantage of plant's weakened defense (Ali *et al.*, 2011). Also, host exudates are hatching factors for the cyst nematodes, *Globodera rostochiensis* and *G. pallida* which have a narrow host range (Perry *et al.*, 2009). Specific triterpene compounds, glycinoeclepins and solanoeclepin A (**14**) isolated from roots of kidney bean and potato stimulate hatching of the soy cyst nematode and potato cyst nematode respectively (Masamune *et al.*, 1982; Schenk *et al.*, 1999). In dose dependent assays, lower concentrations of the potato glykoalkaloids, α-solanine (**15**) and α-chaconine (**16**), significantly stimulated hatching than higher concentrations (Devine *et al.*, 1996; Ochola, 2021).

Since the cyst nematodes are more specific plant parasites, they have evolved to detect the most suitable environment that will ensure their survival such that concentrations are also very critical for their hatching.

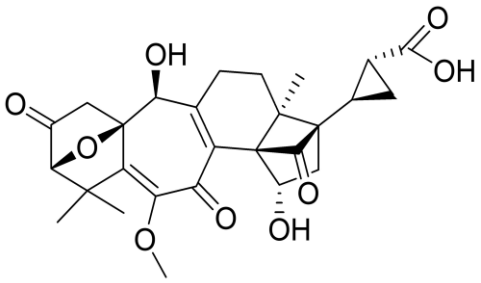

(**14**)

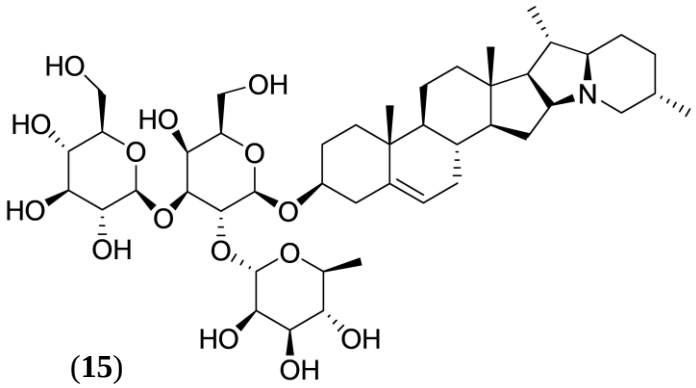

(**15**)

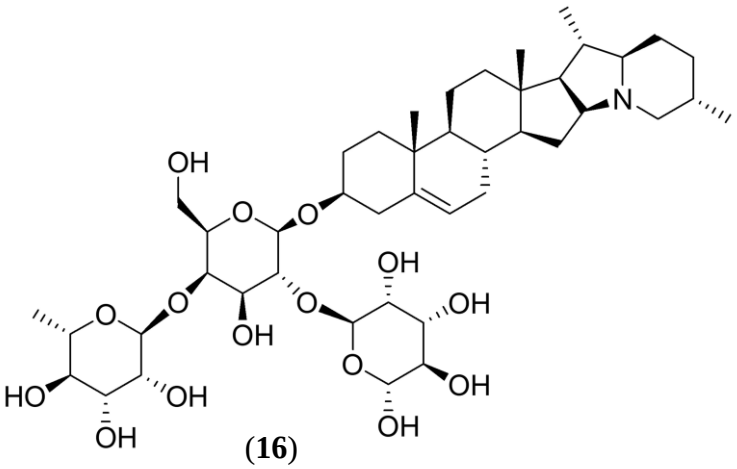

(**16**)

In RKNs however, the influence of host diffusates are not apparent for hatching since they have a broad host range, but plant chemical cues chemo-orient the infective juveniles during host seeking (Ali *et al.*, 2011; Kihika *et al.*, 2017). Nematodes utilize this distinctive character, concentration or combination of stimulus in soil environment to find roots for them to feed and complete their life cycle (Perry *et al.*, 2009).

Secretions from the nematodes are the principal signaling molecules in the interface of plant-nematode interactions and can be considered as the most highly evolved adaptations facilitating plant parasitism (Perry *et al.*, 2009; Haegeman *et al.* 2012). These secretions contain enzymes that degrade the cell wall and are also major effectors of RKN parasitism. They can be released in response to root exudates before nematodes reach the invasion site to influence responsiveness of host roots to the infective juveniles (Perry *et al.*, 2009; Jones *et al.*, 2011). The plant cell wall is the initial barrier, and is primarily made up of carbohydrate polymers, such as cellulose, hemicellulose and pectin, wall proteins and possibly phenolic compounds. These PPNs, like bacteria and fungi, have developed enzyme systems for degradation of plant cell walls (Jones *et al.*, 2011).

2.5 Plant response to root knot nematodes

The RKNs go through three molting phases during parasitism and this poses a different challenge for the host plant because the cuticle changes its composition after each molt (Holbein *et al.*, 2016). This leads to the induction of PTI and ETI which activate the salicylic acid (SA (**17**)), jasmonic acid (JA (**18**)), and ethylene (ET (**19**)) signaling pathways. Previously, it was suggested that biotrophic pathogens activate the SA pathway while wounding or necrotrophic pathogens trigger the JA and ET pathways (Wondafrash *et al.*, 2013). However, some molecular studies

reported that the biotrophic RKNs induce the three signaling pathways differentially in the different stages of parasitism (Kumari *et al*., 2016; Ling *et al.*, 2017).

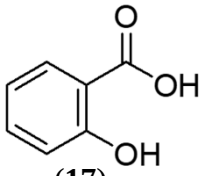

(**17**)

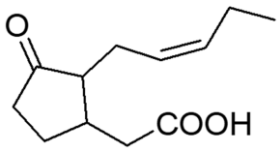

(**18**)

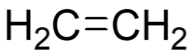

(**19**)

Molecular studies have shown remarkable transcriptomic differences (Kumari *et al*., 2016; Ling *et al.*, 2017) as well as proteomic differences (Ha *et al.*, 2017) between resistant and susceptible crops after RKN infection. Another study showed that systemic defense signaling after rice infection with *M. graminicola* and a migratory endoparasitic nematode, *Hirschmanniella oryzae* differentially activates and suppresses the three hormonal defense pathways at different time points of infection (Nahar *et al.*, 2011; Kyndt *et al.*, 2012). Additionally, transcriptomic analysis of host tissues during the early stages of nematode invasion have shown that up-regulation or down-regulation of defense-related genes may vary depending on whether the nematodes are still in the migratory phase or have begun forming feeding sites (Bhattarai *et al.*, 2008; Portillo *et al.*, 2013; Kammerhofer *et al.*, 2015). In contrast, gene expression studies in later stages of PPN infection show that the host defense responses are greatly suppressed (Jammes *et al.*, 2005; Szakasits *et al.*, 2009; Barcala *et al.*, 2010; Ji *et al.*, 2013). However, it's important to determine whether the early defense activation is based on the recognition of nematodes by the host (NAMPs) or it's a general response to tissue damage (DAMPs).

In studies examining plant-mediated interactions between root-feeding nematodes and aboveground herbivorous insects, there were varying effects of nematode infection to leaf feeding insects, where in some cases, nematode parasitism favored the pest (Alston *et al.*, 1991;

Kaplan *et al.*, 2008), while in others, there was a negative effect of reduced performance or lower population when compared to non-infected controls (Hol *et al.*, 2010; Kaplan *et al.*, 2011). In other interactions, leaf-feeding insects impact the PPN population positively or negatively (Russin *et al.*, 1989; Alston *et al.*, 1993; Russin *et al.*, 1993; Kaplan *et al.*, 2009; Tiwari *et al.*, 2009). In *M. incognita*-infested *Nicotiana,* the amount of nicotine (**20**), an alkaloid used in defense, was two-fold lower compared to non-infected controls (Kaplan *et al.*, 2008). On the contrary, gossypol (**21**) and gossypol-like compounds produced by cotton, *Gossypium hirsutum*, were not affected by the root herbivory of *M. incognita* (Olson *et al.*, 2008). Beyond these studies, no investigations have been done on the root system chemical signals when RKNs invade and parasitize the plant or even compare local and systemic chemical responses.

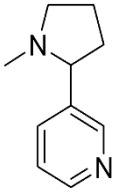

(**20**)

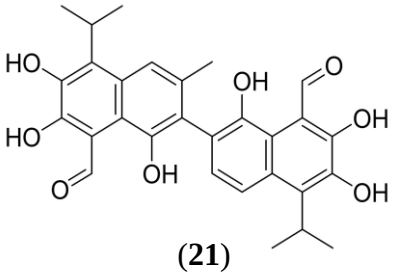

(**21**)

CHAPTER THREE

MATERIALS AND METHODS

3.1 Collection of Nematode cultures

The nematodes, *M. javanica* and *M. incognita*, used for the experiments were sustained on the 'Cal J' tomato cultivar in the screen house at 27 ± 2 °C, 60-70% relative humidity at *icipe.* To obtain the J2 and egg masses that were used for the laboratory and pot experiments, RKN-infected roots were washed gently to remove the soil and Phloxine B (0.15 g/L water) was used to stain the egg masses. Thereafter, the roots were rinsed with running tap water for 5 min, placed in distilled water, and each egg mass was individually removed using a fine needle by observing under a stereomicroscope (Leica M125, Leica microsystems, USA). For the emergence of J2, they were placed in 24-well culture plates containing 2 mL distilled H_2O and incubated at 27 ± 2 °C for 2 to 5 days (Coyne *et al*., 2007; Kihika *et al.*, 2017).

3.2 Preparation of experimental plant materials

Tomato (cv. 'Cal J') (*Solanum lycopersicum L.*) and black nightshade (*Solanum nigrum Linn*) (commonly referred to as managu, mnavu in Kenya), were obtained locally (SimLaw Seeds Company, Nairobi, Kenya). *Bidens pilosa L.*, commonly known as black-jack were sourced from the field at the *icipe*, Duduville campus, Nairobi, Kenya (1° 13' 18.96"S, 36° 53' 47.94"E). Tomato (cv. 'Cal J') and black nightshade are plants in the Solanaceae family that are susceptible to RKNs (Murungi *et al.*, 2018; Kirwa *et al*., 2018). Blackjack is used in the experiments as a non-host Asteraceae plant (Mwamba *et al.*, 2021). Images of the plants used in the study are shown in Plate 3.1.

Plate 3.1: Plants used in the experiments (**a)** Tomato (**b**) Black nightshade (**c**) Blackjack

The seedlings were transplanted two weeks after germination into a sterilized soil and sand mixture (1:1) in 5-liter plastic pots (29 cm depth). Plants were used for experiments at three to four weeks after transplanting. The plants were watered on alternate days with nutrient solution containing macro- and micro-nutrients (Appendix I: Kihika *et al.*, 2017; Kirwa *et al.*, 2018; Murungi *et al.*, 2018).

3.3 Determination of behavioral responses of *M. javanica* infective juveniles to infected tomato plants

A dual-choice olfactometer was used to determine the responses of *M. javanica* J2 to root volatiles of healthy and infected tomato plants (Kihika *et al.*, 2017; Murungi *et al*., 2018) (Figure 3.1). The healthy, non-infected plants, served as the control. The different sections of the olfactometer are shown in Figure 3.1.

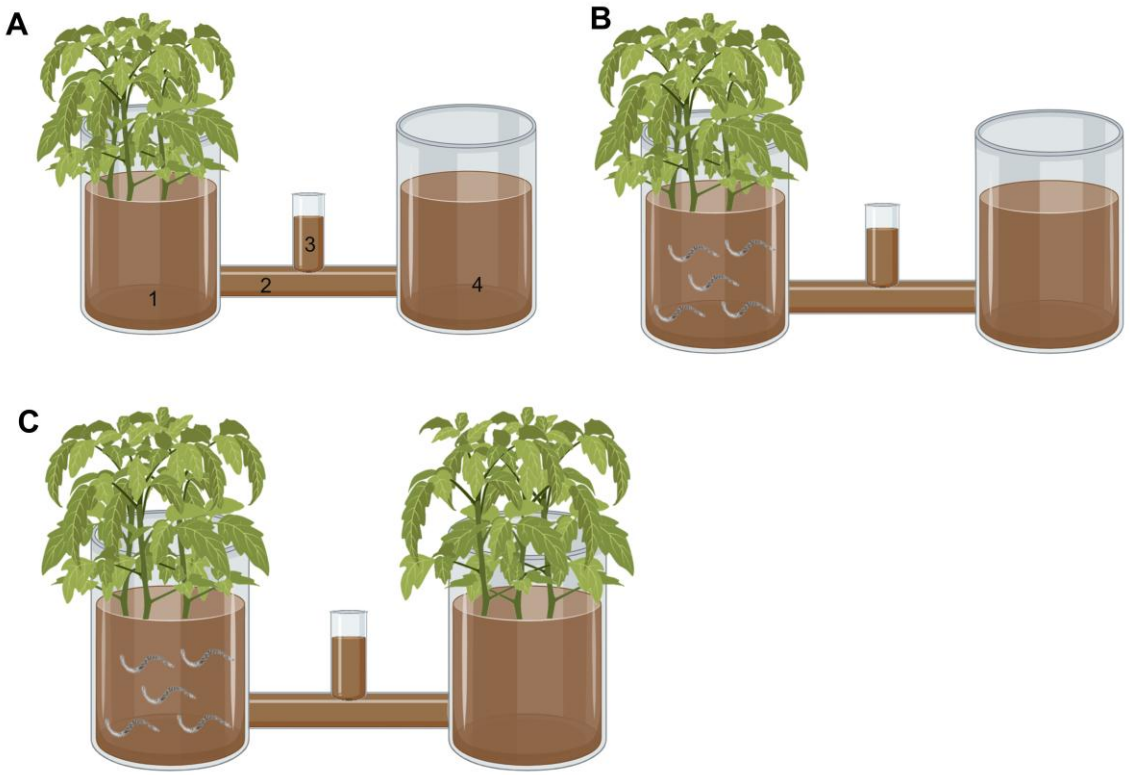

Figure 3.1: A schematic representation showing the dual choice olfactometer assays. Test responses of *Meloidogyne javanica* infective juveniles (J2) to plant root volatiles were compared; (**A**) Healthy vs. control (sand) (**1**) Stimulus chamber (**2**) Connecting arm (**3**) Release arm (**4**) Control chamber (**B**) RKN-infected (2- or 7- DPI) versus a control (sand) (**C**) RKN-infected vs. healthy (used as the control). Images created in Biorender.com

Five plants were placed in a growth chamber (85 mm diameter x 140 mm depth) that contained 300 g of sterilized sand. Nutrient solution (20 mL) was used to water the plants every other day before conducting the experiments in the laboratory at 25 ± 2 °C. After 3-5 days, approximately 1, 000 J2 were used to inoculate the plants to obtain the RKN-infected plants. The healthy (non-infected) plants were prepared in the same way but were not inoculated. The control chamber was filled with 300 g of sterilized sand and nutrient solution (20 mL) was used to moisten the sand on alternate days.

The J2 responses were assayed using (i) healthy (0 days post-infection (DPI)) and infected plants (2- DPI and 7- DPI) tested against sand controls and (ii) healthy vs infected plants in pairwise

treatments. For each treatment, four replicates were conducted and approximately 600 J2 were introduced in the release arm. The experiment was disassembled after 4 h and nematodes in each olfactometer section were recovered using the Baermann sieving method over a 48 h period after which a stereomicroscope was used to count the recovered J2.

3.4 Collection and analysis of volatiles associated with root-knot nematode infection

The volatiles were collected from healthy and infected plants using solid-phase microextraction (SPME). For trapping the root odors, the plants were prepared in the same way described in section 3.3. Thereafter, they were removed from the sand gently, washed with tap water to remove the sand, put in sodium hypochlorite (0.05%) in H_2O for 2 min, and finally rinsed with distilled water.

A round bottom glass flask (100 mL) was used to place five intact plants and a cotton wool moistened with distilled H_2O was placed inside the flask to prevent the roots from dehydration. A charcoal filter was used to cover the glass at the top to ensure that only root volatiles were sampled and aluminum foil was used to wrap the flask to simulate a dark natural root environment. A 65 μm polydimethylsiloxane/divinylbenzene (PDMS/DVB) SPME fiber (Supelco, Bellefonte, USA) was pre-cleaned by thermal desorption at 250°C for 30 min. The fiber was then inserted at the side arm of the glass flask for 1 h at 25 ± 2 °C to trap the root volatiles (Plate 3.2).

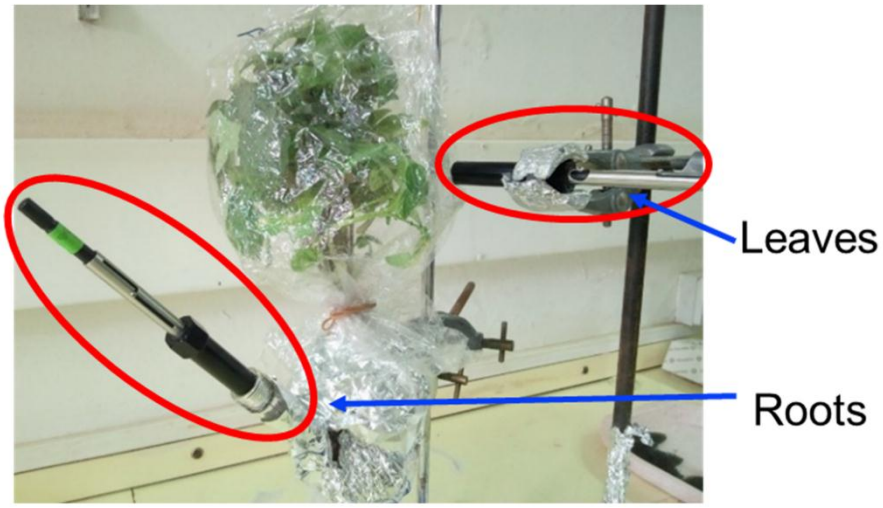

Plate 3.2: Collection of tomato root and leaf volatiles

The leaf volatiles were collected as previously described (Njuguna *et al*., 2018). Briefly, an oven bag was used to enclose the plants and a pre-cleaned SPME fiber was inserted to trap the volatiles for 1 h at 25 ± 2 °C as shown in Plate 3.2. Volatiles were collected in triplicates from the roots and leaves of tomato at 0 DPI, 2 DPI, and 7 DPI. The volatiles collected from the roots and leaves were analyzed using gas chromatography coupled to mass spectrometry (GC/MS) with a HP-7890B series gas chromatograph (Agilent Technologies, Wilmington, USA) linked to a HP 5977 mass spectrometer (Agilent, Wilmington, USA) operated in electron ionization mode (Kihika *et al*., 2020). Plate 3.3 shows the GC/MS and the conditions used for analysis.

B

Injector port temperature: 250 °C

HP-5 MS ultra-inert capillary column: 5%-phenyl methyl polysiloxane; 30 m x 0.25 mm i.d., 0.25 µm film thickness, J & W Scientific, Folsom, USA

Carrier gas: helium at 1.2 ml min^{-1}

Column temperature: 35 °C for 5 min to 280 °C at 10 °C/min

Ion source temperature: 230 °C

EI energy: 70 eV

m/z range: 38-550 Daltons (Da)

Scan time: 0.73 scans/sec

Plate 3.3: Gas chromatography-mass spectrometer (A) and conditions used for analysis (B)

The retention indices (RI) were calculated comparative to C_8-C_{31} *n*-alkanes. Analytes were first identified by comparing their mass spectra with those in the GC/MS library (Adams2 terpenoid/natural product library, 1995; National Institutes of Standards and Technology, 2008) and then their RI were compared with those reported in the literature. The identities of the compounds were then confirmed by comparing the RI and mass spectra of the available authentic standards analyzed under the same conditions. Calibration curves generated from authentic standards of the identified synthetic standards were used for quantification.

The equivalent source amounts were determined using different concentrations (0.2-1,000 ng/µl) of the synthetic standards (1 mL each) contained in an air-tight 4 mL vial. The volatiles were collected by inserting a pre-cleaned SPME fiber into the headspace of the vial for 1 h and analysis was done by GC/MS using the same conditions described earlier for the root and leaf volatiles.

3.5 Nematode responses to synthetic compounds of volatiles associated with root-knot nematode infection

The available synthetic standards of the compounds identified from the infected plants were used to determine the J2 responses using the dual-choice assays described in section 3.3. The RKN species used for these experiments was *M. javanica.* For each compound, three concentrations were prepared in hexane and these were tested in four replicates (Kihika *et al.*, 2017; Murungi *et al*., 2018). The concentrations of individual compounds were prepared based on amounts estimated to be present in healthy and infected plants at the three time points of infection (Table 3.1). The 6-component blend comprised of three doses as follows: Dose 1 ((+)-(2)-carene (4.4 µg), β-phellandrene (20.6 µg), and 2.75 µg of β-pinene, α-phellandrene, MeSA, and MeDiJA),

Dose 2 ((+)-(2)-carene (8.8 µg), β-phellandrene (10.2 µg), and 5.5 µg of β-pinene, α-phellandrene, MeSA, and MeDiJA) and Dose 3 ((+)-(2)-carene (34.1 µg), β-phellandrene (69.2 µg), and 11 µg of β-pinene, α-phellandrene, MeSA, and MeDiJA).

Table 3.1: Concentrations of the compounds used in bioassays

Compound	Concentration 1 (ng/µl)	Concentration 2 (ng/µl)	Concentration 3 (ng/µl)
Methyl salicylate (MeSA)	55	110	220
Methyl dihydrojasmonate (MeDiJA)	55	110	220
β-pinene	55	110	220
α-phellandrene	55	110	220
(+) -(2)-carene	88	176	682
β-phellandrene	412	203	1,384

The treatments (50 µl aliquots) of the compounds and hexane were introduced into the stimulus and control chambers, respectively. Separate bioassays tested the J2 responses to the infected plant at 2-DPI spiked with MeSA against the 2-DPI (control). Another experiment determined the effect of spiking a healthy plant with MeDiJA vs healthy plant (control) using the similar concentrations tested for individual compounds.

3.6 Determination of the effect of blackjack root exudates in *M. incognita* infected susceptible plants

The effect of blackjack root exudates in reducing the infection of *M. incognita* in two susceptible host plants, tomato and black nightshade, was evaluated using two different experiments (Figure 3.2): (i) intercrop whereby each pot contained one non-host plant and one susceptible plant inoculated with one egg mass of *M. incognita*, and (ii) drip experiments whereby a pot containing blackjack was watered with 300 ml nutrient solution, and an excess of 300 ml of the

nutrient solution was saturated and allowed to drip through a Teflon tube into a pot containing the host plant inoculated with one egg mass of the RKN. As a control, the different plants were separately inoculated with one egg mass to check for host status.

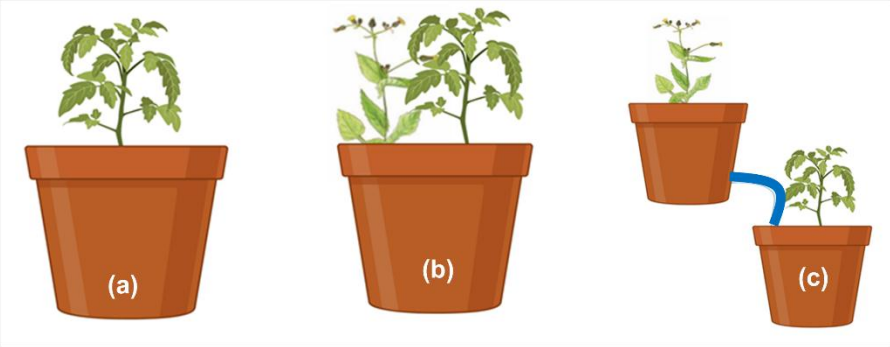

Figure 3.2: A schematic representation showing the pot experiments. (**a**) control (**b**) intercrop and (**c**) drip experiments. Images created in Biorender.com

Approximately 60 days post inoculation, the plants were uprooted and the roots were washed to remove the soil. The roots were stained by placing them in 500 ml beakers containing 300 ml Phloxin B (0.15 g/L water) for 20 min (Kihika *et al.*, 2017). The number of galls and egg masses per root system was counted (Taylor and Sasser, 1978; Kihika *et al.*, 2017).

3.7 Collection of root exudates from the susceptible and non-host plants

The plants were uprooted gently, washed under slow running tap water, dipped in 0.05% NaOCl in H_2O for 2 min, and finally rinsed with distilled water. The exudates were collected by immersing 100 intact plants in a 500 ml beaker containing 250 ml distilled water and wrapped with aluminum foil. This represented a replicate and the collection was done in triplicates. After 24 h the exudates were filtered, stored in – 80°C, and then lyophilized in a VirTis AdVantage 2.0 benchtop freeze drier (SP Scientific, Gardiner, NY), weighed, then stored at – 80^{o}C until use in either bioassays or chemical analysis.

3.8 Determination of the effect of root exudates on the *in vitro* hatching and mortality of *M. incognita*

A stock solution (25 mg/ml) of the freeze-dried exudates was prepared in distilled water, vortexed for 2 min, sonicated for 10 min and centrifuged for 5 min at 14,000 rpm. Three concentrations (1, 2.5, and 5 mg/ml) were prepared by serial dilution (Kirwa *et al*., 2018; Ochola *et al*., 2020a).

Hatching assays were conducted by placing each egg mass in a well of a 96-well polypropylene plate containing 100 µl of the treatment. The set up was incubated at 27°C, monitored for seven days, and the total number of emerged J2 and unhatched eggs were counted. Mortality assays were conducted by introducing 20 µl of aqueous suspension containing about 100 J2s in each well of a 96-well polypropylene plate containing a 100 µl of the treatment. After 48 h in the dark at 27 °C, J2s that were dead and alive were counted. For a control, 100 µl of distilled water was used in similar set ups and 12 wells for each treatment and control represented replicates.

3.9 Chemical analysis of the root exudates

A concentration of 1 mg/ml was constituted by dissolving 80 mg of the lyophilized root exudates in 30 % methanol in double distilled water (Kirwa *et al*., 2018; Ochola *et al*., 2020a). The sample was vortexed (1 min), sonicated (20 min), and centrifuged (14,000 rpm; 10 min). The supernatant was transferred into a sample vial and 5 µl analyzed on a Nexera X2 Series HPLC system (Shimadzu, Kyoto, Japan), equipped with a Prominence SPD-M30A diode array detector (190-700 nm). The HPLC conditions for the analysis and fractionation of the root exudates are shown in Table 3.2.

Table 3.2: High performance liquid chromatographic conditions for the analysis and fractionation of root exudates

Time (min)	Solvent A (%)	Solvent B (%)	Solvent A: H_2O (0.01% Formic acid) Solvent B: Acetonitrile Flow rate: 0.7 ml/min Oven temperature: 30°C Column: 250 mm x 10 mm i.d., 3.5 µm, SB C18 (Advance Chromatography Technologies, Aberdeen, Scotland)
0.01	95	5	
5	80	20	
15	60	40	
20	60	40	
27	40	60	
30	40	60	
37	20	80	
40	0	100	
46	0	100	
49	95	5	
52	95	5	

The three fractions that were collected: fraction 1 (2.5-20 min); fraction 2 (20.1-30 min); and fraction 3 (30.1-46 min) were concentrated using a rotary evaporator to give 30 mg, 20 mg, and 17 mg, respectively. Three concentrations (1, 2.5 and 5 mg/ml) of each fraction were prepared and their bioactivity was tested on *M. incognita* following the procedures described in section 3.8.

A concentration of 1000 ng μl^{-1} of the root exudates of tomato, black nightshade, and the most bioactive fraction of blackjack were prepared in 30% methanol in double distilled H_2O. The mixture was vortexed (1 min), sonicated (20 min), and centrifuged (14,000 rpm; 10 min). The sample was then diluted to 100 ng μl^{-1} and transferred into a sample vial (1 ml) for analysis using the Ultra Performance Liquid Chromatography coupled to a triple quadrupole tandem mass spectrometry (UPLC-QQQ-MS/MS). The ACQUITY UPLC I-class system (Waters Corp., Milford, 151 MA) was used for chromatographic separation. An electrospray ionization (ESI) Waters Xevo TQ-S operated in full scan MS in both positive and negative ionization modes was interfaced with the UPLC. The data was attained using MassLynx version 4.1 SCN 712 (Waters). The UPLC-QQQ-MS conditions used for analysis are shown in Table 3.3. The

potential identities of the compounds were assigned by generating the mass spectrum for each peak, establishing the molecular ion peaks using adducts, common fragments, literature and where available, confirmed with authentic standards.

Table 3.3: Liquid chromatography tandem mass spectrometry conditions for the analysis of root exudates

Time (min)	Solvent A (%)	Solvent B (%)	Solvent A: H_2O (0.01% Formic acid) Solvent B: Methanol Flow rate: 0.2 ml min^{-1} Autosampler tray temperature: 5°C Oven temperature: 45°C Column: ACQUITY UPLC BEH C18 column (2.1 mm × 150 mm, 1.7 µm particle size; Waters Corp., Wexford, Ireland)
0.01	95	5	
2	80	20	
4	60	20	
7	60	60	
8.5	40	60	
10	40	80	
19	20	80	
20.5	0	100	
23	0	100	
24	95	5	
26	95	5	
m/z range: 100 – 2000, Capillary voltage: 0.5 kV, Sampling cone voltage: 30 V Source temperature: 150°C, Desolvation temperature: 250°C, Nitrogen desolvation flow rate: 550 l h^{-1}			

3.10 Determination of the bioactivity of the identified compounds

The eight available standards, which included ascorbic acid and nicotinic acid, malic acid, tyrosine and phenylalanine, *p*-coumaric acid and 2-hydroxybenzoic acid, and kaempferol were tested. Five concentrations (0.1, 1, 10, 100, 1000 ng μl^{-1}) were prepared by serial dilution from a stock solution of 10 mg/ml prepared in distilled water containing 10% DMSO. The control was constituted by preparing 2% DMSO in water. The treatments and control were tested in five replicates using the *in vitro* egg hatching and J2 mortality assays described in section 3.8.

3.11 Chemicals and reagents

The synthetic standards identified using GC/MS analysis and were available, included *o*-cymene; *p*-cymene; 95% nonanal; >95% tridecane; ≥97% of (*R*)-(-)-α-phellandrene and 3-isopropyl-2-methoxypyrazine; 99% of (*R*)-(+)-α-pinene and (1*S*)- (-)-β-pinene; a mixture of cis and trans MeDiJA from Sigma Aldrich (St, Louis, MO, USA). 97% MeSA was acquired from Sigma Aldrich (Steinhelm, Germany), 97% (+) -(2)-carene from Sigma Aldrich, Switzerland and 99% (-)-*trans* caryophyllene from Fluka. The (*S*)-(+)-β-phellandrene (89%) was obtained from Angelica seed oil.

The solvents and synthetic standards used for UPLC-QQQ-MS analysis included ≥98% of phenylalanine, tyrosine, kaempferol, nicotinic acid, and *p*-coumaric acid; ≥ 99.9% of analytical grade methanol, acetonitrile, DMSO, L-ascorbic acid, DL-malic acid, and 2-hydroxybenzoic acid; water (LC-MS Chromasolv); formic acid (98-100%) from Sigma- Aldrich (St. Louis, MO, United States).

3.12 Statistical analysis

Results from the dual-choice assays were expressed using the formula:

$$[(n/N) \times 100]$$

Where, n is the number of nematodes that responded to a specific treatment and N is the sum of nematodes that responded to the treatment and control. The non-responding nematodes were not considered in the analysis which was done using the Chi-square (χ^2) goodness-of-fit analysis.

The concentration of the volatiles was checked for normality using the Shapiro−Wilk test ($P > 0.05$) and then analyzed using ANOVA or Kruskal-Wallis test followed by SNK post hoc tests and Post hoc Dunn's test for mean separation, respectively. The unpaired *t*-test was used for the

pairwise comparison of mean concentrations of volatiles for healthy and infected plants. All the statistical results were considered significant at $P < 0.05$.

SIPMER followed by one-way ANOSIM using the Bray–Curtis dissimilarity matrix was performed to compare the chemical profiles of the leaf volatiles of healthy and infected plants. The data was visualized using NMDS prepared on the Past 3 free software (Hammer and Harper, 2001). The results from the pot experiments on number of galls and egg masses were analyzed using ANOVA and SNK post hoc multiple comparison test to separate the means. Galling and egg mass indices were analyzed using Kruskal-Wallis test followed by the post hoc Dunn's test after checking for normality. The unpaired *t*-test compared the galling and reproduction for tomato and black nightshade and this data was visualized using the principal co-ordinate analysis (PCoA).

The data from the hatching and mortality assays was analyzed using GLM with a binomial distribution due to the binary nature of the parameters (hatched vs. unhatched and dead vs. alive, respectively). Analysis of deviance (with chi-squared test) was used to establish the significance of the model. The "emmeans" R package (Lenth, 2018) was used to perform the Tukey's multiple comparisons test to separate the means for each treatment. The data was expressed as a percentage using the formula:

$$(C_o\text{-}T_\alpha)/C_o \times 100,$$

Where, C_o is the number of J2 hatched in control or number of live J2 in control and T_α is the number of J2 hatched in the treatment or number of live J2 for hatching and mortality assays, respectively.

The R statistical software 64 (version 3.5.1) and the R Studio graphical user interface (version 1.1.383) were used to perform the analyses (R Core Team, 2020).

CHAPTER FOUR

RESULTS AND DISCUSSION

4.1 Response of *Meloidogyne javanica* to root volatiles of healthy and infected tomato

The results from the dual choice assays demonstrated that volatiles from the non-infected tomato roots significantly attracted J2 of *M. javanica* (Table 4.1; Figure 4.1) compared to sand controls. These findings are consistent with those reported by Murungi *et al.*, (2018) where this tomato cultivar attracted J2 of *M. incognita*. The time points investigated in this study were found to influence the J2 responses to RKN infected tomato. Specifically, significant avoidance was recorded at 2-DPI whereas significant attraction was observed at 7-DPI compared to a sand control (Table 4.1; Figure 4.1). Equally, in the pairwise experiments, J2 significantly avoided the root volatiles of 2-DPI tomato but preferred the 7-DPI plant over healthy plants (Table 4.1; Figure 4.1).

Table 4.1: Chi-square analysis for test of proportions of the nematode responses to root volatiles

Treatments	Proportions and chi-square analysis
0 DPI vs control	97%, $\chi^2 = 599.2$, df = 1, $P < 0.001$
2 DPI vs control	86%, $\chi^2 = 599.2$, df = 1, $P < 0.001$
7 DPI vs control	98%, $\chi^2 = 1384.6$, df = 1, $P<0.001$
2 DPI vs 0 DPI	71%, $\chi^2 = 221.36$, df = 1, $P < 0.001$
7 DPI vs 0DPI	58%, $\chi^2 = 21.43$, df = 1, $P < 0.05$

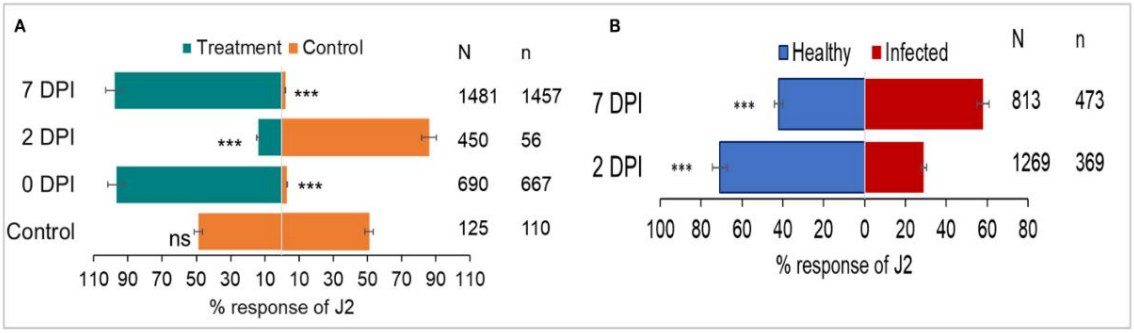

Figure 4.1: Response of *Meloidogyne javanica* infective juveniles (J2) to tomato "Cal J" root volatiles. (**A**) Healthy (0 DPI) and infected (2- and 7- DPI) versus a control (**B**) Healthy vs. RKN-infected. (N corresponds to the total number of responding J2 while n is the number of J2 corresponding to a given treatment. The level of significance is indicated by: ***$P < 0.001$; ns = not significant) DPI; days post infection.

These findings may indicate that nematode infection triggers the plant to produce volatiles that inhibit nematode attraction to the host plant at 2 DPI. This is consistent with the initial stages of RKN infection when the nematodes migrate between the cells before they begin forming the feeding sites (Pierre *et al.*, 2009). Subsequently, the J2 may link these chemical signals with reduced food resources and therefore evade this treatment to avoid competition when too many J2 infect the plant. On the contrary, nematodes preferred the plants at 7 DPI and these differential responses could be associated with the ratio and composition of attractive and repellent compounds released by the healthy and infected plants at the different post-infection times. Consequently, the nematodes may release diverse chemical signals for nematode-nematode interaction during attraction or avoidance to different treatments, which requires further research.

4.2 Constitutive and induced volatiles produced by tomato roots in response to RKN infection

The root volatile profiles of healthy and infected tomato were collected and analyzed using SPME and GC/MS, respectively. Twenty-eight compounds were identified that were consistent in the three replicates sampled for each treatment and consisted of thirteen monoterpenes, nine

sesquiterpenes, two aldehydes, a pyrazine, an alkane, a benzenoid, and a jasmonate (Figure 4.2). Table 4.2 shows the compounds detected and their quantitative variations at the different time points of root infection. There was a significant difference in the amounts released for the different compounds at the different times of infection compared to the non-infected tomato plant (Table 4.2). β-phellandrene (**26**) was the most abundant compound in the non-infected plant, with a two-fold decrease and relatively three-fold increase in the amounts at 2-DPI and 7-DPI, respectively.

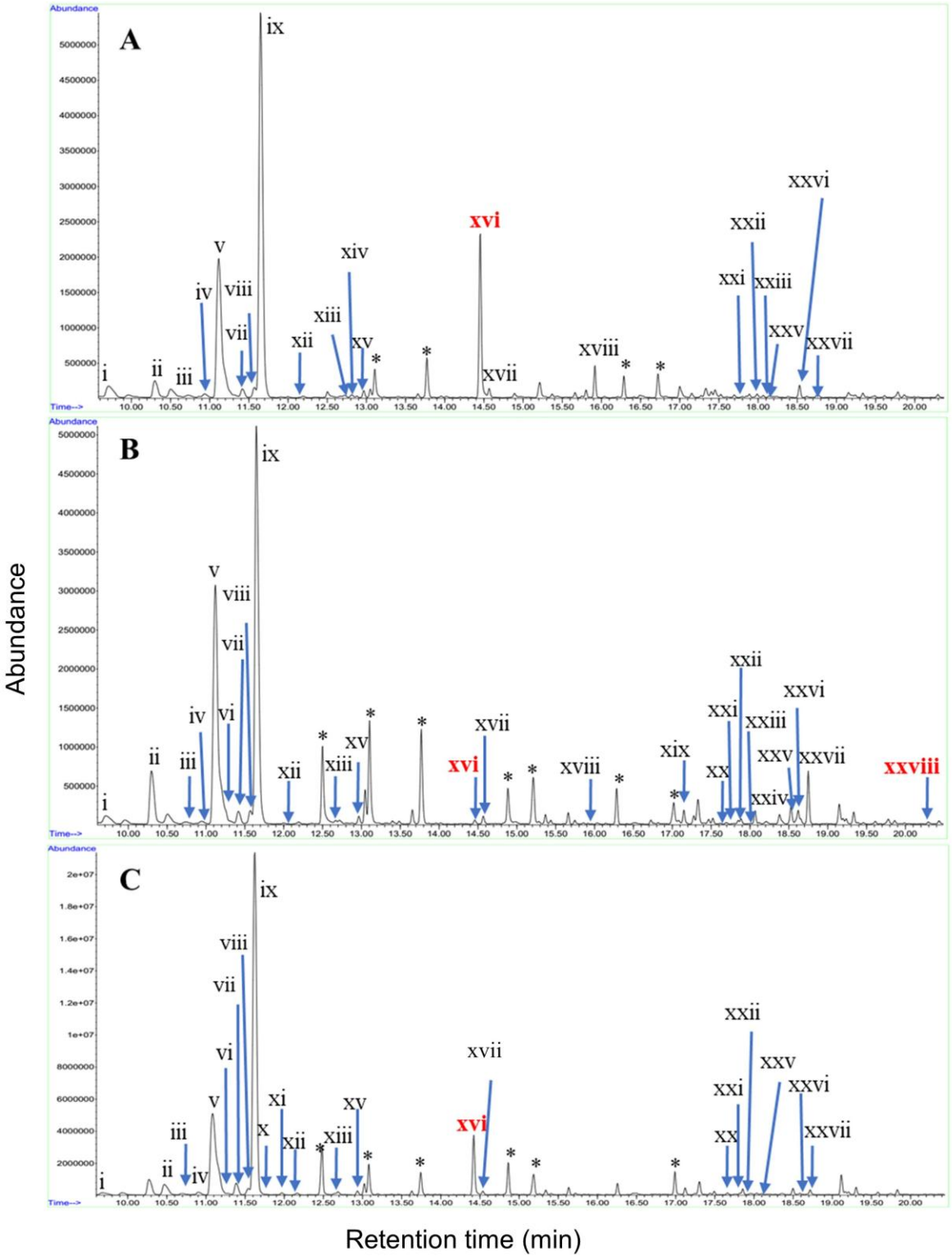

Figure 4.2: Gas chromatography-mass spectrometry profiles of root volatiles collected from healthy and RKN-infected tomato. **(A)**Healthy (Day 0) and *Meloidogyne javanica* infected (Day 2 **(B)** and 7**(C)**) tomato ('Cal-J') plants by SPME. Asterisk (*) indicates column contaminants.

Table 4.2: Compounds detected in root volatiles from non-infected and *Meloidogyne javanica infected* tomato plants collected by SPME and analyzed by gas chromatography-mass spectrometry.

	t_R(min)	Compound	RI^{Calculated}	RI^{Literatue}	Mean amount adsorbed (ng ± SE)		
					Healthy	2-DPI	7-DPI
i.	9.71	*α-Pinene^{Mono} (**1**)	915	918	2.95 ± 0.75^{a}	2.29 ± 0.70^{a}	6.21 ± 2.32^{a}
ii.	10.50	**o*-Cymene^{Mono} (**22**)	951	956	2.96 ± 1.33^{a}	1.61 ± 0.29^{a}	10.98 ± 1.79^{b}
iii.	10.73	* * (*E*)-Isolimonene^{Mono} (**23**)	961	960	0.49 ± 0.19^{a}	0.19 ± 0.07^{a}	1.85 ± 0.43^{b}
iv.	10.94	*β-Pinene^{Mono} (**24**)	971	965	0.40 ± 0.07^{a}	0.23 ± 0.05^{a}	1.84 ± 0.23^{b}
v.	11.12	* (+) -(2)-Carene^{Mono} (**25**)	979	981	18.68 ± 9.02^{a}	34.40 ± 4.89^{a}	127.03 ± 34.79^{b}
vi.	11.20	*α-Phellandrene^{Mono} (**26**)	988	985	trace	0.32 ± 0.01^{a}	1.10 ± 0.28^{b}
vii.	11.42	*α-Terpinene^{Mono} (**27**)	993	996	17.86 ± 16.64^{a}	1.07 ± 0.27^{a}	10.09 ± 2.68^{a}
viii.	11.57	**p*-Cymene^{Mono} (**28**)	1000	1000	0.81 ± 0.29^{a}	0.66 ± 0.34^{a}	3.14 ± 0.90^{b}
ix.	11.65	*β-Phellandrene^{Mono} (**29**)	1005	1010	78.46 ± 30.53^{a}	39.66 ± 6.95^{a}	252.79 ± 50.34^{b}
x.	11.81	**3-Carene^{Mono} (**30**)	1014	1011	trace	trace	0.10 ± 0.01
xi.	12.00	* (*E*)-β-Ocimene^{Mono} (**31**)	1024	1029	trace	0.13 ± 0.03^{a}	0.94 ± 0.15^{b}
xii.	12.20	**γ-Terpinene^{Mono} (**32**)	1036	1041	2.08 ± 1.99^{a}	0.09 ± 0.02^{a}	1.06 ± 0.23^{a}
xiii.	12.72	**Terpinolene^{Mono} (**33**)	1066	1073	1.43 ± 1.29^{a}	0.1 ± 0.01^{a}	2.46 ± 0.45^{a}
xiv.	12.82	*3-Isopropyl-2-methoxypyrazine ^{Pyr} (**34**)	1075	1079	0.02 ± 0.03	trace	trace
xv.	12.96	*Nonanal^{Ald} (**35**)	1082	1088	0.27 ± 0.25^{a}	0.69 ± 0.26^{ab}	1.09 ± 0.08^{b}
xvi.	14.46	*Methyl salicylate^{Est} (**3**)	1170	1176	7.24 ± 0.28^{a}	1.18 ± 0.03^{a}	8.62 ± 4.15^{a}
xvii.	14.57	*Decanal^{Ald} (**36**)	1177	1183	0.50 ± 0.18^{a}	0.57 ± 0.24^{a}	1.11 ± 0.08^{b}
xviii.	15.91	*Tridecane^{Alka} (**5**)	1234	1271	0.47 ± 0.63^{a}	0.10 ± 0.09^{a}	trace

xix.	17.09	*α-Copaene^{Sesq} (**37**)	1348	1351	trace	0.14 ± 0.03^{a}	trace
xx.	17.61	**Di-epi-α-cedrene^{Sesq} (**38**)	1385	1385	trace	0.06 ± 0.01^{a}	0.15 ± 0.07^{a}
xxi.	17.70	* (*E*)-Caryophyllene^{Sesq} (**13**)	1389	1396	0.10 ± 0.05^{a}	0.07 ± 0.00^{a}	0.17 ± 0.01^{a}
xxii.	17.99	**Geranyl acetone^{Ket} (**39**)	1411	1424	0.07 ± 0.01^{a}	0.11 ± 0.09^{a}	0.24 ± 0.07^{a}
xxiii.	18.07	**α-Guaiene^{Sesq} (**40**)	1419	1433	0.04 ± 0.00^{a}	0.30 ± 0.07^{a}	trace
xxiv.	18.22	**9,10-Dehydro-isolongifolene^{Sesq} (**41**)	1431		ND	0.28 ± 0.07	ND
xxv.	18.38	**α-Selinene^{Sesq} (**42**)	1441	1475	0.04 ± 0.00^{a}	0.32 ± 0.06^{a}	0.30 ± 0.06^{a}
xxvi.	18.62	**Valencene^{Sesq} (**43**)	1459	1484	0.03 ± 0.00^{a}	0.42 ± 0.07^{b}	0.30 ± 0.09^{b}
xxvii.	18.75	**Viridiflorene^{Sesq} (**44**)	1469	1489	0.06 ± 0.00^{a}	0.66 ± 0.13^{b}	0.65 ± 0.15^{b}
xxviii.	20.43	* (*Z*)-Methyl dihydrojasmonate^{Jas} (**45**)	1606	1655	BDL	0.11 ± 0.02	trace

Ald= Aldehyde; Alka=Alkanes; Est = Esters; Ket= Ketone; Jas= Jasmonate; Mono=Monoterpenes; Pyr = Pyrazine and Sesq=Sesquiterpenes.

Means with different letters for each compound are significantly different from each other (ANOVA followed by SNK post hoc test; $P < 0.05$, $n = 3$). DPI; days post infection, $RI^{Calculated}$; Retention index relative to C_8-C_{31} n- alkanes of a HP-5 MS column, $RI^{Literature}$; Retention index obtained from literature. ND; not detected. BDL; below detection limit. *Compound whose identity was established based on comparison of retention time and mass spectra data with authentic standard. **Compound identified tentatively based on library data, calculated RI values and comparison to literature.

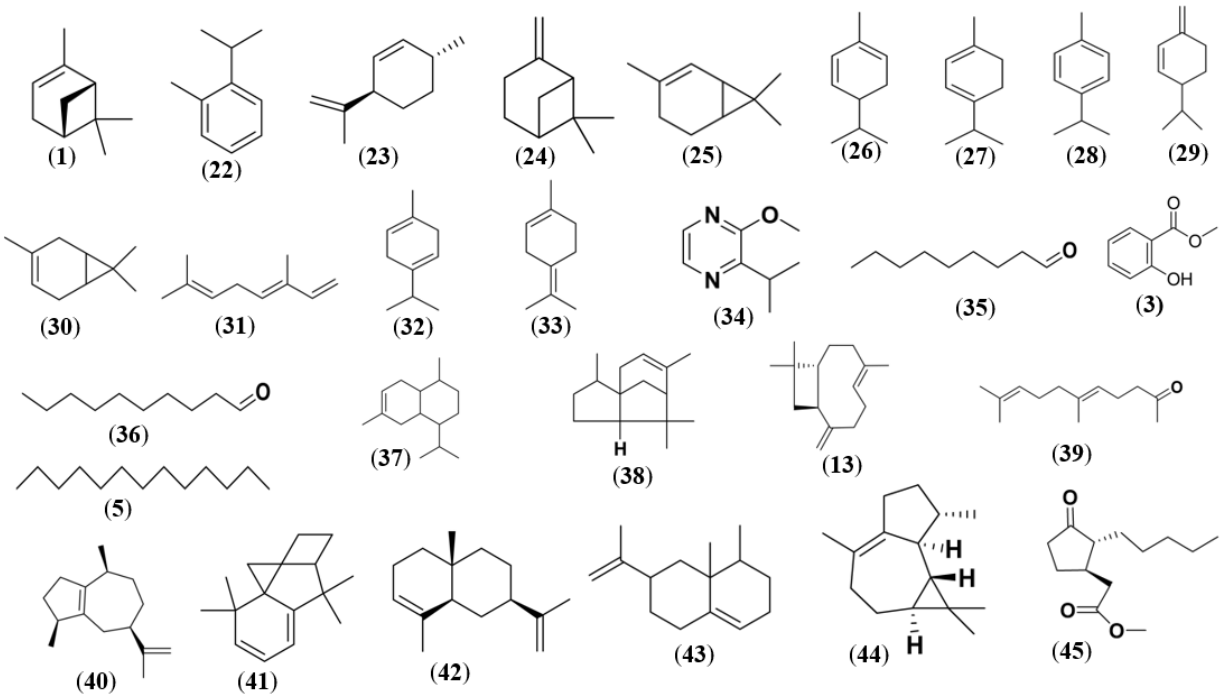

Sampling and analysis of volatiles from the intact plant using SPME-GC/MS was a more sensitive technique likened to a method that was previously used which utilized Super Q as the adsorbent (Kihika *et al.*, 2017; Murungi *et al.*, 2018). However, the technique of using Super Q connected to a probe and inserted in sand may be a more accurate representation of the natural situation where matrix interference from sand-specific compounds is present. The effect of sand-released compounds on the behavior of J2 was not investigated in the previous studies (Kihika *et al.*, 2017; Murungi *et al.*, 2018). Additionally, different compounds may have varied diffusion rates in the sand matrix which can influence the concentrations detected and thus differ from the natural concentrations released by the roots. For example, using selected ion monitoring mode (*m/z* 83, 156, 226), MeDiJA (**45**) was detected in the root volatiles of healthy tomato in the current study. However, this compound was not reported in a previous study (Murungi *et al.*, 2018) that sampled volatiles from the same tomato cultivar when the roots were snap frozen. In the current study, volatiles were collected from the intact tomato plant with the roots retained in

moist cotton wool and the sampling was done within a short period (1 h). This was especially important since this approach facilitated the reduction of stress-associated volatiles released by the roots. Nevertheless, the differences in the procedures used to collect the root volatiles and authentic standards may influence the precision of the amounts determined for the adsorbed volatiles.

Nematodes of *Meloidogyne* species are endoparasitic biotrophs (Pierre *et al.*, 2009) that cause negligible damage as they move intercellularly to the vascular tissue where they form galls (Gheysen and Mitchum, 2011) in a confined area and withdraw nutrients from living plant cells using their stylet (Pierre *et al.*, 2009). Notably, when tomato was infected with *M. javanica*, it caused a significant difference in certain monoterpenes, particularly (+) -(2)-carene (**25**) and β-phellandrene (**26**), but this was not observed for the sesquiterpenes. It is likely that the time frame and extent of *M. javanica* infection were only sufficient to activate a burst of monoterpenes but not sesquiterpenes. Different scenarios such as the degree of nematode infection over an extended duration should be considered in future studies.

In the current study, methyl dihydrojasmonate (**45**), derived from the jasmonic acid (JA) pathway (Haegeman *et al.*, 2012), was identified at 2-DPI when the J2 are migrating between the cells and initiating the formation of feeding sites (Haegeman *et al.*, 2012). This could be triggered by specific nematode secretions that are produced to counter plant defense responses at this phase of RKN parasitism (Haegeman *et al.*, 2012). MeDiJA (**45**) may be formed through the hydrogenation of methyl JA (**46**) or through the hydrogenation of the JA (**18**) isomer, (+)-7-iso JA (**47**), which is then methylated to MeDiJA (**45**) (Figure 4.3). However, the biosynthesis of MeDiJA (**45**) in plants like tomato is yet to be fully elucidated.

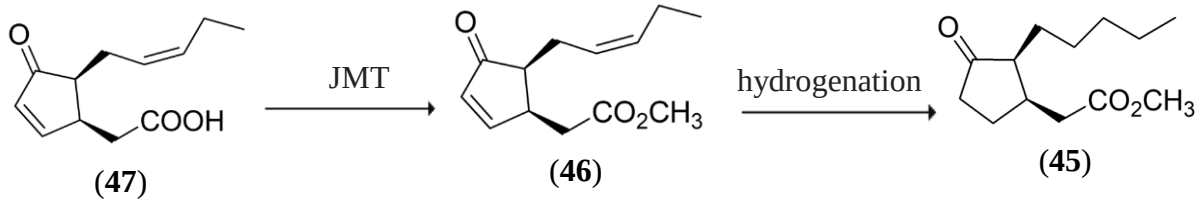

(**47**) (**46**) (**45**)

Figure 4.3: Putative biosynthesis of methyl dihydrojasmonate (**45**). (+)-7-iso JA (**47**) is methylated to methyl JA (**46**) by jasmonic acid carboxyl methyltransferase (JMT). Methyl jasmonate is then hydrogenated to give MeDiJA (**45**).

On the other hand, methyl salicylate (MeSA) (**3**), derived from SA (**17**), is a constituent of insect- and pathogen-induced plant volatiles (De Backer *et al*., 2015; Engelberth *et al*., 2004; Silva *et al*., 2017; Zebelo *et al*., 2014; Zhang *et al*., 2009; 2013) and is well known for its significant ecological role in indirect defense of recruiting natural enemies (De Boer and Dicke, 2004). The amount of MeSA (**3**) in this study reduced at 2-DPI, and the asynchronous quantifiable detection of MeSA (**3**) and MeDiJA (**45**) may indicate a likely cross-talk between the JA (**18**) and SA (**17**) signaling pathways in response to *M. javanica* infection. The amount of MeSA (**3**) may decrease when it is being converted to its precursor, SA (**17**), (Figure 4.4) to enable the production of other defense compounds.

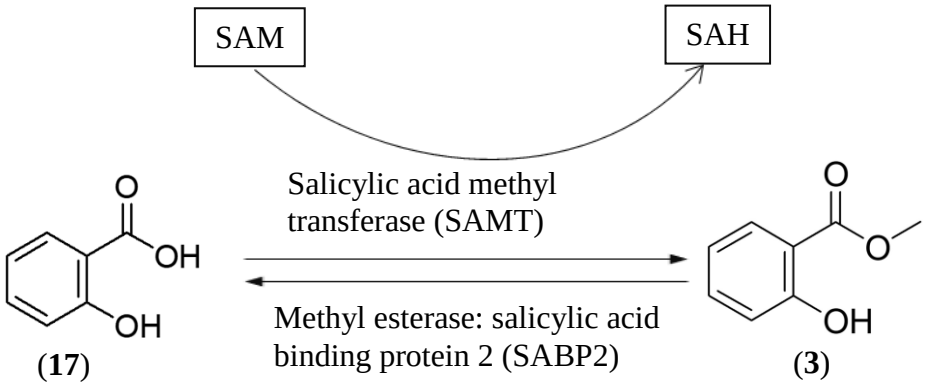

(**17**) (**3**)

Figure 4.4: Biosynthesis of methyl salicylate in plants. *S*-adenosyl-l-methionine (SAM)-dependent methylation of SA (**17**) into MeSA (**3**) by salicylic acid methyl transferase. SAM donates a methyl group and is converted into *S*-adenosyl homocysteine (SAH). (Singewar *et al.*, 2021)

4.3 Constitutive and induced leaf volatiles of tomato released in response to RKN infection

4.3.1 Gas chromatography-mass spectrometric analysis of tomato leaf volatiles

Analysis of aerial volatiles collected from healthy tomato, *M. incognita*- and *M. javanica*-infected plants by GC-MS, detected a total of 41, 55 and 52 VOCs, respectively. The volatiles generally belonged to nine classes of compounds namely, monoterpenes, sesquiterpenes, aldehydes, a pyrazine, alkanes, an ester, alcohol, fatty acids, and a jasmonate (Table 4.3). For the *M. incognita* -infected plants, 52 and 48 VOCs were identified from tomato at 2- and 7- DPI (Figure 4.5) while 51 and 46 VOCs were detected from tomato infected with *M. javanica* at 2- and 7- DPI (Figure 4.6).

Table 4.3: Compounds detected in leaf volatiles from healthy and *RKN*-infected tomato ('Cal-J') plants collected by SPME and analyzed by gas chromatography-mass spectrometry.

			Mean amount adsorbed (ng ± SE)						
	t_R(min)	Compound name	Healthy	*M. incognita*-infected		*M. javanica*-infected		RI^{calc}	RI^{lit}
				2-DPI	7-DPI	2-DPI	7-DPI		
i.	9.72	*α- Pinene^{Mono} (**1**)	0.96 ± 0.40^{a}	13.47 ± 4.72^{a}	29.56 ± 4.83^{b}	3.87 ±1.53^{a}	11.12 ± 1.79^{b}	915	918
ii.	10.51	**o*-Cymene^{Mono} (**22**)	1.77 ± 0.59^{a}	37.01 ± 8.66^{b}	91.69 ± 14.78^{c}	10.32 ± 2.93^{a}	36.94 ± 8.70^{b}	951	956
iii.	10.73	** (*E*) -Isolimonene^{Mono} (**23**)	0.15 ± 0.08^{a}	3.77 ± 0.92^{b}	9.44 ± 1.43^{c}	0.89 ± 0.28^{a}	3.13 ± 0.28^{b}	961	960
iv.	10.93	*β-Pinene^{Mono} (**24**)	0.52 ± 0.26^{a}	21.08 ± 9.25^{a}	50.77 ± 8.82^{b}	5.02 ± 0.79^{b}	11.39 ± 1.17^{c}	971	971
v.	11.12	*2-δ-Carene^{Mono} (**25**)	21.10 ± 9.14^{a}	257.91 ± 68.99^{a}	645.11 ± 113.25^{b}	96.93 ± 23.93^{b}	243.52 ± 27.65^{c}	979	981
vi.	11.17	*α-Phellandrene^{Mono} (**26**)	0.96 ± 0.88^{a}	3.78 ± 0.91^{a}	10.92 ± 1.73^{b}	trace	3.55 ± 0.56^{a}	988	985
vii.	11.43	*α- Terpinene^{Mono} (**27**)	2.47 ± 0.87^{a}	39.53 ± 11.89^{a}	96.56 ± 17.11^{b}	12.74 ± 3.86^{a}	36.49 ± 5.62^{b}	993	996
viii.	11.58	**p*-Cymene^{Mono} (**28**)	2.98 ± 0.60	trace	trace	trace	trace	1000	1000
ix.	11.66	*β-phellandrene^{Mono} (**29**)	77.81 ± 25.78^{a}	549.14 ± 109.53^{a}	1571.05 ± 239.69^{b}	273.07 ± 44.70^{b}	551.60 ± 35.82^{c}	1002	1005
x.	11.81	*Sabinene^{Mono} (**48**)	0.30 ± 0.21^{a}	3.61 ± 1.70^{a}	9.75 ± 1.81^{b}	0.78 ± 0.14^{a}	2.08 ± 0.48^{b}	1014	1011
xi.	11.97	** (*E*)-β-Ocimene^{Mono} (**31**)	0.85 ± 0.52^{a}	11.14 ± 5.34^{a}	27.90 ± 5.68^{b}	2.92 ± 0.32^{a}	5.67 ± 2.38^{a}	1025	1029
xii.	12.16	**γ-Terpinene^{Mono} (**32**)	1.25 ± 0.20^{a}	8.65 ± 2.66^{a}	22.08 ± 3.65^{b}	3.06 ± 0.81^{a}	7.87 ± 1.64^{b}	1037	1041
xiii.	12.32	**Endo-arbozol^{Mono} (**49**)	0.73 ± 0.30	-	-	-	-	1046	
xiv.	12.72	*Terpinolene^{Mono} (**33**)	1.62 ± 0.60^{a}	19.60 ± 3.92^{a}	44.85 ± 8.84^{b}	5.94 ± 1.57^{a}	17.80 ± 3.55^{b}	1068	1073
xv.	12.88	*Undecane^{Alk} (**50**)	0.02 ± 0.00^{a}	-	1.79 ± 0.69^{a}	0.03 ± 0.09^{a}	trace	1079	
xvi.	12.97	*Nonanal^{Ald} (**35**)	0.32 ± 0.08^{a}	2.21 ± 0.10^{a}	12.17 ± 1.07^{b}	1.50 ± 0.64^{a}	2.26 ± 1.05^{a}	1083	1088
xvii.	13.23	*Iso-sylvestrene^{Mono} (**51**)	0.52 ± 0.12^{a}	6.58 ± 2.03^{a}	16.13 ± 3.03^{b}	1.76 ± 0.51^{a}	6.62 ± 1.71^{b}	1098	
xviii.	13.38	**Allo-ocimene^{Mono} (**52**)	0.36 ± 0.28^{a}	2.72 ± 1.23^{a}	7.60 ± 1.07^{b}	0.48 ± 0.09^{a}	1.44 ± 0.41^{a}	1109	1114
xix.	13.48	**1,3,8-*p*-Menthatriene^{Mono} (**53**)	-	1.10 ± 0.12^{a}	3.83 ± 0.48^{b}	0.27 ± 0.12^{a}	0.84 ± 0.16^{a}	1115	1118
xx.	13.55	**Neo-allo-ocimene^{Mono} (**54**)	-	0.59 ± 0.25^{a}	1.97 ± 0.84^{a}	0.01 ± 0.07^{a}	0.34 ± 0.22^{a}	1119	1128
xxi.	14.05	**2-Methoxy-3-(1-methylpropyl)-pyrazine^{Pyr}	-	1.16 ± 0.28	-	-	-	1148	1156

		(**55**)							
xxii.	14.46	*Methyl salicylate^{Est} (**3**)	0.32 ± 0.23^{a}	1.26 ± 0.20^{a}	3.57 ± 0.49^{b}	0.60 ± 0.48^{a}	0.84 ± 0.15^{a}	1170	1176
xxiii.	14.57	*Decanal^{Ald} (**36**)	0.87 ± 0.27^{a}	-	7.29 ± 0.90^{b}	2.00 ± 0.80^{a}	1.78 ± 0.60^{a}	1177	1183
xxiv.	15.11	**Cumin aldehyde^{Ald} (**56**)	-	0.36 ± 0.08^{a}	1.84 ± 0.24^{a}	trace	0.22 ± 0.02^{a}	1212	1211
xxv.	15.85	***p*-Cymen-7-ol^{Alc} (**57**)	-	-	-	0.26 ± 0.19	-	1261	1267
xxvi.	15.92	*Tridecane^{Alk} (**5**)	trace	0.46 ± 0.12^{a}	2.12 ± 0.44^{b}	0.02 ± 0.07^{a}	0.18 ± 0.06^{a}	1234	1234
xxvii.	15.96	*Thymol$^{Mono-Alc}$ (**6**)	0.10 ± 0.05^{a}	0.29 ± 0.06^{a}	1.81 ± 0.21^{b}	trace	0.20 ± 0.08^{a}	1269	1272
xviii.	16.54	**δ- Elemene^{Sesq} (**58**)	1.18 ± 0.25^{a}	36.14 ± 9.66^{a}	203.87 ± 45.69^{b}	17.19 ± 8.06^{ab}	39.12 ± 11.89^{b}	1308	1313
xxix.	16.78	*Eugenol^{Alc} (**59**)	0.07 ± 0.03	-	-	-	-	1325	
xxx.	17.09	**α-Copaene^{Sesq} (**37**)	0.10 ± 0.01^{a}	0.35 ± 0.09^{a}	5.11 ± 0.94^{b}	0.08 ± 0.00^{a}	0.19 ± 0.08^{a}	1347	1351
xxxi.	17.28	**β-Elemene^{Sesq} (**60**)	0.15 ± 0.05^{a}	3.68 ± 1.15^{a}	26.50 ± 6.13^{b}	0.35 ± 0.17^{a}	3.86 ± 1.36^{b}	1361	1366
xxxii.	17.56	**α-Funebrene^{Sesq} (**61**)	-	0.23 ± 0.05	-	-	-	1381	
xxiii.	17.70	*Caryophyllene^{Sesq} (**13**)	2.86 ± 1.45^{a}	109.59 ± 34.07^{a}	534.77 ± 128.74^{b}	30.43 ± 13.87^{a}	113.63 ± 21.49^{b}	1391	1396
xxiv.	17.78	**γ- Elemene^{Sesq} (**62**)	0.14 ± 0.05^{a}	3.53 ± 1.36^{a}	23.03 ± 4.83^{b}	0.91 ± 0.58^{a}	3.25 ± 0.96^{b}	1397	1405
xxxv.	17.81	**Germacrene D^{Sesq} (**63**)	0.35 ± 0.03	trace	trace	trace	trace	1399	
xxvi.	17.97	**6,9- Guaiadiene^{Sesq} (**64**)	0.08 ± 0.04^{a}	5.49 ± 2.00^{a}	30.86 ± 7.83^{b}	1.23 ± 0.74^{a}	4.94 ± 1.27^{b}	1412	1418
xxvii.	18.06	**γ-Muurolene^{Sesq} (**65**)	0.67 ± 0.31^{a}	2.40 ± 1.33^{a}	17.31 ± 3.79^{b}	0.27 ± 0.10^{a}	2.04 ± 0.74^{b}	1419	
xviii.	18.14	*α- Humulene^{Sesq} (**66**)	0.67 ± 0.24^{a}	30.20 ± 11.29^{a}	150.44 ± 40.20^{b}	7.48 ± 4.46^{a}	28.99 ± 6.95^{b}	1425	1429
xxix.	18.24	**Dauca-5,8-diene^{Sesq} (**67**)	-	2.87 ± 1.48^{a}	17.70 ± 4.08^{b}	0.42 ± 0.22^{a}	2.07 ± 0.77^{a}	1432	
xl.	18.28	**β-Cubebene^{Sesq} (**68**)	0.12 ± 0.04^{a}	6.30 ± 2.77^{b}	8.50 ± 1.76^{b}	-	-	1435	
xli.	18.38	**Sibirene^{Sesq} (**69**)	0.32 ± 0.11^{a}	10.90 ± 5.49^{a}	54.86 ± 13.79^{b}	1.74 ± 1.46^{a}	9.06 ± 2.85^{b}	1443	
xlii.	18.45	**Germacrene B^{Sesq} (**70**)	-	0.25 ± 0.06^{a}	3.03 ± 0.60^{a}	0.12 ± 0.04^{a}	0.23 ± 0.05^{a}	1449	1456
xliii.	18.53	**α-Cubebene^{Sesq} (**71**)	0.17 ± 0.14^{a}	6.30 ± 2.77^{a}	31.51 ± 6.61^{b}	1.05 ± 0.72^{a}	4.96 ± 1.31^{b}	1455	
xliv.	18.57	**δ- Selinene^{Sesq} (**72**)	0.23 ± 0.09^{a}	7.59 ± 3.93^{a}	40.60 ± 10.26^{b}	0.52 ± 1.09^{a}	6.44 ± 2.09^{b}	1458	
xlv.	18.66	**α- Selinene^{Sesq} (**42**)	0.11 ± 0.03^{a}	1.29 ± 1.00^{a}	11.23 ± 2.86^{b}	0.31 ± 0.18^{a}	1.04 ± 0.52^{a}	1465	1469
xlvi.	18.69	**α-Gurjunene^{Sesq} (**73**)	0.08 ± 0.03^{a}	2.02 ± 0.01^{a}	7.85 ± 3.72^{b}	0.15 ± 0.07^{a}	0.62 ± 0.16^{a}	1467	1479
xlvii.	18.77	** (*Z*)-β-Guaiene^{Sesq} (**74**)	-	-	-	0.14 ± 0.00	-	1473	

xlviii.	18.87	**γ- Cadinene^{Sesq} (**75**)	0.04 ± 0.01^{a}	0.20 ± 0.04^{a}	4.17 ± 0.65^{b}	0.11 ± 0.03^{a}	0.27 ± 0.05^{b}	1481	
xlix.	18.95	**β-Vatirenene^{Sesq} (**76**)	-	-	2.77 ± 0.36	-	-	1487	
l.	18.97	**δ- Cadinene^{Sesq} (**77**)	0.08 ± 0.03^{a}	0.69 ± 0.49^{a}	8.50 ± 3.04^{b}	0.21 ± 0.08^{a}	0.60 ± 0.24^{a}	1489	
li.	19.05	**(*E*)-Cadina-1,4-diene^{Sesq} (**78**)	-	0.18 ± 0.03	-	-	0.14 ± 0.02	1495	
lii.	19.47	**Cyprene^{Sesq} (**79**)	0.08 ± 0.02^{a}	1.52 ± 1.04^{a}	11.48 ± 2.64^{b}	0.10 ± 0.03^{a}	0.95 ± 0.50^{a}	1529	
liii.	20.43	**Methyl dihydrojasmonate^{Jas} (**45**)	-	trace	-	0.08 ± 0.01	-	1606	1606
liv.	21.08	**Cadina-1(10),6,8-triene^{Sesq} (**80**)	-	trace	3.33 ± 0.48	-	-	1666	
lv.	21.22	**9,10-Neoisolongifolene^{Sesq} (**81**)	-	trace	trace	0.07 ± 0.01^{a}	0.16 ± 0.03^{a}	1678	
lvi.	21.87	**Guaiazulene^{Sesq} (**82**)	-	0.18 ± 0.02^{a}	2.57 ± 0.27^{b}	0.07 ± 0.02^{a}	0.21 ± 0.07^{a}	1751	
lvii.	23.52	*Hexadecanoic acid^{FA} (**83**)	-	0.08 ± 0.01	-	trace	-	1916	
lviii.	25.25	**6-Octadecenoic acid^{FA} (**84**)	-	trace	-	trace	-	2102	
lix.	25.48	**(*Z, Z*)-9,12-Octadecadienoic acid^{FA} (**85**)	-	trace	-	trace	-	2127	

Alc= Alcohol; Ald= Aldehyde; Alka=Alkanes; Est= Esters; FA=Fatty acids; Jas= Jasmonate; Mono=Monoterpenes; Pyr= Pyrazine and Sesq=Sesquiterpenes.

DPI; days post infection. *Compound whose identity was established based on comparison of retention time and mass spectra data with authentic standard. **Compound identified tentatively based on library data, calculated RI values and comparison to literature. RI^{calc} = Retention index relative to C_8-C_{23} *n*- alkanes of a HP-5 MS column. RI^{lit} = Retention index obtained from literature (Hassaballa *et al.*, 2020; Kihika *et al*., 2020). Means with different lower-case letters on the same row are significantly different from each other (ANOVA followed by SNK post hoc test and Kruskal-Wallis test followed by the post hoc Dunn's test; $P < 0.05$, n = 3).

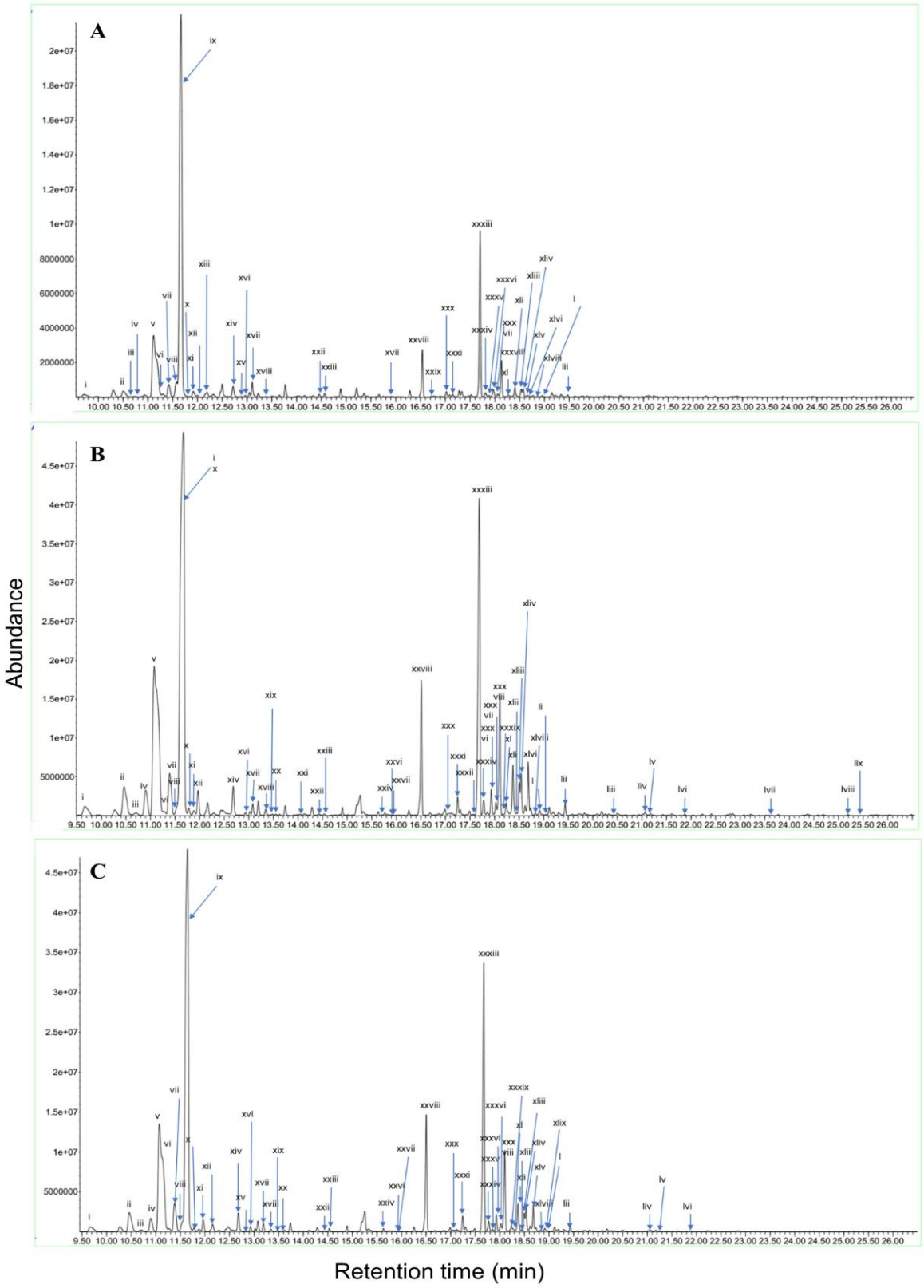

Figure 4.5: Gas chromatography-mass spectrometry profiles of leaf volatiles collected from healthy tomato and *M. incognita*-infected tomato. **(A)** Healthy tomato and *M. incognita*-infected tomato ('Cal-J') plants at 2 DPI **(B)** and 7 DPI **(C)** by SPME. DPI; days post infection.

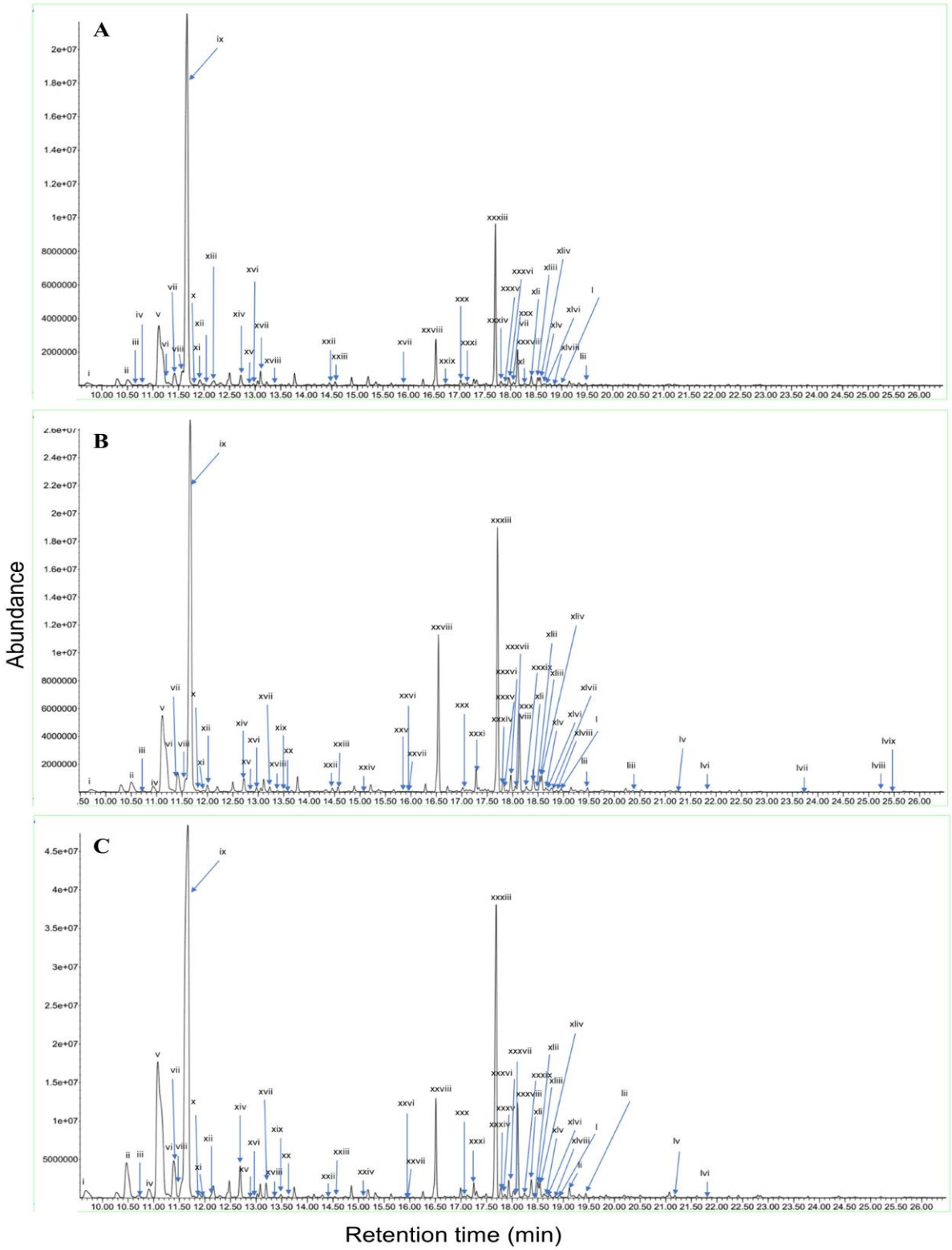

Figure 4.6: Gas chromatography-mass spectrometry profiles of leaf volatiles collected from healthy and *M. javanica*-infected tomato. **(A)** Healthy tomato and *M. javanica*-infected tomato ('Cal-J') plants at 2 DPI **(B)** and 7 DPI **(C)** by SPME. DPI; days post infection.

Quantitatively, there were statistical variations between the healthy and infected plants at 7-DPI by the two species for the different monoterpenes (Table 4.3). However, there were compounds that showed significant differences at 7-DPI for tomato infected with *M. incognita* but not *M. javanica*. These include decanal (**36**), nonanal (**35**), tridecane (**5**), α-copaene (**37**), α-gurjenene (**73**), cyperene (**79**) and guaiazulene (**82**). Furthermore, the fatty acids hexadecanoic acid (**83**), 6-octadecenoic acid (**84**) and (*Z, Z*)-9,12-octadecadienoic acid (**85**) were only detected in trace amounts in the infected plants at 2-DPI. In contrast, some compounds were not significantly different in the volatiles of healthy and infected plants, and these include neo-allo-ocimene (**54**), cumin aldehyde (**56**), germacrene B (**63**) and 9,10-neoisolongifolene (**81**).

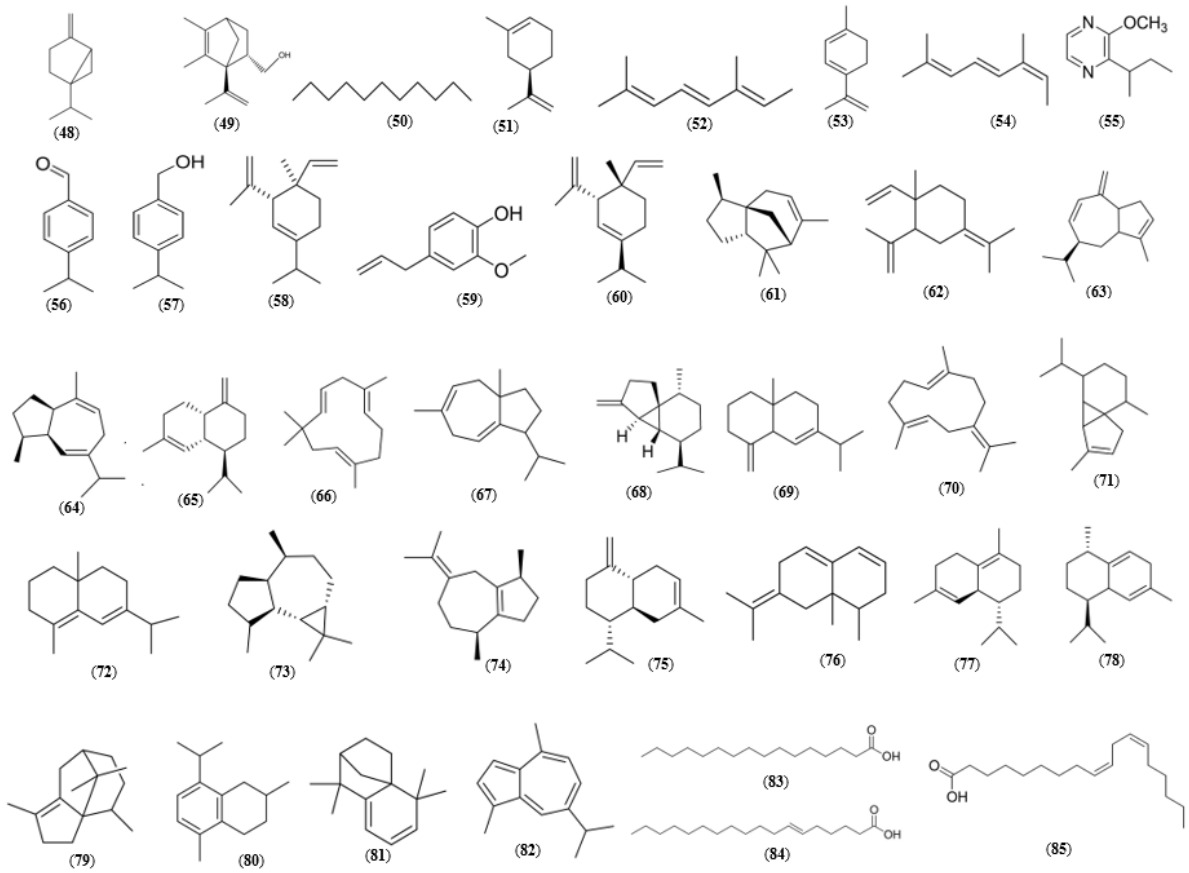

Sedentary and endoparasitic nematodes such as the RKNs have a complex interaction with the host plants (Escudero *et al*., 2014). Once the J2 locates the host plant, they travel between the

cells and inject a wide range of effectors including proteins, peptides and other small molecules into the host roots (Haegeman *et al*., 2012). This causes changes in the ratio and composition of the released plant compounds, which in turn influence the activity of pathogenic and beneficial microbes in the rhizosphere (Escudero *et al.*, 2014; Kihika *et al*., 2020) The findings from the current study show that systemic responses of tomato to RKN infection by both *M. javanica* and *M. incognita* induced changes in the foliar volatile chemistry. However, quantitative variations of VOCs were detected in nematode-infected and healthy plants between the two nematode species. The results also show that qualitatively more compounds were present in infected plants than in the healthy plants. This suggests that RKN infection in the plant roots trigger biosynthesis and release of different plant compounds from plant shoots, either causing an increase or decrease in the amounts of volatiles.

Previously, a number of transcriptomic and proteomic studies were carried out to enhance the understanding on plant-nematode interactions (Kumari *et al.*, 2016; Ha *et al.*, 2017; Ling *et al.*, 2017) and their observations led to the proposition that nematode infection may activate changes in the primary and secondary metabolites. Subsequent metabolomic studies demonstrated that *M. incognita* infection in tomato caused an increase in the levels of sugars, amino acids, organic acids and phosphorylated metabolites, in tomato 60 days post infection (Eloh *et al.*, 2016). Another study found that tomato infected with *M. javanica* led to increase in aromatic compounds even though that study did not identify the specific compounds (Escudero *et al.*, 2014). Volatile organic compounds such as the terpenes β-phellandrene (**29**), α-terpinene (**27**), β-caryophyllene (**13**), and α-humulene (**66**) were also shown to reduce in amounts following *M. incognita* infection when chemical analysis was carried out at 20 days post infection (Arce *et al*., 2017). This shows that the effect of RKN parasitism on plant volatile chemistry varies during

different stages of the entire life cycle since these same compounds were quantitatively more in the current study which investigated earlier stages (2-7 DPI) of RKN infection. Future studies should evaluate the concurrent changes in gene expression, phytohormonal levels, and VOCs profiles during the different stages of the RKN life cycle in order to determine the resultant inter-species ecological above-ground interactions.

Importantly, the changes in odor profiles of the foliar VOCs occasioned by RKN infection influence the interactions between insect pests above-ground since these associations are driven by the ability of the insects to perceive plant odors for host location, oviposition and feeding (Bruce and Pickett, 2011; Wondafrash *et al*., 2013). Previously, root parasitism by *M. incognita* affected the oviposition preferences of *T. absoluta* and this was associated with the qualitative and quantitative changes in β-phellandrene (**29**), α-terpinene (**27**), β-caryophyllene (**13**), and α-humulene (**66**) which are physiologically important compounds (Arce *et al*., 2017). The terpenes, α-pinene (**1**), (*E*)-β-caryophyllene (**13**), α-humulene (**66**) were previously reported to attract the whitefly, *Trialeurodes vaporariorum*, in tomato and eggplants (Darshanee *et al.*, 2017). In another study, the melon fly, *Zeugodacus curcubitae* expanded its host plants from cucumber, its natural host, to tomato plants and this was attributed to shared host finding volatiles, and α-phellandrene (**26**) and β-phellandrene (**29**) were identified as important kairomonal signals of the melon fly. Thus, this study agrees with these previous findings showing that these compounds play multiple roles in the biology/ecology of different insects as attractants.

4.3.2 Determination of leaf volatiles contributing to dissimilarities between healthy and RKN-infected tomato.

The composition and ratio of volatiles was analyzed using one-way ANOSIM based on the Bray-Curtis dissimilarity. The results showed significant differences between the healthy and RKN-infected plants at 2 DPI (Figure 4.7A; R = 0.75, p = 0.0007) and 7 DPI (Figure 4.7B; R = 0.60, p = 0.004). The order of contribution of VOCs to the dissimilarity trends between healthy and infected plants at 2 DPI were β-phellandrene (**9**) (34.6 %), 2-δ-Carene (**25**) (19.1 %), (*E*)-caryophyllene (**13**) (13.1 %), δ- elemene (**58**) (4.5 %) and α- humulene (**66**) (4 %) (Figure 4.7C). Clustering of volatiles profiles of the diverse stages of infection by non-metric multidimensional scaling, sowed that β-phellandrene (**29**) contributed more to the dissimilarity (33.9 %) between the healthy and RKN-infected plants at 7 DPI followed by 2-δ-Carene (**25**) (17.6 %), caryophyllene (**13**) (15.7 %), δ- elemene (**58**) (5.2 %) and α- humulene (**66**) (4.6%) (Figure 4.7D).

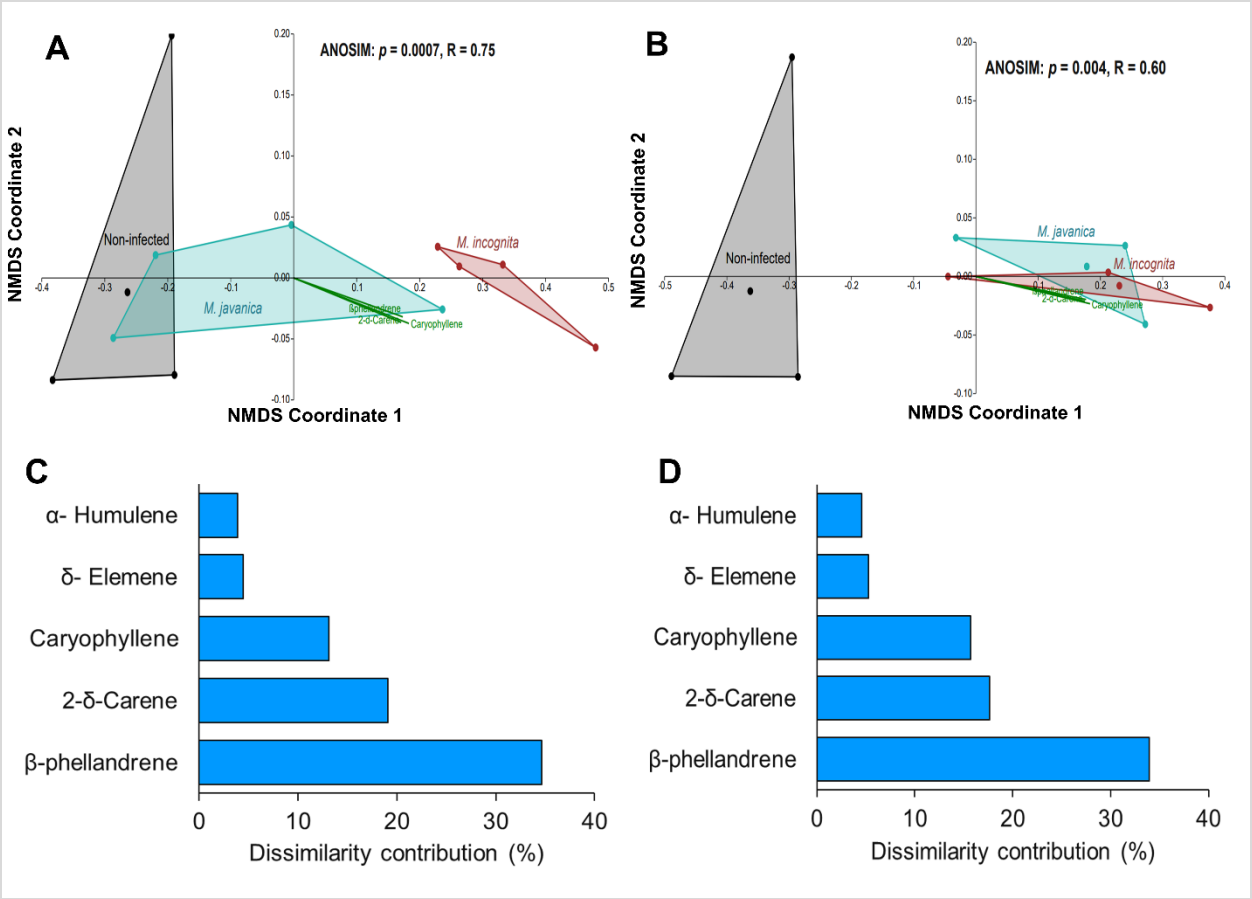

Figure 4.7: Non-metric multidimensional scaling plot (NMDS) showing the clustering of volatile organic compounds of healthy and RKN-infected tomato at 2-DPI (**A**) and 7-DPI (**B**). Histogram depicting the contribution of the five most important volatiles to the differentiation of the different stages of infection (**C**) 2-DPI and (**D**) 7-DPI, based on Analysis of similarities (ANOSIM), DPI; days post infection.

The quantitative differences of the detected compounds at the varied time points of infection are shown in Table 4.3. The mean concentrations of the VOCs contributing to the dissimilarity trends from healthy and *M. javanica* infected plants were significantly different for 2-δ-carene (**25**) ($F_{(2,6)} = 27$, $P < 0.001$), β-phellandrene (**29**) ($F_{(2,6)} = 43.11$, $P < 0.0001$), δ- elemene (**58**) ($H = 6.49$, df = 2, $P < 0.05$), caryophyllene (**13**) ($F_{(2,6)} = 15.2$, $P < 0.001$), and α-humulene (**66**) ($H = 6.48$, df = 2, $P < 0.05$) (Figure 4.8). Additionally, the amounts of the VOCs increased by 5-, 4-, 15-, 11-, and 11-fold at 2 DPI and 12-, 7-, 33-, 40- and 43-fold at 7 DPI for 2-δ-carene (**25**), β-phellandrene (**29**), δ- elemene (**58**), caryophyllene (**13**), and α-humulene (**66**), respectively.

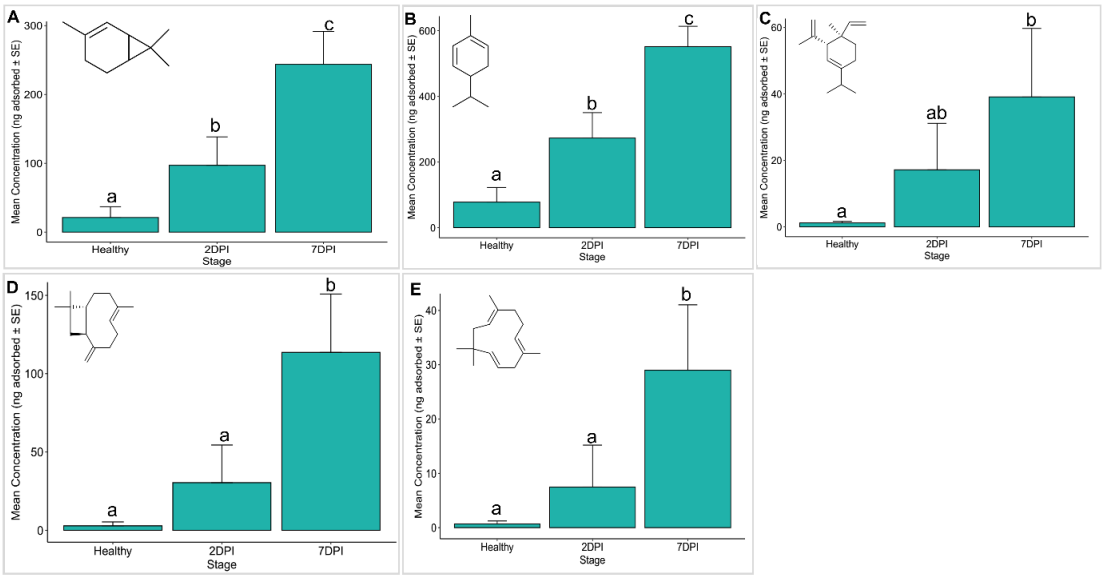

Figure 4.8: Mean concentration of the aerial volatile organic compounds that contributed the differentiation of healthy and *M. javanica*-infected tomato. Bar plots of VOCs from 2-δ-Carene (**5**) (**A**), β-phellandrene (**9**) (**B**), δ- elemene (**40**) (**C**), caryophyllene (**21**) (**D**), and α- humulene (**48**) (**E**) (ANOVA followed by SNK post hoc test and Kruskal-Wallis test followed by the post hoc Dunn's test; $P < 0.05$, n = 3).

Similarly, the mean concentrations of the VOCs contributing to the dissimilarity trends from healthy and *M. incognita* infected plants varied significantly for 2-δ-carene (**25**) (H = 7.2, df = 2, $P < 0.05$), β-phellandrene (**29**) ($F_{(2,6)}$ = 24.93, $P < 0.01$), δ- elemene (**58**); (H = 7.2, df = 2, $P <$ 0.05), caryophyllene (**13**) (H = 7.2, $P < 0.05$), and α-humulene (**66**) (H= 7.3, df = 2, $P < 0.05$) (Figure 4.9). Additionally, the amounts of the VOCs increased by 8-, 7-, 31-, 38-, and 45-fold at 2 DPI and 31-, 20-, 173-, 186- and 225-fold at 7 DPI for 2-δ-carene (**25**), β-phellandrene (**29**), δ-elemene (**58**), caryophyllene (**13**), and α-humulene (**66**), respectively.

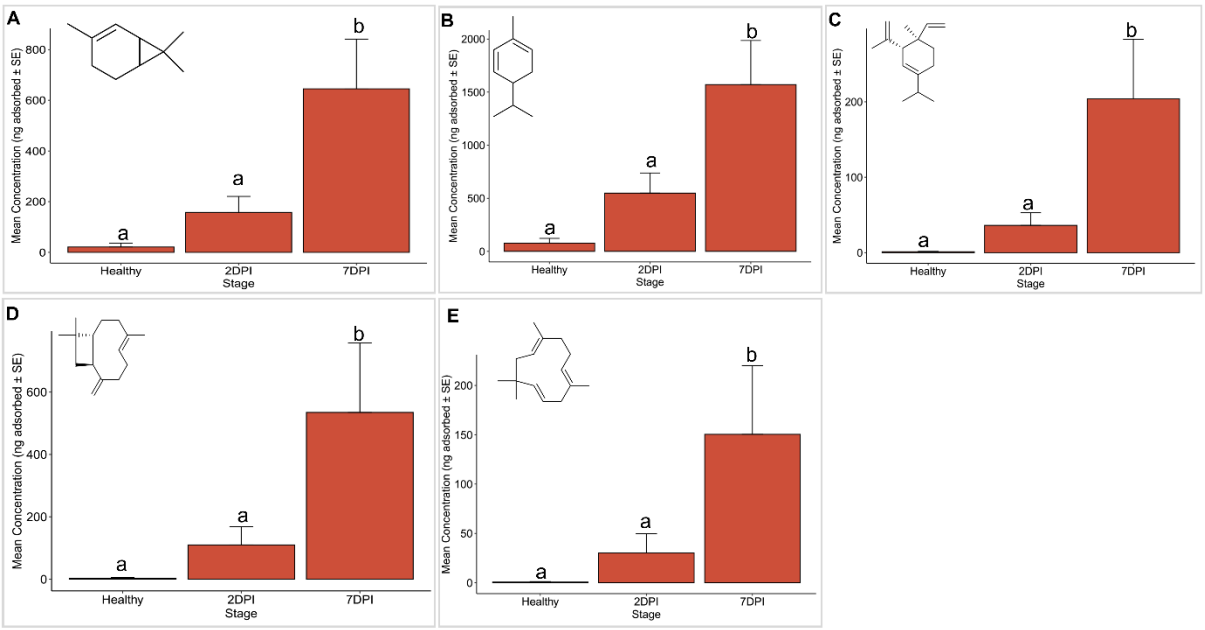

Figure 4.9: Mean concentration of aerial volatile organic compounds that contributed to the differentiation of healthy and *M. incognita*-infected tomato. Bar plots of VOCs from 2-δ-Carene (**25**) (**A**), β-phellandrene (**29**) (**B**), δ- elemene (**58**) (**C**), caryophyllene (**13**) (**D**), and α- humulene (**66**) (**E**) (ANOVA followed by SNK post hoc test and Kruskal-Wallis test followed by the post hoc Dunn's test; $P < 0.05$, n = 3).

However, pairwise comparison between the mean concentrations of the VOCs that contributed to dissimilarity trends produced in response to *M. incognita*- and *M. javanica* -infected plants did not differ significantly at 2 DPI (carene (**25**); t = -1.40, df = 3.47, $P > 0.05$, β-phellandrene (**29**); t = -2.33, df = 2.65, $P > 0.05$, δ- elemene (**58**); t = -1.51, df = 3.88, $P > 0.05$, caryophyllene (**13**); t = -2.15, df = 2.65, $P > 0.05$, and α-humulene (**66**); t = -1.87, df = 2.61, $P > 0.05$) and 7-DPI (carene (**25**); t = -3.44, df = 2.24, $P > 0.05$, β-phellandrene (**29**); t = -4.21, df = 2.09, $P > 0.05$, δ-elemene (**58**); t = -3.49, df = 2.27, $P > 0.05$, caryophyllene (**13**); t = -3.23, df = 2.11, $P > 0.05$, and α-humulene (**66**); t = -2.98, df = 2.12, $P > 0.05$).

These results demonstrated that RKN-infection played a crucial role in altering the above-ground plant volatile emissions since NMDS analysis showed a clear separation of RKN-infected plants from healthy plants. Additionally, quantitative differences were evident in 2-δ-carene (**25**),

β-phellandrene (**29**), δ- elemene (**58**), caryophyllene (**13**), and α- humulene (**66**) emissions, compounds that contributed significantly to the dissimilarity trends of nematode-infested plants compared to healthy plants irrespective of the nematode-species. Some of these compounds are reported to have an important role in indirect defense by attracting parasitoids as they are also produced by tomato in response to above-ground pest infestation as herbivore-induced plant volatiles (De Backer et al., 2015; Arce *et al*., 2017; Ayelo *et al.*, , 2021). In these interactions, level of infestation was important for generalist parasitoids as this influenced the quality and quantity of volatile emissions.

Some of the tomato-pest-parasitoid interactions involved high infestation density of the whitefly, *Trialeurodes vaporariorum*, on tomato which led to the release of β-elemene and (*E*)-caryophyllene which were not detected in low infestation density and these attracted the parasitoid, *Encarsia Formosa* (Ayelo *et al.*, 2021). Terpenes such as β-phellandrene (**29**), 2-carene (**25**), α-pinene (**1**), β -caryophyllene (**13**), and α-phellandrene (**26**) were significantly increased in high density *T. absoluta* -infested plants and these attracted the generalist predator, *Macrolophus pygmaeus*(De Backer *et al*., 2015; Arce *et al*., 2017). Qualitative similarities were also observed in tomato infested with the whiteflies, *T. vaporariorum* and *Bemisia tabaci* and the aphid *Myzus persicae*, resulting in increased production of mono- and sesqui-terpenes (Silva *et al*., 2017). These findings compare with other findings showing that tomato plants may have a generic response to both above- and below-ground intruders by production of terpene compounds.

4.4 Response of *M. javanica* second-stage juveniles to volatiles associated with RKN-infection.

The available compounds, (β-pinene (**24**), (+) - (2)-carene (**25**), α-phellandrene (**26**), β-phellandrene (**29**), MeSA (**3**) and, MeDiJA (**45**)), were tested in bioassays and the findings showed significant differences at the diverse time points of root infection. The individual compounds and a blend of the six components tested against a solvent control elicited dose-dependent response in the J2 (Figure 4.10). MeSA (**3**) was preferred by the nematodes at all the tested doses (Table 4.4) whereas MeDiJA (**45**) was unattractive at 2.75µg but not at 5.5µg and 11µg (Table 4.4). A different experiment tested the importance of MeSA (**3**) and MeDiJA (**45**) in the infected and non-infected plants respectively. The findings showed that nematodes significantly preferred the roots of the plant at 2-DPI spiked with MeSA (**3**) at all the doses but the preference of J2 to the roots of the healthy plant diminished when the roots of a healthy plant were spiked with MeDiJA (**45**) (Table 4.4; Figure 4.10).

Table 4.4: Chi-square analysis for test of proportions of the nematode responses to compounds

Treatment	Dose (µg)	Proportions and chi-square analysis
MeSA vs control	2.75	86%, $\chi^2 = 203.98$, df = 1
	5.5	75%, $\chi^2 = 61.77$, df = 1
	11	80%, $\chi^2 = 100.09$, df = 1
MeDiJA vs control	2.75	75%, $\chi^2 = 37.33$, df = 1
	5.5	54%, $\chi^2 = 1.62$, df = 1
	11	53%, $\chi^2 = 0.32$, df = 1
2 DPI + MeSA vs control	2.75	87%, $\chi^2 = 126.68$, df = 1
	5.5	74%, $\chi^2 = 115.43$, df = 1
	11	83%, $\chi^2 = 242.42$, df = 1
Healthy plant + MeDiJA vs control	2.75	59%, $\chi^2 = 21.39$, df = 1
	5.5	39%, $\chi^2 = 22.873$, df = 1
	11	58%, $\chi 2 = 6.0036$, df = 1

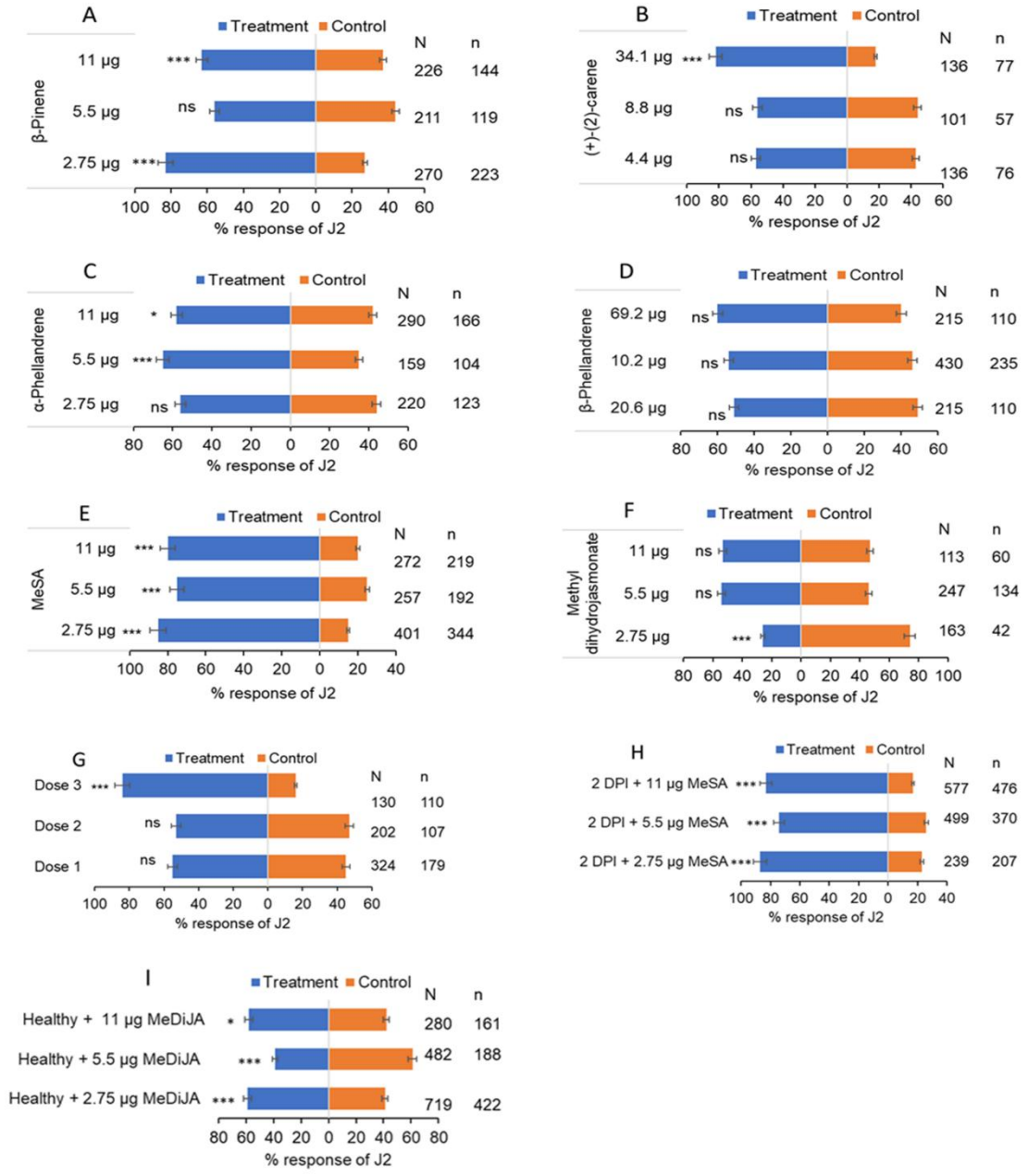

Figure 4.10: Response of *Meloidogyne javanica* infective juveniles (J2) to compounds associated with RKN infection at different doses. (**A**) β-pinene, (**B**) (+)-(2)-carene, (**C**) α-phellandrene, (**D**) β-phellandrene, (**E**) Methyl salicylate (MeSA), (**F**) methyl dihydrojasmonate, and (**G**) 6-component blend vs. sand control. (**H**) 2-DPI plant spiked with MeSA vs. 2-DPI plant (control), (**I**) healthy tomato spiked with different doses of MeDiJA vs healthy tomato (control). (N corresponds to the total number of responding J2 while n is the number of J2 corresponding to a given treatment. The level of significance is indicated by: ***$P < 0.001$, $^{*}P < 0.05$, ns = not significant).

The bioactivity of MeSA (**3**) in attracting J2 appeared to be concentration-dependent since the decreased levels of MeSA (**3**) at 2-DPI concurred with avoidance behavior, but when the plant was spiked with MeSA (**3**), the roots became more attractive again. While the diminished amount of MeSA (**3**) at 2-DPI was not statistically significant in our analyses, the drop appeared to have ecological significance since it elicited an avoidance response in J2. Perhaps, the other compounds associated with RKN-infection interfere or mask this significant kairomonal signal. The volatile compounds that were not tested in this study may also contribute to the avoidance response observed at 2-DPI. However, this defense response appears not to be sustained long enough to deter further nematode attack. Previous studies have demonstrated a concentration-dependent attraction with other compounds. For example, ethylene (ET (**19**)) signaling was reported to modulate the attractiveness of *M. javanica, M. halpa* and *M. incognita* (Fudali *et al.*, 2013; Čepulytė *et al*., 2018). Specifically, the roots of wild types of Arabidopsis and tomato that constitutively overproduced ET (**19**) were less preferred by the J2 of these nematode species while those with diminished ET (**19**) synthesis were more preferred. The high amounts of ethylene may be associated with diminished food reserves for the J2 since a previous study showed that ET (**19**) increased during the second week of *M. javanica*-infection in tomato (Glazer *et al.*, 1983). In the same way, the results of this study may indicate the significance of SA (**17**) signaling in the attractiveness of tomato roots. These findings are consistent with previous studies which reported that MeSA (**3**) was detected in tomato and pepper as an important kairomonal signal for *M. incognita* J2 (Kihika *et al.*, 2017; Murungi *et al.*, 2018). The exogenous application of JA (**18**) and MeJA (**46**) in tomato shoots was reported to induce systemic root defenses against RKNs attack (Cooper *et al*., 2005; Fan *et al*., 2015). Additionally, plants treated with JA(**18**) are reported to boost Mi-mediated resistance at high temperatures

(Cooper *et al*., 2005) demonstrating that jasmonates have an important role in protecting crops against RKNs.

Notably, β-phellandrene (**29**), which was the most abundant compound detected in the root volatiles of the healthy tomato plant, decreased two-fold at 2-DPI and increased three-fold at 7-DPI. Nevertheless, in the soil olfactometer assays, this monoterpene had a neutral effect on the J2 at all the doses tested (Table 4.5; Figure 4.10). The chirality of β-phellandrene (**29**) produced by the tomato plants was not determined in this study, and in the behavioral assays only the (*S*)-(+)-enantiomer was tested. These findings indicate that β-phellandrene (**29**) and other root volatiles may influence the attraction of J2 as background signals, however this warrants further research. Conversely, the dose of 34.1 µg (+) - (2)-carene (**25**) consistent with the 7-DPI was significantly preferred by J2 (Table 4.5), while the lower doses corresponding to 0-DPI and 2-DPI, respectively, were weakly attractive (Table 4.5; Figure 4.10).

Table 4.5: Chi-square analysis for test of proportions of the nematode responses to monoterpenes and a 6-component blend

Treatment	Dose (µg)	Proportions and chi-square analysis
β-phellandrene vs control	20.6	51%, $\chi^2 = 0.07$, df = 1
	10.2	55%, $\chi^2 = 3.54$, df = 1
	69.2	60%, $\chi^2 = 11.60$, df = 1
(+)-(2)-carene vs control	4.4	57%, $\chi^2 = 2.13$, df = 1
	8.8	56%, $\chi^2 = 1.43$, df = 1
	34.1	82%, $\chi^2 = 59.38$, df = 1
β-pinene vs control	2.75	83%, $\chi^2 = 113.43$, df = 1
	5.5	56%, $\chi^2 = 3.20$, df = 1
	11	63%, $\chi^2 = 16.47$, df = 1
α-phellandrene vs control	2.75	56%, $\chi^2 = 2.84$, df = 1
	5.5	65%, $\chi^2 = 14.49$, df = 1
	11	57%, $\chi^2 = 5.79$, df = 1
6-component blend	Dose 1	55%, $\chi^2 = 3.15$, df = 1
	Dose 2	53%, $\chi^2 = 0.59$, df = 1
	Dose 3	84%, $\chi^2 = 60.93$, df = 1

Other compounds differentially attracted J2 and these included the monoterpenes, β-pinene (**24**) and α-phellandrene (**26**). The infective juveniles significantly preferred β-Pinene (**24**) at doses of 2.75 µg and 11 µg, but not at the dose of 5.5 µg that corresponded to the infected plants at 2-DPI (Table 4.5; Figure 4.10). The nematodes were more attracted to α-phellandrene (**26**) at doses of 5.5 µg and 11 µg, than at 2.75 µg (Table 4.5; Figure 4.10). The chirality of the β-pinene (**24**) and α-phellandrene (**26**) released by the tomato roots was not established and only the (1S)-(-)- and (R)-(-)-enantiomers, respectively, were tested in the olfactometer assays. In previous studies that investigated interactions in the rhizosphere and above-ground, β-pinene (**24**) was identified as a herbivore induced plant volatile that attracted the citrus root nematode *Tylenchulus semipenetrans* (Ali *et al.*, 2011) and constitutively attracted the bark beetle, *Hylastus nigrinus.*(Johnson *et al.*, 2012) The monoterpenes, α-pinene (**1**), limonene (**2**) and sabinene (**48**) have previously been identified in the root volatiles of pepper and tomato and also as signals contributing to the attraction of *M. incognita* J2 (Kihika *et al.*, 2017; Murungi *et al.*, 2018). The blend of all six components was attractive to J2 at the highest dose corresponding to 7-DPI, but not at doses corresponding to 0-DPI or 2-DPI (Table 4.5; Figure 4.10). This may have been influenced by the dose of (+)-(2)-carene corresponding to 7-DPI (34.1 µg) that was also highly attractive to the J2 when tested individually.

The monoterpenes appear to have differential attraction effect which is plausible since they are common in numerous host plant species (Degenhardt *et al.*, 2010; Kihika *et al.*, 2017; Murungi *et al.*, 2018) of these polyphagous nematodes. Nevertheless, the root plant volatiles stimulated more J2 responses than the individual compounds tested alone or in the 6-component blend, suggesting that other yet-to-be identified compounds contribute to J2 attraction. This indicates

that J2 chemoreception is attuned to determine a suitable host that will best support its survival and reproduction.

4.5 Blackjack reduces the prevalence of root-knot infestation in tomato and black nightshade

The number of galls and egg masses per root system was counted and used to determine the galling and egg mass indices to assess the infection and reproduction of root-knot nematodes on a plant, as previously reported. Galling and egg mass indices were done using the scale: 0 = no galls or no egg masses, 1 = 1 to 2, 2 = 3 to 10, 3 = 11 to 30, 4 = 31 to 100, and 5 = more than 100 galls or more than 100 egg masses per plant (Taylor and Sasser, 1978; Kihika *et al.*, 2017). Results from the pot experiments showed a 3- to 9-fold significant reduction in nematode infection on tomato ($F_{(2,57)} = 55.46$, $P < 0.0001$) and 3- to 4-fold reduction in black nightshade ($F_{(2,57)} = 61.04$, $P < 0.0001$) when blackjack was present in the intercrop and drip experiments compared to the control (Table 4.6). Additionally, galling and egg mass indices showed a similar trend of reduced root-knot disease incidence in tomato ($H = 36.84$, df = 2, $P < 0.0001$) and black night shade ($H = 27.11$, df = 2, $P < 0.0001$). When investigating whether Blackjack had a different effect on tomato and black nightshade, galling ($t = 4.72$, df = 15.81, $P < 0.001$) and reproduction ($t = 4.11$, df = 15.25, $P < 0.001$) of RKN varied significantly in the intercrop experiment but not in the drip and control experiments; (galling: control; $t = 0.10$, df = 16.87, $P > 0.05$ and drip; $t = -1.54$, df = 15.09, $P > 0.05$ and reproduction: control; $t = -0.01$, df = 16.36, $P > 0.05$), drip; $t = -1.59$, df = 17.17, $P > 0.05$) (Figure 4.11, Table 4.6).

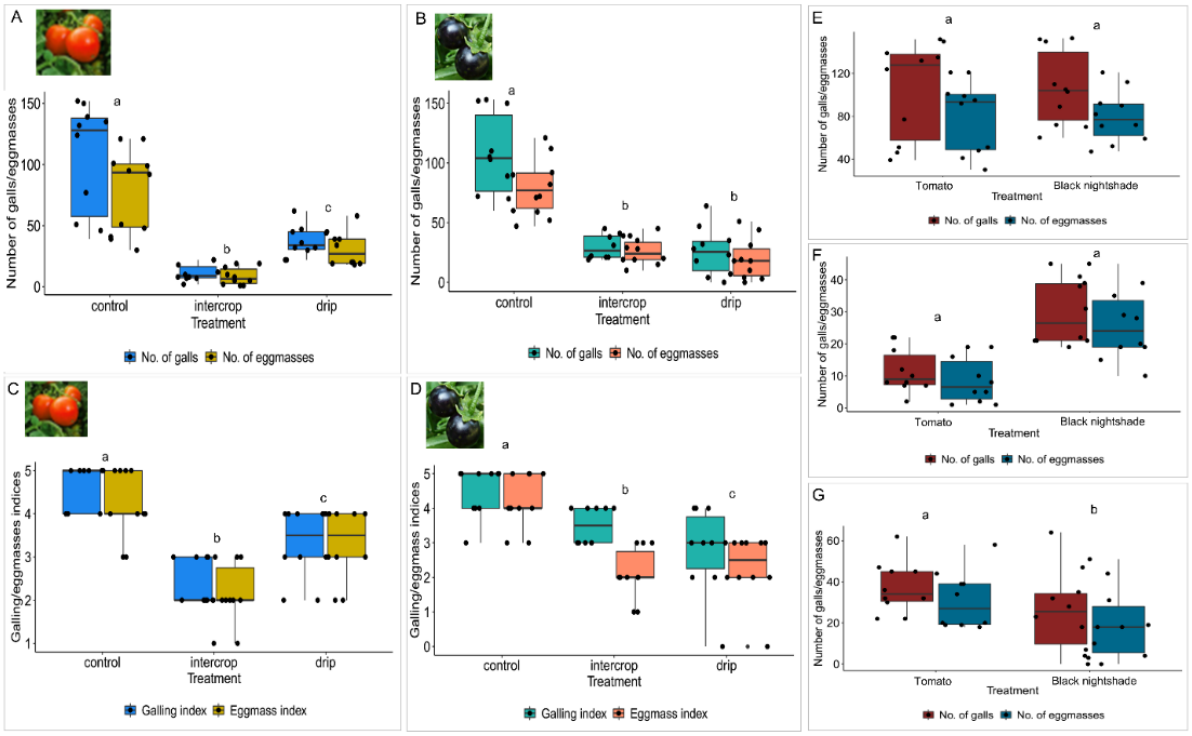

Figure 4.11: Effect of blackjack root exudates in reducing the infection of root knot nematode in susceptible crops. (**A**) and (**B**) Boxplots are means (± SEM) of number of galls and egg masses across the different treatments for tomato and black nightshade, respectively (ANOVA test followed by SNK's *post-hoc* test, $P < 0.05$, n = 10). (**C**) and (**D**) Box plots are means (± SEM) of galling and egg mass indices across the different treatments for tomato and black nightshade, respectively (Kruskal-Wallis test followed by Dunn's *post-hoc* test, $P < 0.05$, n = 10). (**E**) to (**G**) Box plots are means (± SEM) of number of galls and egg masses showing pairwise comparison of tomato and black nightshade for the control (**E**), intercrop (**F**) and drip (**G**) experiments (Unpaired *t*-test, $P < 0.05$, n = 10). Treatments with different lower-case letters are significantly different from each other.

Table 4.6: Mean number of galls (galling) and egg masses (reproduction) in tomato and black nightshade.

		Mean ± SE (fold reduction)	
	Treatment	Tomato	Black nightshade
Galling	control	104.5 ± 14.5[a]	106.4 ± 11.1[a]
	intercrop	11.6 ± 2.2 (9)[a]	29.8 ± 3.2 (4)[b]
	drip	37.3 ± 3.9 (3)[a]	25.8 ± 6.3 (4)[a]
Reproduction	control	79.9 ± 10.8[a]	79.8 ± 7.8[a]
	intercrop	8.6 ± 2.3 (9)[a]	25.9 ± 3.6 (3)[b]
	drip	31.0 ± 4.4 (3)[a]	19.8 ± 5.5 (4)[a]

Means with different letters in the same row are significantly different (Unpaired *t*-test, $P < 0.05$, n = 10). Fold reduction indicates the diminished root-knot infestation in intercrop and drip pot experiments when compared to the control.

Results from the PCoA showed that the PC1 and PC2 accounted for 99.2% and 0.8% of the variance between the treatments, respectively. As shown in Figure 4.12, clustering was based on the treatments; the control experiments of tomato and black nightshade group to the right while the intercrop and drip experiments and clustered to the left of the plot.

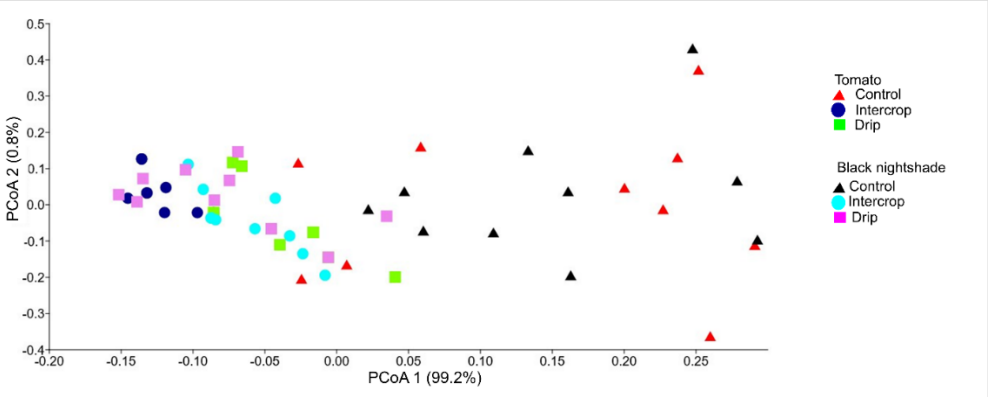

Figure 4.12: Principal coordinate analysis (PCoA) plot showing clustering of the different treatments of the pot experiments.

The results from the pot experiments showed that tomato and black nightshade supported the development and reproduction of *M. incognita*, which is consistent with previous reports (Nchore *et al.*, 2012; Mwangi *et al.*, 2017), demonstrating that both crops are highly susceptible to RKN infection. This suggests that the rhizospheres of these plants provide a favorable environment that facilitates detection of chemical cues by *M. incognita* for egg hatching, successful host plant location by the infective juveniles, and their growth and reproduction. However, using the Asteraceae plant, *Bidens pilosa*, as an intercrop companion crop caused reduction in the prevalence of the root-knot infestation in the two susceptible solanaceous crops as indicated by the lower rate of galling and production of egg masses.

With the drip experiments exhibiting the same trends as the intercropping experiments, the results suggest direct or indirect effects of the root chemical components of blackjack on the

different life stages of *M. incognita*. The root exudate of blackjack may directly affect egg hatching of RKNs or interfere with J2 behavior by disrupting its chemoreception of host chemical signals and cause nematicidal activity. In addition, the root exudates of blackjack may indirectly impact nematode behavior by influencing the composition of the microbial community in the rhizosphere that have different modes of action against the nematodes through direct parasitism, production of nematicidal compounds and lytic enzymes (Goodell and Ferris, 1989; Hallman and Sikora, 1996; Kerry, 2000; Migunova and Sasanelli, 2021), but this would require additional research.

4.6 *In vitro* experiments demonstrate the influence of root exudates on egg hatching and mortality of *Meloidogyne incognita*

The root exudates of tomato and black nightshade stimulated varied egg hatching at the different concentrations when tested individually and in combination with the root exudate of blackjack. The root exudates of tomato significantly inhibited egg hatching (χ^2 = 32.96, df = 4, $P < 0.001$) at all the concentrations when tested alone or combined with the root exudates of blackjack (χ^2 = 135.19, df = 4, $P < 0.0001$) compared to controls. A similar trend was observed for the root exudates of black nightshade tested alone (χ^2 = 15.12, df = 4, $P < 0.0001$) and when combined with blackjack (χ^2 = 118.18, df = 4, $P < 0.0001$). The percent inhibition in egg hatching of the root exudates of blackjack was significantly higher (χ^2 = 243.77, df = 4, $P < 0.0001$) at all the concentrations tested compared to the control. Interestingly, the root exudates of tomato had a lower egg hatching inhibition effect (16-28%) when tested alone (Figure 4.13), but when combined with blackjack the egg hatching inhibition effect increased by 4-fold (65 – 99%). The root exudate from black nightshade elicited a similar low inhibition effect (9-38%) at the concentrations 1 and 2.5 mg/ml but at 5 mg/ml the inhibition effect was 83% (Figure 4.13).

When black nightshade was combined with blackjack, the inhibition effect increased by 1.2- 9-fold (85-98%) at 1-5 mg/ml.

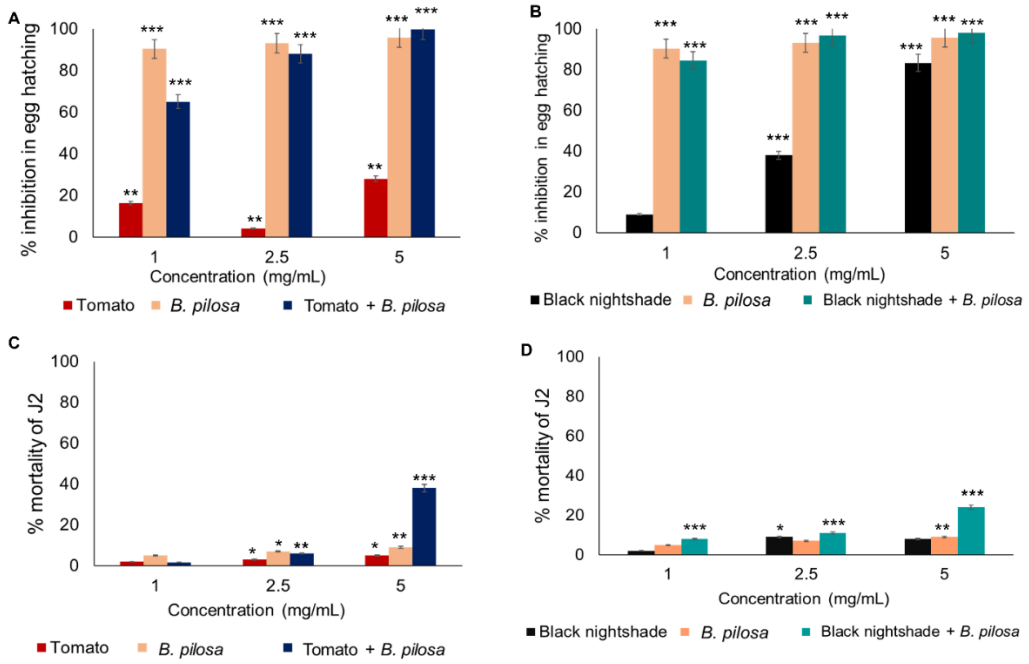

Figure 4.13: Egg hatching of *M. incognita* in the root exudates of blackjack with tomato (**A**) and black nightshade (**B**) Percent mortality of J2 in the root exudates of tomato (**C**) and black nightshade (**D**) (GLM with binomial distribution followed by Tukey *post-hoc* mean separation test, $P < 0.05$, n = 12). The level of significance is indicated by: ***$P < 0.0001$, **$P < 0.001$, *$P < 0.05$.

In the *in vitro* mortality assays, the root exudates of tomato caused significant mortality ($\chi^2 = 45.77$, df = 4, $P < 0.001$) when tested alone or when combined with the root exudates of blackjack ($\chi^2 = 48.1$, df = 4, $P < 0.0001$) relative to a control. Similarly, the root exudates of black nightshade caused significantly higher mortality when tested alone ($\chi^2 = 46.78$, df = 4, $P < 0.0001$) and when combined with blackjack ($\chi^2 = 46.80$, df = 4, $P < 0.0001$). The percent mortality of the root exudates of blackjack was significantly higher ($\chi^2 = 46.02$, df = 4, $P < 0.0001$) than the control at all tested concentrations (Figure 4.13). The root exudates of blackjack exerted the highest nematicidal activity with $LC_{50/48\ h}$ of 2.4 mg/ml followed by blackjack

combined with black nightshade (5.6 mg/ml), blackjack combined with tomato (5.8 mg/ml), then black nightshade (7.1 mg/ml) and tomato (7.5 mg/ml) when tested alone.

Since the drip and intercrop pot experiments of both tomato and black nightshade showed reduced nematode infection by blackjack, we hypothesized that the root exudates may inhibit egg hatching and/or cause mortality of J2. We therefore tested the root exudates of the three plants to determine their interactive effects. The water control stimulated more hatching than all the other treatments in the *in vitro* experiments. Additionally, the percent inhibition in egg hatching and nematicidal activity of the tomato root exudates were significantly lower than those found for the root exudate of black nightshade (Figure 4.13).

4.7 Bioactivity of blackjack root exudate fractions

All the three fractions of the blackjack root exudate significantly inhibited hatching compared to the control (Fraction 1; $\chi^2 = 18.13$, df = 3, $P < 0.0001$, fraction 2; $\chi^2 = 16.16$, df = 3, $P < 0.0001$, fraction 3; $\chi^2 = 15.73$, df = 3, $P < 0.0001$) and these effects were concentration-dependent (Figure 4.14).

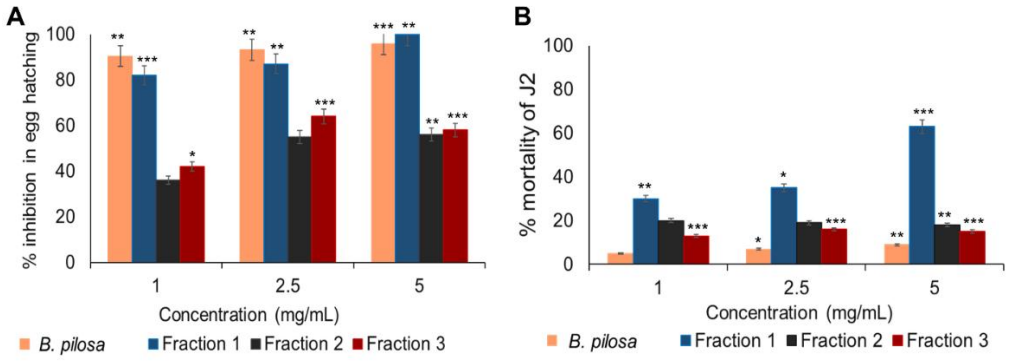

Figure 4.14: Bioactivity of blackjack root exudate fractions. (**A**) Egg hatching and (**B**) J2 mortality of *M. incognita* in blackjack root exudate fractions (GLM with binomial distribution followed by Tukey *post-hoc* mean separation test, $P < 0.05$, n = 12). The level of significance is indicated by: ***$P < 0.0001$, **$P < 0.001$, *$P < 0.05$.

Fraction 1 had a significantly higher inhibition effect on egg hatching at all concentrations: 1 mg/ml; (82%, $P < 0.0001$, n = 5), 2.5 mg/ml; (87%, $P < 0.0001$, n = 5) and 5 mg/ml; (100%, $P < 0.0001$, n = 5), than fraction 2: 1 mg/ml; (36%, $P > 0.05$, n = 5), 2.5 mg/ml; (55%, $P < 0.05$, n = 5), and 5 mg/ml; (56%, $P < 0.05$, n = 5) and fraction 3: 1 mg/ml; (42%, $P < 0.05$, n = 5), 2.5 mg/ml; (64%, $P < 0.0001$, n = 5), and 5 mg/ml; (58%, $P < 0.001$, n = 5). The fractions elicited varied significant concentration-dependent nematicidal effects on the J2 (Fraction 1; $\chi^2 = 17.33$, df = 3, $P < 0.0001$, fraction 2; $\chi^2 = 16.25$, df = 3, $P < 0.0001$, fraction 3; $\chi^2 = 13.43$, df = 3, $P < 0.0001$) compared to the control. Fraction 1 exhibited the highest J2 mortality followed by fraction 3 and 2 ($EC_{50/48\ h}$ = 1.0, 1.7 and 2.4 mg/ml, respectively).

4.8 Liquid chromatography tandem mass spectrometric identification of metabolites in the root exudates

Chemical analysis of the tomato, black nightshade and the bioactive fraction of blackjack root exudates using LC-QQQ-MS identified 14 compounds belonging to eight classes; vitamins, a dicarboxylic acid, amino acids, phytohormone (cytokinin), pentacyclic triterpene glycoside, aromatic acids, a flavonoid and alkaloids (Table 4.7). Additionally, the chemical profile of the root exudates showed several unidentified components (Figure 4.15).

Table 4.7: Identified compounds in root exudates of tomato, black nightshade and blackjack most bioactive fraction

Peak No.	t_R (min)	Compound	Tomato	Black nightshade	Blackjack	$[M + H]^+$	$[M - H]^+$	Key fragment ions
i.	1.36	Ascorbic acid* (**86**)	+	+	+	177.9	175.1	159.3, 140.8
ii.	1.89	Malic acid* (**87**)	-	+	+	135.8	133.6	117.9, 103.8
iii.	2.37	Nicotinic acid* (**88**)	-	+	+	124.7	122.8	106.8
iv.	2.87	Tyrosine** (**89**)	-	+	+	182.2	180.1	165.1, 147.0, 136.0, 119.0
v.	5.41	Phenylalanine** (**90**)	-	+	+	166.1	164.1	149.1, 131.1, 120.0, 103.0
vi.	6.11	Zeatin* (**7**)	+	+		220.0	218.2	202.0, 136.2
vii.	9.45	Diosgenin 3-O-beta-D-glucoside** (**91**)	-	-	+	577.2	-	455.1 [M+Na], 433. 1, 345.2
viii.	10.05	*p*-coumaric acid* (**92**)	-	-	+	165.9	163.6	147.9, 119.8
ix.	10.91	2-hydroxybenzoic acid* (**17**)	-	-	+	137.8	135.6	120.7
x.	10.93	Dehydrotomatine** (**93**)	+	-	-	1032.8	-	576.3, 527.7, 414.2, 273.1
xi.	11.20	Tomatine** (**94**)	+	-	-	1034.8	-	578.7, 528.8, 416.2
xii.	11.35	Kaempferol* (**95**)	-	-	+	287.7	-	268.5, 256.7
xiii.	13.76	Tomatidine* (**96**)	+	+	-	416.2	-	398.3, 273.2, 255.2
xiv.	13.95	Solasodine* (**97**)	+	+	-	414.4	-	396.3

*Compound whose identity was established based on comparison of retention time and mass spectra data with authentic standard.
**Compound identified tentatively based on mass fragmentation pattern and literature data. (+) and (-) indicates presence or absence of a compound, respectively.

The identified vitamins included ascorbic acid (**86**) and nicotinic acid (**88**). The dicarboxylic acid, malic acid (**87**) and the amino acids include tyrosine (**89**) and phenylalanine (**90**). A pentacyclic triterpene glycoside, diosgenin 3-O-beta-D-glucoside (**91**). The aromatic acids, *p*-coumaric acid (**92**) and 2-hydroxybenzoic acid (**17**) and the flavonoid kaempferol (**95**) were also detected in fraction 1 (Figure 4.15). Compounds identified exclusively in tomato and black nightshade included the phytohormone, zeatin (**7**), the steroidal glycoalkaloids dehydrotomatine (**93**) and tomatine (**94**) and their aglycones tomatidine (**96**) and solasodine (**97**). All these compounds were identified in both positive and negative ionization modes with key fragments illustrated in Table 4.7. The chemical structures of the identified compounds are shown in (Figure 4.15).

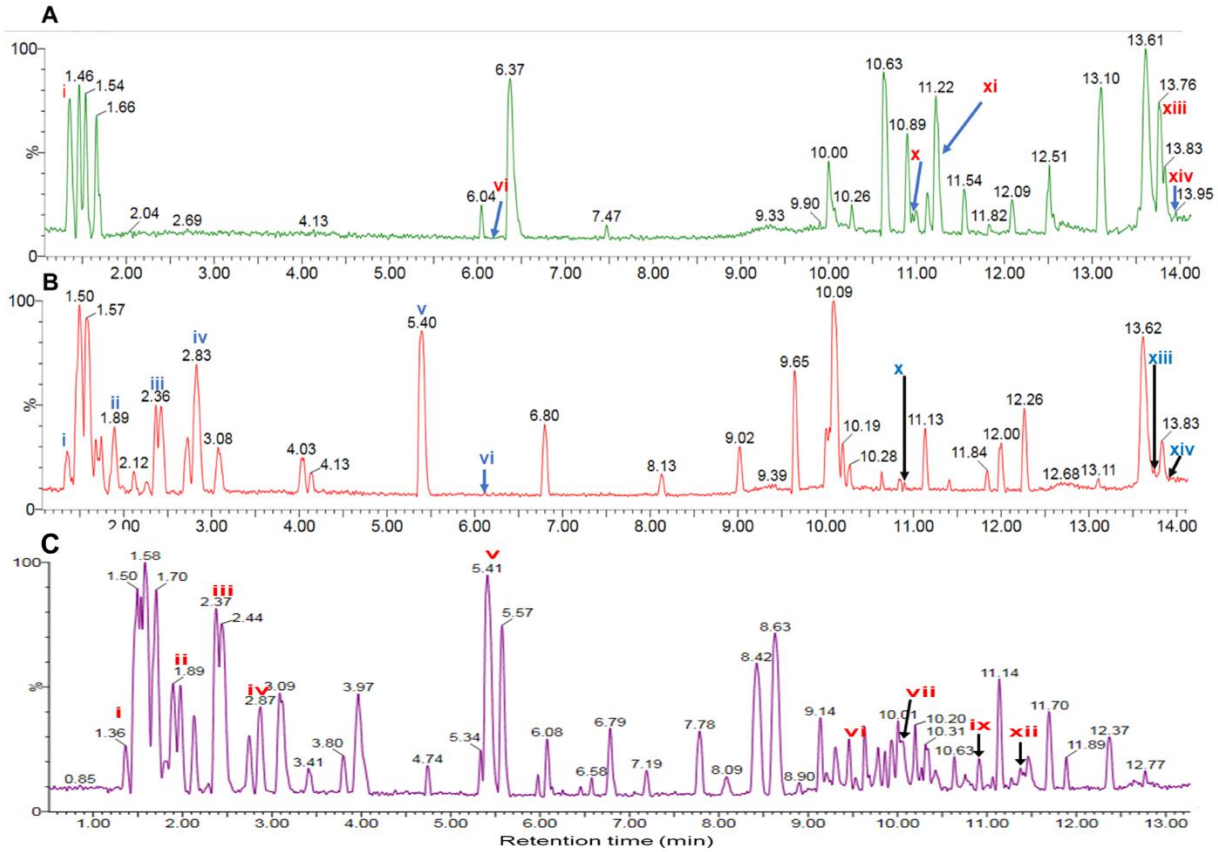

Figure 4.15: Liquid chromatography tandem mass spectrometry profiles of the root exudates. (**A**) tomato, (**B**) black nightshade and (**C**) fraction 1 of blackjack root exudates. Peak number assignments of the compounds are shown in Table 4.7.

Ascorbic acid (**86**) eluted at RT 1.36 min, with a molecular ion peak at m/z 177.9 and 175.8 on positive $[M+H]^+$ and negative $[M-H]^+$ ionization modes, respectively (Appendix II). The product ions at m/z 159.3 and 140.8 are attributed to sequential loss of two water molecules [M+H-$2H_2O$]. Sodium and potassium adducts were identified at m/z 199.1 and 215.2 and also confirmed with an authentic standard. The fragments were consistent with those reported in Al-Yousef *et al*., (2020).

A dicarboxylic acid, malic acid (**87**) which eluted at RT 1.89 min, had a molecular ion peak at m/z 135.8 and 133.6 on positive $[M+H]^+$ and negative $[M-H]^+$ ionization modes, respectively (Appendix III). The product ion at m/z 117.9 correspond to loss of H_2O [M+H-H_2O] (Fernandez-Fernandez *et al.*, 2010).

Nicotinic acid (**88**) eluted at RT 2.37 min and had a molecular ion peak at m/z 124.7 and 122.8 on positive $[M+H]^+$ and negative $[M-H]^+$ ionization modes, respectively (Appendix IV). The product ion at m/z 106.8 correspond to loss of H_2O [M+H-H_2O] and the fragmentation pattern was confirmed with authentic standard. Similar fragmentation was reported by Goldschmidt and wolf (2007).

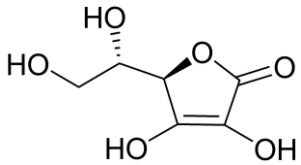

(**86**)

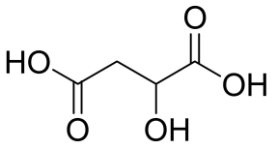

(**87**)

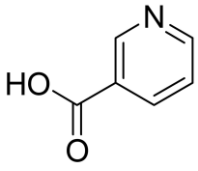

(**88**)

Tyrosine (**89**), eluted at RT 2.87 min, with a molecular ion peak at m/z 182.2 and 180.1 on positive $[M+H]^+$ and negative $[M-H]^+$ ionization modes, respectively (Appendix V). The product ion at m/z 165.2, 147.1, 136.1, 119.0 and 107.0 are attributed to sequential loss of NH_3 [M+H-

$NH_3]^+$, H_2O $[M+H-NH_3-H_2O]^+$, CO $[M+H-H_2O-CO]^+$, and CO $[M+H-NH_3-H_2O-CO]^+$. Sodium adduct peak was identified at m/z 204.2. The fragments were consistent with those reported in El Aribi *et al*., (2004) and Ochola (2021).

An aromatic acid, phenylalanine (**90**) which eluted at RT 5.41 min had a molecular ion at m/z 166.2 and 164.1 for $[M+H]^+$ and $[M-H]^+$ and product ions at m/z 149.1, 131.1 and 103.0 were formed from sequential loss of NH_3 $[M+H-NH_3]^+$, H_2O $[M+H-NH_3-H_2O]^+$ and CO $[M+H-NH_3-H_2O-CO]^+$, respectively (Ochola, 2021), and m/z 120.1 which corresponded to loss of water and CO $[M+H-H2O-CO]^+$ (El Aribi *et al.*, 2004). The sodium and potassium adducts were also detected at m/z 188.2 and 205.2, respectively (Appendix VI).

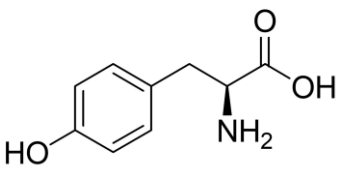

(**89**)

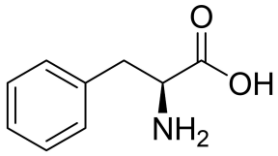

(**90**)

Plant hormone zeatin (**7**) eluted at RT 6.11 min and was identified based on the molecular ion peaks at m/z $[M+H]^+$ 220.0 on positive and m/z and [M-H]+ 218.2 on negative ionization modes (Appendix VII). Fragment ions at m/z 202.0 and 137.1 corresponded to the loss of water $[M+H-H_2O]$ and an adenine derivative ion $C_5H_6N_5^+$ and a sodium adduct were identified at m/z 242.0 (Kirwa *et al*., 2018; Ochola *et al*., 2020a). Zeatin was previously reported in the root exudates of two Solanaceae crops, *S. tuberosome* and *S. lycopersicon* (Kirwa *et al*., 2018; Ochola *et al*., 2020a).

The pentacyclic triterpene glycoside, diosgenin 3-O-beta-D-glucoside (**91**) which eluted at RT 9.45 min was identified based on the molecular ion $[M+H]^+$ peak at m/z 577.2 (Appendix VIII).

The major product ion was at m/z 433.1 $[M+H–C_8H_{16}O_2]^+$ and a sodium adduct of this fragment was identified at m/z 455.1 (Li, *et al.*, 2006).

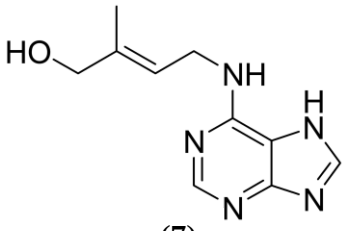

(**7**)

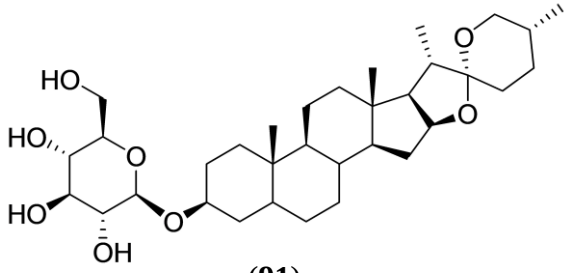

(**91**)

The phenol carboxylic aromatic acid, *p*-coumaric acid (**92**) eluted at RT 10.05 min and was identified based on the molecular ion peaks at m/z $[M+H]^+$ 165.9 on positive and m/z and $[M-H]^+$ 163.6 on negative ionization modes (Appendix IX). In addition, the fragment ion peaks at m/z 147.9 and 119.8 corresponding to the loss of H_2O $[M+H-H_2O]^+$ and CO $[M+H-CO]^+$ were identified. Similar fragmentation was reported by Li *et al*., (2018).

The aromatic acid, 2-hydroxybenzoic acid (**17**) which eluted at RT 10.91 min, had a molecular ion peak at m/z 137.8 and 135.6 on positive $[M+H]^+$ and negative $[M-H]^+$ ionization modes, respectively (Appendix X). The fragment ion at m/z 120.7 was attributed to the loss of a hydroxyl ion $[M+H-OH]^+$ and this was confirmed with the fragmentation pattern of an authentic standard. The fragments were consistent with those reported by (Liu *et al.*, 2008).

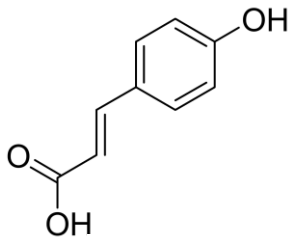

(**92**)

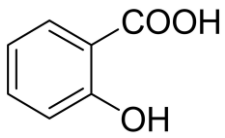

(**17**)

Dehydrotomatine (**93**) which eluted at RT 10.93 min was identified based on the molecular ion $[M+H]^+$ peak at m/z 1032.8 and a sodium adduct $[M+H+Na]^+$ at m/z 1054.4 (Appendix XI). In

addition, the fragment ions corresponding to [tomatidenol+Gal+H] at m/z 576.3 due to the loss of xylose (Xyl) and two glucose (Glc) moieties and a doubly charged ion $[M+H+Na]^{2+}$ at m/z 527.7 were detected. The aglycone tomatidenol at m/z 414.2 due to loss of the whole sugar chain, (i.e. lycotetraose $[M+H\text{-Xyl-Glc-Glc-Gal}]^{+}$) was also identified. Similar fragmentation was reported by Kirwa *et al*., (2018) and Cataldi *et al*., (2005).

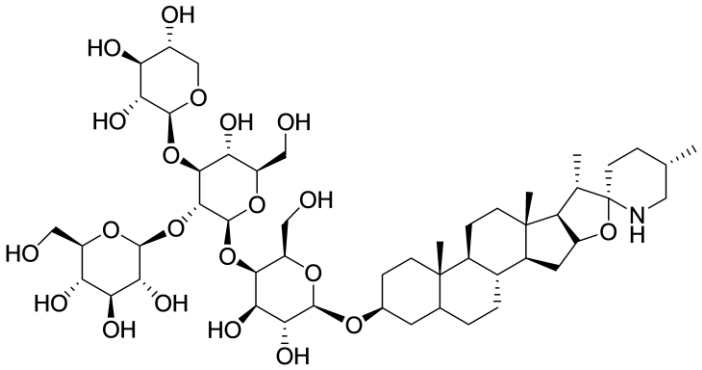

(**93**)

A major steroidal glycoalkaloid in tomato namely tomatine (**94**) eluted at RT 11.20 min and had a molecular ion $[M+H]^{+}$ peak at m/z 1034.8. The abundant fragment ions at 578.7, 528.8, 416.2 were identified. Ions at m/z 416.2 and 578.4 correspond to the aglycone [tomatidine + H] mainly produced by the loss of lycotetraose and [tomatidine + Gal +H] which is produced by the loss of xylose and two glucose moieties, respectively (Appendix XII). The ion at m/z 528.8 is due to the formation of a doubly charged ion, $[M+H+Na]^{2+}$, an adduct that is detected because ^{13}C isotope peak occurs than the corresponding ^{12}C peak. The fragments were consistent with those reported by (Cataldi *et al*., 2005).

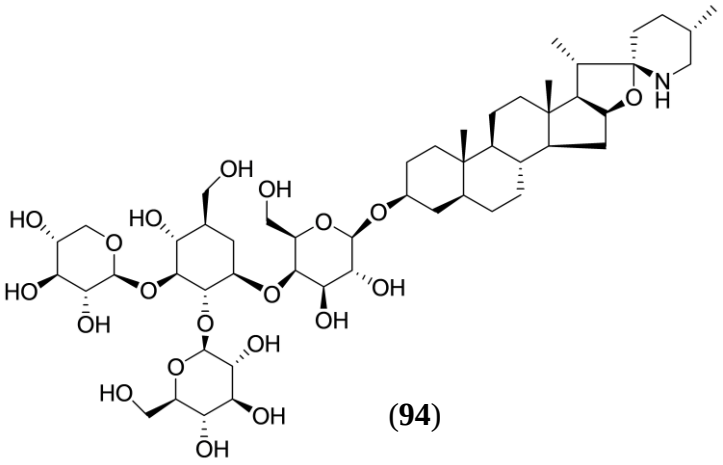

(**94**)

The flavonoid kaempferol (**95**) eluted at RT 11.35 min based on the molecular ion $[M+H]^+$ at m/z 287.7 and both sodium and potassium adducts at 309.2 and 325.7 (Appendix XIII). Fragment ion at m/z 268.5 and 256.7 corresponding to the loss of CH_3O^+ $[M+H-CH_3O]^+$ and H_2O $[M+H-H_2O]^+$ were also identified (Devaraj *et al.*, 2011).

Steroidal alkaloid tomatidine (**96**), eluted at RT 13.76 min was identified based on the molecular ion peak $[M+H]^+$ at m/z 416.3, and a fragment ion $[M+H-H_2O]^+$ at m/z 398.3 (Appendix XIV). The same spectrum also showed a specific loss of 143 Da yielding the product ions at m/z 273.2 and 255.2 from the precursor ions at m/z 416.2 and 398.3, respectively (Cataldi *et al.*, 2005). Solasodine (**97**) was also identified and it eluted at RT 13.95 min with a molecular ion peak $[M+H]^+$ at m/z 414.4 (Appendix XIV), and a fragment ion $[M+H-H_2O]$ at m/z 396.3 (Kirwa *et al*., 2018).

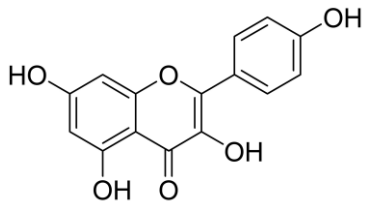

(**95**)

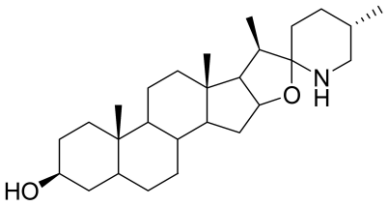

(**96**)

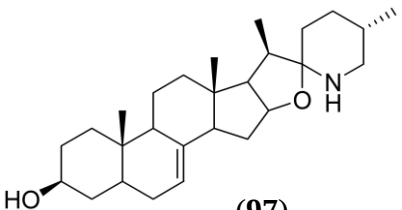

(**97**)

LC-QQQ-MS analysis showed differences in the compounds detected from the root exudates of tomato and black nightshade (Table 4.7) and these variations may be influenced by age and cultivar differences but this requires further investigation. It is likely that some of the compounds were present but in trace amounts and therefore below the detection limits. This shows that the two Solanaceae crops vary constitutively in the composition and ratios of root components and these variations may account for the observed differences in nematode response and behavior. Some of these chemical components influence the behavior of PPNs, specifically, the phytohormone, zeatin (**7**) attracted the polyphagous *M. incognita* J2 (Kirwa *et al.*, 2018) but had the least stimulatory effect on hatching of potato cyst nematodes, *Globodera rostochiensis* (Ochola *et al*., 2020a). On the other hand, the steroidal alkaloids, solasodine (**97**) and tomatidine (**96**) stimulated hatching of *G. rostochiensis* and stylet thrusting in *M. incognita* J2 but did not elicit attraction.

4.9 Bioactivity of the compounds identified in the most bioactive fraction of blackjack

All the identified compounds elicited significantly higher egg hatching inhibition than the control (2% DMSO), and the inhibition effect varied across the different classes of compounds. Both the vitamins nicotinic acid (**88**) and ascorbic acid (**86**) significantly inhibited hatching (80-99%, χ^2 = 26.52, df = 5, $P < 0.0001$) and χ^2 = 21.90, df = 5, $P < 0.0001$), respectively, at all the tested doses. The effect of the dicarboxylic acid, malic acid (**87**), on inhibiting egg hatching was significantly higher (80-88%, χ^2 = 25.27, df = 5, $P < 0.0001$) than the control. The amino acids had a lower inhibition effect on egg hatching (9-40%) at 0.1 – 100 ng µl^{-}1. Of the amino acids, tyrosine (**89**) exhibited significantly higher inhibition in egg hatching (9-40%, χ^2 = 28.32, df = 5, $P < 0.0001$) than phenylalanine (**90**) (11-18%, χ^2 = 23.48, df = 5, $P < 0.0001$), but both compounds significantly inhibited (77%, $P < 0.0001$, n = 5) egg hatching at the highest tested

concentration. Both the aromatic acids, 2-hydroxybenzoic acid (**17**) and *p*-coumaric acid (**92**) significantly inhibited egg hatching (80-98%, $\chi^2 = 26.52$, df = 5, $P < 0.0001$ and $\chi^2 = 25.07$, df = 5, $P < 0.0001$, respectively) at all the tested doses. The flavonoid, kaempferol (**95**) had a concentration-dependent effect on egg hatching of *M. incognita* which was significantly higher (64-100%, $\chi^2 = 24.41$, df = 5, $P < 0.0001$) than the control (Figure 4.16).

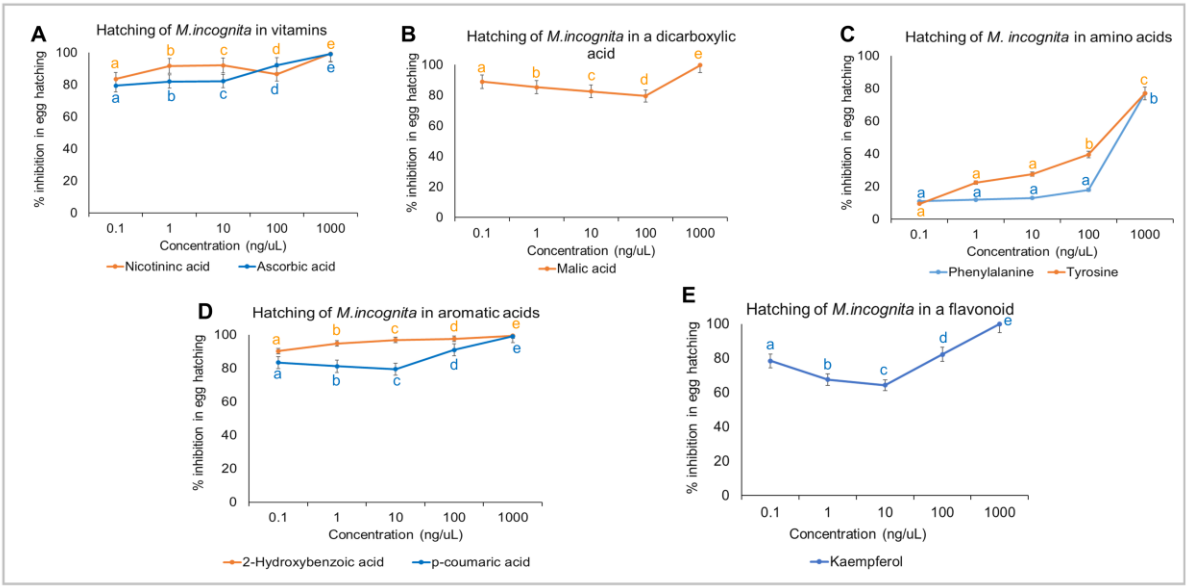

Figure 4.16: Egg hatching of *M. incognita* in the identified compounds. Hatching of *M. incognita* in vitamins (**A**), dicarboxylic acids (**B**), amino acids (**C**), aromatic acids (**D**) and a flavonoid (**E**). (GLM with binomial distribution followed by Tukey *post-hoc* mean separation test, $P < 0.05$, n = 12). Treatments with different lower-case letters are significantly different from each other.

The *in vitro* mortality assays with the identified compounds had varied concentration-dependent nematicidal effects that were significantly higher than the control. The nematicidal activity differed with the class of compound. Of the vitamins, ascorbic acid (**86**) had a significantly higher (68-81%, $\chi^2 = 24.05$, df = 5, $P < 0.0001$) nematicidal activity than nicotinic acid (**88**) (12 – 26%, $\chi^2 = 22.44$, df = 5, $P < 0.0001$) at 0.1 – 100 ng μl^{-1}, but both compounds elicited significantly higher (90 – 92%, $P < 0.0001$, n = 5) percent mortality at the highest (1000 ng μl^{-1}) dose. The dicarboxylic acid, malic acid (**87**), had a significantly higher (41-82%, $\chi^2 = 23.68$, df =

5, $P < 0.0001$) nematicidal activity than the control. Both amino acids elicited significantly low percent mortality in J2; phenylalanine (**90**) (13 -20%, $\chi^2 = 23.54$, df = 5, $P < 0.0001$) and tyrosine (**89**) (12 – 23%, $\chi^2 = 23.82$, df = 5, $P < 0.0001$) at 0.1 – 100 ng μl^{-1} but they elicited significantly high (80%, $P < 0.0001$, n = 5) mortality in J2 at the highest dose 1,000 ng μl^{-1}. Of the aromatic acids, 2-hydroxybenzoic acid (**17**) caused significant higher percent mortality in J2 (17-94%, $\chi^2 = 23.10$, df = 5, $P < 0.0001$) than *p*-coumaric acid (**92**) (15-68%, $\chi^2 = 22.58$, df = 5, $P > 0.05$) at all the tested doses (Figure 4.17). The flavonoid, kaempferol (**95**), caused significantly higher (21-66%, $\chi^2 = 22.45$, df = 5, $P < 0.0001$) mortality in J2 than the control. Ascorbic acid (**86**) exerted the highest nematicidal activity with $EC_{50/48\ h}$ = 0.12 µg μl^{-1}followed by 2-HBA (0. 30 µg μl^{-1}), nicotinic acid (**88**) (0. 54 µg μl^{-1}), malic acid (**87**) (0. 61 µg μl^{-1}), kaempferol (**95**) (0. 63 µg μl^{-1}), tyrosine (**89**) (0.65 µg μl^{-1}), phenylalanine (**90**) (0.67), and *p*-coumaric acid (**92**) (>1 µg μl^{-1}).

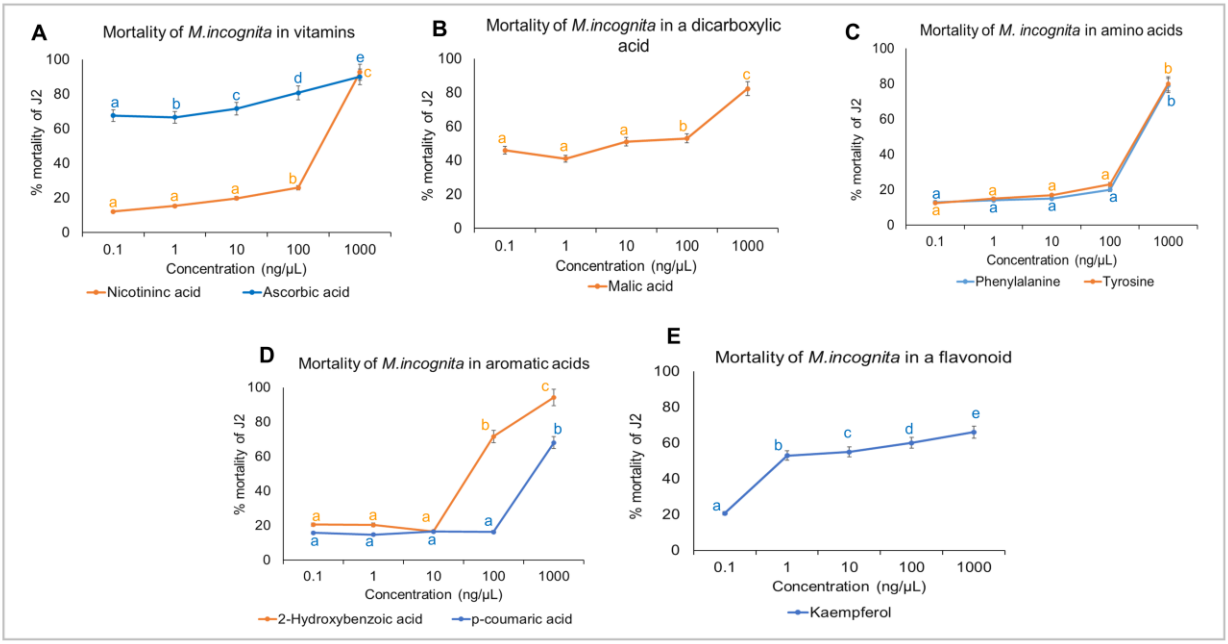

Figure 4.17: Mortality of *M. incognita* J2 in the identified compounds. Mortality of *M. incognita* in vitamins (**A**), dicarboxylic acids (**B**), amino acids (**C**), aromatic acids (**D**) and a flavonoid (**E**). (GLM with binomial distribution followed by Tukey *post-hoc* mean separation test, $P < 0.05$, n = 12). Treatments with different lower-case letters are significantly different from each other.

Several studies have evaluated the nematicidal activity of extracts from aboveground tissue of blackjack applied in different formulations against various plant-parasitic nematodes (Taba *et al.*, 2007, 2010, 2012, 2020). For instance, aqueous and ethanolic extracts of blackjack variety 'radiata' caused significant immobilization, mortality, repellence and egg hatching inhibition of *M. incognita* (Taba *et al.*, 2007; Chaudhary *et al.*, 2013). Additionally, boiled aqueous extracts showed a concentration-dependent nematicidal activity against the pinewood nematode (Taba *et al.*, 2020) and root-knot nematodes (Taba *et al.*, 2010, 2012) without adverse effects on beneficial free-living micro-organisms. This study investigated the chemical constituents from the root exudates of blackjack.

Organic acids have shown potential in reducing RKN infection when applied as soil amendments and foliar sprays or released from organic matter during plant decomposition processes. Following RKN infection, they induce systemic resistance in plants (McBride *et al.*, 2000), or serve as inhibitors of egg hatching (Wuyts *et al.*, 2006), and nematicidal compounds (Aoudia *et al.*, 2012; Seo and Kim, 2014). Previous studies demonstrated that microbes containing high amounts of organic acids also exhibit strong nematicidal activity against different PPNs, including the RKN (Kim *et al.*, 2016; Seo *et al.*, 2019). Additionally, resistant cultivars of tomato produced significantly higher amounts of ascorbic acid (**86**) than susceptible ones (Arrigoni *et al.*, 1978; Rani *et al.*, 2008) and the amounts increased significantly upon nematode infection in the resistant but not the susceptible cultivar (Arrigoni *et al.*, 1978). Further, there was evidence of reduced galling and reproduction when ascorbic acid (**86**) was applied on plants before inoculation in tomato (Arrigoni *et al.*, 1978; Al-Sayed and Thomas, 1988) and okra (Baheti *et al.*, 2018) by inducing systemic resistance and this led to increased crop yields. This suggests that ascorbic acid (**86**) plays various roles beyond plant defense against RKN namely,

inhibiting egg hatching of RKN by impairing the normal embryonic development and causing concentration-dependent toxic effect on the infective juveniles thereby disrupting host location. On the other hand, nicotinic acid (**88**) was intermediate in its nematicidal activity compared to other phenolic compounds (Aoudia *et al.*, 2012) and in another study, it was found to be an attractant for *M. incognita* J2 (Kuang *et al*., 2020). This may explain its low nematicidal activity recorded in the current study, which may be attributed to its binding affinity to J2 receptors, but this should be investigated.

In the current study, both aromatic acids, *2*-hydroxybenzoic acid (**17**) (also known as salicylic acid, SA) and *p*-coumaric acid (**92**), had a significant effect on inhibiting egg hatching compared to their nematicidal activity. However, SA (**17**) recorded a significantly stronger nematicidal activity at higher concentrations. This corroborates with a previous study that found SA (**17**) to irreversibly inhibit egg hatching and J2 motility in addition to its nematicidal activity (Wuyts *et al*., 2006). However, the same study reported that SA (**17**) attracted J2 contrary to Fleming *et al.,* 2017 findings that reported that SA (**17**) repelled J2, which was considered a concentration-dependent effect. Previously, soil drenching and foliar application of SA (**17**) and its derivative acetyl SA (2-acetyloxybenzoic acid) significantly (70 and 100%, respectively) reduced J2 in soil and enhanced growth indices of tomato (Rawdan *et al.*, 2017). This was associated with induced systemic resistance due to the signaling role of SA (**17**) in inducing plant resistance to pathogens (Klessig *et al.*, 2000). In another study, benzoic acid and SA (**17**) recorded higher nematicidal activity (Fleming *et al.,* 2017) while 4-hydroxybenzoic acid (*p*-hydroxybenzoic acid*),* caused a 2-fold reduction in the activity against J2 (Aoudia *et al.*, 2012). In this study, *p*-hydroxybenzoic acid had lower and comparable activity to *p*-coumaric acid (**92**), which in the current study had the lowest nematicidal activity. In other studies *p*-coumaric acid (**92**) repelled the sedentary *M.*

incognita but not the migratory *Radophollus similis* and *Pratylenchus penetrans* J2 (Wuyts *et al.*, 2006; Fleming *et al.*, 2017). Structurally, *p*-coumaric acid (**92**) is a hydroxycinnamic acid and SA (**17**) is a hydroxybenzoic acid but both are derived from the phenylpropanoid pathway, associated with plant defense (Iberkleid *et al.*, 2015). The differences in chemical structures may imply varying modes of actions against RKN, which could be beneficial by reducing the probability of nematodes developing resistance.

The dicarboxylic acid, malic acid (**87**), was elevated in plants exposed to nematode infection (Khanna *et al*., 2019) suggesting its critical role in induced systemic resistance. In another study, malic acid (**87**) in *Arapidopsis thaliana* recruited the beneficial microbe, *Bacillus subtilis* (Rudrappa *et al.*, 2008), which is linked to inducing systemic resistance and promoting plant growth (Rudrappa *et al.*, 2008; Siddiqui and Futai, 2009), and protection against fungal infection (Govindappa *et al*., 2010) and *M. incognita* (Siddiqui and Futai, 2009). In the current study, malic acid (**87**) had a stronger effect on egg hatching inhibition than on mortality of J2, but the defense responses of blackjack *to M. incognita* was not investigated. The abundance of *p*-coumaric (**92**), malic (**87**), nicotinic (**88**), vanillic, and ferulic p-hydroxybenzoic, caffeic acids, in fruit pulp of *M. azedarach* (Aoudia *et al.*, 2012), aqueous extract of dry and fresh leaves of *Eucalyptus citriodora* (El-Rokiek and El-Nagdi, 2011) and root leachate of *Lantana camara* (Shazaukat *et al.*, 2003) contributed to the highest nematicidal activity against *M. incognita.* This suggests a synergistic effect of the organic acids to counteract the nematode cryptic behavior of producing secretion to counter plant defense (Bellafiore *et al*., 2008).

Flavonoids are known to play different roles in plant-nematode interactions (Chin *et al*., 2018). For example, they are induced in plant roots during nematode infection, with higher quantities in

resistant that in susceptible plants (Wuyts *et al.*, 2006; Jones *et al.*, 2007). They also affect different stages of the nematode life cycle such as kaempferol (**95**) which irreversibly inhibits egg hatching of the PPN, *R. similis*, but not *M. incognita* (Wuyts *et al*., 2006). In the current study, we observed concentration-dependent effects of kaempferol (**95**) on egg hatch inhibition and mortality of *M. incognita*, even though its bioactivity was intermediate compared to the other compounds tested. The bioactivity of the flavonoids has been associated with their structure, which contain a three-ring structure but differ in the number and positioning of the hydroxyl groups (Faizi *et al*., 2011; Chin *et al*., 2018; Kirwa *et al*., 2018).

In the current study, the amino acids had the lowest inhibitory effect on egg hatching and had a low nematicidal effect, but tyrosine (**89**) recorded higher egg hatch inhibition than phenylalanine (**90**). The two amino acids are structurally similar and phenylalanine (**90**) is a precursor for tyrosine (**89**), which has a hydroxyl group at the C4 position, causing differences in hydrophilicity and may account for the differences in hatching. As primary metabolites that are present in both monocots and dicots (Carvalhais *et al.*, 2011; Li *et al.*, 2013; Ochola *et al.*, 2020*b*), their presence in the root exudates may signal the availability of food resources for the polyphagous *M. incognita*, even though their bioactivity in blackjack and black nightshade may be masked by the presence of the organic acids that exhibited significant inhibitory effect on hatching and higher nematicidal activity. In a previous study, phenylalanine (**90**) and tyrosine (**89**) had the lowest stimulatory effect on hatching the PPN *G. rostochiensis* (Ochola *et al*., 2020a), suggesting that it's a non-specific signal for the specific PPN with limited host range. The unidentified compounds found in this study may also contribute to the nematode response and this requires further research.

CHAPTER FIVE
CONCLUSIONS AND RECOMMENDATIONS

5.1 CONCLUSIONS

In summary, RKNs induce volatile chemical changes in tomato both locally and systemically with significant variations between healthy and RKN infected plants at the different time points of infection. Additionally, root volatiles associated with RKN infection provide important olfactory cues that disrupt J2 chemoreception. Further, the root exudates of the non-host Asteraceae plant, *B. pilosa*, contributed to reduced nematode infection in tomato and black nightshade with a higher bioactivity against *M. incognita* egg hatching than in mortality of the infective juveniles. Finally, selected compounds from the root exudates of *B. pilosa* had differential activity on egg hatching and J2 mortality. Ascorbic acid had the highest bioactivity in inhibiting egg hatching and causing mortality of the infective juveniles.

5.2 RECOMMENDATIONS

i. Further work should identify the genetic factors responsible for production of MeDiJA (**45**) for crop improvement of RKN-resistant tomato cultivars varieties. It would be critical to determine the impact of such varieties on other soil pathogens and beneficial microorganisms. Additionally, chemical and transcriptomic profiling between resistant and susceptible tomato cultivars can be studied to identify specific genes that can be deployed in crop improvement for management of RKNs.

ii. RKN infection elicits volatile chemical changes in the plant shoot chemistry. Further studies should investigate the changes in above-ground pest populations, parasitoids and natural enemies in field conditions occasioned by RKN infection.

iii. Companion cropping of non-host Asteraceae plants can be extended to other RKN-susceptible crops such as pepper and egg plants and tested in field conditions. Additionally, future work should determine the effect of root exudates of non-host plants on soil microbial populations and evaluate their influence in RKN behavior.

iv. Ascorbic acid and plant-based products containing high content of ascorbic acid can be tested in field conditions to determine their influence in suppressing RKN populations.

REFERENCES

Abad, P., Favery, B., Rosso, M-N., and Castagnone-Sereno, P. (2003). Root-knot nematode parasitism and host response: molecular basis of a sophisticated interaction. *Molecular Plant Pathology*, *4* (4), 217–224.

Abad, P., Gouzy, J. and Aury, M.-J. (2008). Genome sequence of the metazoan plant-parasitic nematode *Meloidogyne incognita*. *Nature Biotechnology*, *26*, 909–915.

Adams2 terpenoid/natural product library, A. R. (1995). Identification of essential oil components by gas chromatography/mass spectrometry, Allured, Carol Stream.

Al-Sayed, A. A. and Thomas, I. J. (1988). *Meloidogyne incognita* and Tomato Response to Thiamine, Ascorbic Acid, L-arginine, and L-glutamic Acid. *Journal of Nematology*, *20*, 451–456.

Al-Yousef, H. M., Hassan, W. H. B., Abdelaziz, S., Amina, M., Adel, R., and El-Sayed, M. A. (2020). UPLC-ESI-MS/MS profile and antioxidant, cytotoxic, antidiabetic, and antiobesity acticities of the aqueous extracts of three different *Hibiscus* species. *Journal of Chemistry*, *6749176*.

Ali, J.G., Alborn, H.T., and Stelinski, L. L. (2011). Constitutive and induced subterranean plant volatiles attract both entomopathogenic and plant parasitic nematodes. *Journal of Ecology*, *99*, 26–35.

Ali, J. G., Alborn, H. T., and Stelinski, L. L. (2010). Subterranean herbivore-induced volatiles released by citrus roots upon feeding by *Diaprepes abbreviatus* recruit entomopathogenic nematodes. *Journal of Chemical Ecology*, *36*, 361–368.

Ali, M. A., Azeem, F., Abbas, A., Joyia, F. A., Li, H., and Dababat, A. A. (2017). Transgenic strategies for enhancement of nematode resistance in plants. *Frontiers in Plant Science*, *8*, 750.

Alston, D. G., Bradley, J. R., Schmitt, D. P., and Coble, H. D. (1991). Response of *Helicoverpa zea* (Lepidoptera, Noctuidae) populations to canopy development in soybean as influenced by *Heterodera glycines* (Nematode, Heteroderidae) and annual weed population densities. *Journal of Economic Entomology*, *84*, 267–276.

Alston, D. G., Schmitt, D. P., Bradley, J. R., and Coble, H. D. (1993). Multiple pest interactions in soybean – Effects on *Heterodera glycines* egg populations and crop yield. *Journal of Nematology*, *25*, 42–49.

Aoudia, H., Ntalli, N., Aissani, N., Yahiaoui-Zaidi, R., and Caboni, P. (2012). Nematotoxic Phenolic Compounds from *Melia azedarach* Against *Meloidogyne incognita*. *Journal of Agricultural and Food Chemistry*, *60*, 11675–11680.

Arce, C. C. M., Machado, R. A. R., Ribas, N. S., Cristaldo, P. F., Ataíde, L. M. S., Pallini, Â., Carmo, F. M., Freitas, L. G., and Lima, E. (2017). Nematode root herbivory in tomato increases

leaf defenses and reduces leaf miner oviposition and performance. *Journal of Chemical Ecology*, *43* (2), 120–128.

Arrigoni, O., Zacheo, G., Arrigoni-Liso, R., Bleve-Zachea, T., and Lamberti, F. (1978). Relationship between ascorbic acid and resistnce in tomato plants to *Meloidogyne incognita*. *Phytopathology*, *69*, 578–581.

Ayelo, P. M., Yusuf, A. A., Pirk, C. W. W., Mohamed, S. A., Chailleux, A., and Deletre, E. (2021). The Role of *Trialeurodes vaporariorum*-infested tomato plant in the attraction of *Encarsia farmosa* (Hymenoptera: Aphelinidae). *Journal of Chemial Ecology*, *47*, 192–203.

Baheti B.L., Nama C.P., Bhati S.S., and Khandelwal, S. K. (2018). Chemical Inducers: A Tool for management of root-knot nematode, *Meloidogyne incognita* infecting okra (*Abelmoschus esculentus* L.) under field conditions. *Indian Journal of Nematology*, *48*, 62–67.

Barcala, M., Garcia, A., Cabrera, J., Casson, S., Lindsey, K., Favery, B., Garcia-Casado, G ., Solano, R., Fenoll, C., and Escobar, C. (2010). Early transcriptomic events in microdissected *Arabidopsis* nematode-induced giant cells. *The Plant Journal*, *61*, 698–712.

Bellafiore, S., Shen, Z., Rosso, M.-N., Abad, P., and Shih, P. (2008). Direct identification of the *Meloidogyne incognita* secretome reveals proteins with host cell reprogramming potential. *PLoS Pathogens*, *4* (10), 1000192.

Bhattarai, K. K., Xie, Q. G., Mantelin, S., Bishnoi, U., Girke, T., Navarre, D. A., and Kaloshian, I. (2008). Tomato susceptibility to root-knot nematodes requires an intact jasmonic acid signaling pathway. *Molecular Plant-Microbe Interactions*, *21* (9), 1205–1214.

Birithia, R., Waceke, W., Lomo, P., and Masiga, D. (2012). Identification of root-knot nematode species occurring on tomatoes in Kenya: use of isozyme phenotypes and PCR-RFLP. *International Journal of Tropical Insect Science*, *32* (02), 78–84.

Bruce, T. J. A., and Pickett, J. A. (2011). Perception of plant volatile blends by herbivorous insects - Finding the right mix. *Phytochemistry*, *72*, 1605–1611.

Carvalhais, L. C., Dennis, P. G., Fedoseyenko, D., Hajirezaei, M. R., Borriss, R., and vonWirén, N. (2011). Root exudation of sugars, amino acids, and organic acids by maize as affected by nitrogen, phosphorus, potassium, and iron deficiency. *Journal of. Soil Science and Plant Nutrition.*, *174*, 3–11.

Cataldi, T. R. I., Lelario, F., and Bufo, S. A. (2005). Analysis of tomato glycoalkaloids by liquid chromatography couples with electrospray ionization tandem mass spectrometry. *Rapid Communication in Mass Spectrometry*, *19*, 3103–3100.

Čepulytė, R., Danquah, W. B., Bruening, G., and Williamson, V. M. (2018). Potent attractant for root-knot nematodes in exudates from seedling root tips of two host species. *Scientific Reports*, *8* (1), 10847.

Chaudhary, K. K., Haile, A., Ayresea, Z. G., Semereab, G., and Weldegergish, T. (2013). Nematicidal activity of Eritrean weed plants against the root-knot nematode *Meloidogyne incognita*. *Nematropica*, *43*, 207–215.

Chen, Z.X., Chen, S.Y. and Dickson, D. W. (Ed.). (2004). *Nematology Advances andand Perpectives; Nemtode Management and Utilization* (Volume 2). CABI Publishing.

Chin, S., Behm, C., Mathesius, U., Chin, S., Behm, C. A., and Mathesius, U. (2018). Functions of flavonoids in plant–nematode interactions. *Plants*, *7* (4), 85.

Chitambo, O., Haukeland, S., Fiaboe, K.K.M., Kariuki, G.M., and Grundler, F. M. W. (2016). First report of the root-knot nematode *Meloidogyne enterolobii* parasitizing African nightshades in kenya. *Plant Disease*, *100*, 1954.

Collange, B., Mireille, N., Peyre., G., Mateille, T., and Tchamitchian, M. (2011). Root-knot nematode (*Meloidogyne*) management in vegetable crop production: The challenge of an agronomic system analysis. *Crop Protection*, *30* (10), 1251–1262.

Cooper, W. R., Jia, L., and Goggin, L. (2005). Effects of jasmonate-induced defenses on root-knot nematode infection of resistant and susceptible tomato cultivars. *Journal of Chemical Ecology*, *31* (9), 1953–1967.

Coyne, D. L., Nicol, J. M., and Claudius-Cole, B. (2007). Practical plant nematology: A field and laboratory guide. 2nd edition. SP-IPM Secretariat, International Institute of Tropical Agriculture (IITA) Cotonou, Benin.

Coyne, Danny L., Cortada, L., Dalzell, J. J., Claudius-Cole, A. O., Haukeland, S., Luambano, N., and Talwana, H. (2018). Plant-parasitic nematodes and food security in sub-saharan africa. *Annual Review of Phytopathology*, *56* (1), 381–403.

Curtis, R. H. C. (2007). Plant parasitic nematode proteins and the host-parasite interaction. *Briefings in Functional Genomics and Proteomics*, *6* (1), 50–58.

Curtis, R. H. C. (2008). Plant-nematode interactions: environmental signals detected by the nematode's chemosensory organs controls changes in the surface cuticles and behaviour. *Parasite*, *15*, 310–316.

Darshanee, H. L. C., Ren, H., Ahmed, N., Zhang, Z-F., Liu, Y-H., and Liu, Y.-X. (2017). Volatile-mediated attraction of greenhouse whitefly *Trialeurodes vaporariorum* to Tomato and Eggplant. *Frontiers in Plant Science*, *8*, 1285.

de Almeida-Engler, J., Engler, G., and Gheysen, G. (2011). Current nematode threats to world agriculture. In *Genomics and Molecular Genetics of Plant-Nematode Interactions* (pp. 347–367).

De Backer, L., Megido, R. C., Fauconnier, M.-L., Brostaux, Y., Francis, F., and Verheggen, F. (2015). Tuta absoluta-induced plant volatiles: attractiveness towards the generalist predator *Macrolophus pygmaeus*. *Arthropod-Plant Interactions*, *9* (5), 465–476.

De Boer, J.G., and Dicke, M. (2004). The role of methyl salicylate in prey searching behavior of the ppredatory mite *Phytoseiulus persimilis*. *Journal of Chemical Ecology, 30* (2), 255–271.

Degenhardt, D. C., Refi-Hind, S., Stratmann, J. W., and Lincoln, D. E. (2010). Systemin and jasmonic acid regulate constitutive and herbivore-induced systemic volatile emissions in tomato, *Solanum lycopersicum*. *Phytochemistry*, *71* (17–18), 2024–2037.

Devaraj, A. D., Krishna, B. G., and Viswanantha, G. L. (2011). Simultaneous determinination of quercetin, rutin and kaempferol in the leaf extracts of *Moringa oleifera* Lam. and *Raphinus sativus* Linn. by liquid chromatography-tandem mass spectrometry. *Journal of Chinese Intergrative Medicine*, *9*, 1022–1030.

Devine, K.J., Bryne, J., Maher, N., and Jones, P. w. (1996). Resolution of natural hatching factors for golden potato cyst nematode, *Globodera rostochiensis*. *Annals of Applied Biology, 129*, 323–334.

De Waele, D. and Elsen, A. (2007). Changes in tropical plant nematology. *Annual Review of Phytopathology, 47,* 457.

Djian-Caporalino, C., Farazi, A., Arguel, M.J., Vernie, T., VandeCasteele, C., Faure, I., Brunound, G., and Abad, P. (2007). Root-knot nematode (*Meloidogyne* spp.) Me resistance genes in pepper (*Capsicum annuum* L.) are clustered on the P9 chromosome. *Theoretical and Applied Genetics*, *114* (3), 473–486.

Eisenback, J. D. (1985). Detailed morphology and anatomy of second-stage juveniles, males, and females of the genus *Meloidogyne* (root-knot nematodes). In C. C. Sasse, J.N. and Carter (Ed.), *An Advanced Treatise on Meloidogyne. Volume I. Biology and Control. A cooperative publication of the Department of Plant Pathology and the United States Agency for International Development* (pp. 44–77). North Carolina State University Graphics, Raleigh, North Carolina.

El-Rokiek, K., and El-Nagdi, W. (2011). Dual effects of leaf extracts of *Eucalyptus citriodora* on controlling purslane and root-knot nematode in sunflower. *Journal of Plant Protection Research*, *51*, 121−129.

El Aribi, H., Orlova, G, Hopkinson, A. C., and Michael Siu, K. W. (2004). Gas-phase fragmentation reactions of protonated aromatic amino acids: Concomitant and consecutive neutral eliminations and radical cation formations. *Journal of Physical Chemistry*, *108*, 3844–3853.

Eloh, K., Sasanelli, N., Maxia, A., and Caboni, P. (2016). Untargeted metabolomics of tomato plants after root-knot nematode infestation. *Journal of Agricultural and Food Chemistry*, *64* (29), 5963–5968.

Engelberth, J., Alborn, H. T., Schmelz, E. A., and Tumlinson, J. H. (2004). Airborne signals prime plants against insect herbivore attack Preparation of Crude Regurgitant elicitor (CRE)

from larvae of BAW. *Proceedings of the National Academy of Sciences, 10*, 1781–1785.

Escudero, N., Marhuenda-Egea, F.C., Ibanco-Canete, R., Zavala-Gonzalez, E.A., and Lopez-Llorca, L. V. (2014). A metabolomic approach to study the rhizodeposition in the tritrophic interaction: tomato, *Pochonia chlamydosporia* and *Meloidogyne javanica*. *Metabolomics, 10*, 788-804.

Faizi, S., Fayyaz, S., Bano, S., Yawar Iqbal, E., Lubna, L., Siddiqi, H., and Naz, A. (2011). Isolation of nematicidal compounds from *Tagetes patula* L. yellow flowers: Structure-activity relationship studies against cyst nematode *Heterodera zeae* infective stage larvae. *Journal of Agricultural and Food Chemistry, 59* (17), 9080–9093.

Fan, J. W., Hu, C. L., Zhang, L. N., Li, Z. L., Zhao, F. K., and Wang, S. H. (2015). Jasmonic acid mediates tomato's response to root-knot nematodes. *Journal of Plant Growth Regulation, 34* (1), 196–205.

Fargette, M., Davies, K.G., Robinson, M.P. and Trudgill, D. L. (1994). Characterization of resistance breaking *Meloidogyne incognita*-like populations using lectins, monoclonal antibodies and spores of *Pasteuria penetrans*. *Fundamental and Applied Nematology, 17*, 537–542.

Fargette, M. (1987). Use of esterase phenotype in the taxonomy of the genus *Meloidogyne*. 2. Esterase phenotypes observed in West African populations and their characterization. *Revue de Nématologie, 10*, 45–56.

Fernandez-Fernandez, R., Lopez-Martinez, J. L., Romero-Gonzalez, R., Martinez-Vidal, J. L., Flores, M. I. A., and Frenich, A. G. (2010). Simple LC-MS determination of citric and malic acids in fruits and vegetables. *Chromatographia, 72*, 55–62.

Fleming, T. R., Maule, A. G., and Fleming, C. C. (2017). Chemosensory responses of plant parasitic nematodes to selected phytochemicals reveal long-term habituation traits. *Journal of Nematology, 49*, 462–471.

Fudali, S.L, Wang, C. and Williamson, V. M. (2013). Ethylene signaling pathway modulates attractiveness of host roots to the root-knot nematode *Meloidogyne hapla*. *Molecular Plant-Microbe Interactions, 26* (1), 75–86.

Gheysen, G., and Mitchum, M. G. (2011). How nematodes manipulate plant development pathways for infection. *Current Opinion in Plant Biology, 14* (4), 415–421.

Glazer, I., Orion, D., and Apelbaum, A. (1983). Interrelationships between ethylene production, gall formation, and root-knot nematode development in tomato plants infected with *Meloidogyne javanica*. *Journal of Nematology, 15*, 539–544.

Goldschmidt, R. J., and Wolf, W. R. (2007). Determination of niacin in food materials by liquid chromatography using isotope dilution Mass Spectrometry. *Journal of AOAC International, 90*, 1084–1089.

Goodell, P. B. and Ferris, H. (1989). Influence of environmental factors on the hatch and survival of *Meloidogyne incognita*. *Journal of Nematology, 21*, 328–334.

Govindappa, M., Lokesh, S., Rai, V. R., Naik, V. R., and Raju, S. G. (2010). Induction of systemic resistance and management of safflower *Macrophomina phaseolina* root-rot disease by biocontrol agents. *Archives Of Phytopathology And Plant Protection, 43* (1), 26–40.

Ha, J., Won, J. C., Jung, Y. H., Yang, J-W., Lee, H-U., Nam, K.J., Park, S-C., Jeong, J. C., Lee, S-W., Lee, D. W., Chung, J-S., Lee, J. J., and Kim, Y.-H. (2017). Comparative proteomic analysis of the response of fibrous roots of nematode-resistant and -sensitive sweet potato cultivars to root-knot nematode *Meloidogyne incognita*. *Acta Physiologiae Plantarum, 39*, 262.

Haegeman, A., Mantelin, S., Jones, J. T., and Gheysen, G. (2012). Functional roles of effectors of plant-parasitic nematodes. *Gene, 492*, 19–31.

Hallman, J. and Sikora, R. A. (1996). Toxicity of fungal endophyte secondary metabolites to plant parasitic nematodes and soil-borne plant pathogenic fungi. *European Journal of Plant Pathology, 102*, 155–162.

Hammer Ø, Harper DA, R. P. (2001). Past: paleontological statistics software package for education and data analysis. *Palaeontol Electron., 4* (9).

Hassaballa, I. B., Sole, C. L., Cheseto, X., Torto, B., and Tchouassi, D. P. (2020). Afrotropical sand fly-host plant relationships in a leishmaniasis endemic area. *PLoS Neglected Tropical Diseases, 15*, e0009041.

Hiltpold, I., Jaffuel, G., and Turlings, T. C. J. (2015). The dual effects of root-cap exudates on nematodes: from quiescence in plant-parasitic nematodes to frenzy in entomopathogenic nematodes. *Journal of Experimental Botany, 66*, 603–611.

Hol, W. H. G., De Boer, W., Ter- morshuizen, A. J., Meyer, K. M., Schneider, J. H. M., Van Dam, N. M., Van Veen, J.A., and Van Der Putten, W. H. (2010). Reduction of rare soil microbes modifies plant–herbivore interactions. *Ecology Letters, 13*, 292–301.

Holbein, J., Grundler, F. M. W., and Siddique, S. (2016). Plant basal resistance to nematodes: an update. *Journal of Experimental Botany, 67*, 2049–2061.

Holbrook, C. C., Knauft, D. A. and Dickson, D. W. (1983). A technique for screening peanut for resistance to *Meloidogyne arenaria*. *Plant Disease, 67*, 957–958.

Hooks, C.R., Wang, K-H., and Ploeg, A. (2007). Protecting crops from nematode pests : using marigold as an alternative to chemical nematicides. *Plant Disease, PD-35*, 1–6.

Hooks, C.R.R., Wang, K-H., Ploeg, A., and Robert, M. (2010). Using marigold (*Tagetes* spp.) as a cover crop to protect crops from plant-parasitic nematodes. *Applied Soil Ecology, 46* (3), 307–320.

Iberkleid, I., Sela, N., and Brown, M. S. (2015). *Meloidogyne javanica* fatty acid- and retinol-

binding protein (Mj-FAR-1) regulates expression of lipid-, cell wall-, stress- and phenylpropanoid-related genes during nematode infection of tomato. *BMC Genomics*, *16*, 272.

IITA. (1981). Proceedings of the Third Research Planning Conference on Root-knot Nematodes, Meloidogyne spp.

Nicol, J. M., Turner,S. J., Coyne, D. L., den Nijs, S. H. and Maafi, Z. T. (2011). Current nematode threats to world agriculture. In C. Jones, J., Gheysen, G. and Fenoll (Ed.), *Genomics and Molecular Genetics of Plant-Nematode Interactions* (pp. 21–45). Springer.

Jammes, F ., Lecomte, P., Almeida-Engler, J., Bitton, F., Martin-Magniette, M. L., Renou, J. P., Abad, P., and Favery, B. (2005). Genome-wide expression profiling of the host response to root-knot nematode infection in *Arabidopsis*. *The Plant Journal*, *44*, 447–458.

Ji, H. L., Gheysen, G., and Denil, S. (2013). Transcriptional analysis through RNA sequencing of giant cells induced by *Meloidogyne graminicola* in rice roots. *Journal of Experimental Botany*, *64*, 3885–3898.

Johnson, S. N., and Gregory, P. J., (2006). Chemically-mediated host-plant location and selection by root-feeding insects. *Physiological Entomology*, *31* (1), 1-13.

Johnson, S.N., and Nielsen, U. N. (2012). Foraging in the dark-chemically mediated host plant loction by belowground insect herbivores. *Journal of Chemical Ecology*, *38* (6), 604–614.

Jones, J.; Furlanetto, C.; Phillips, M. (2007). The role of flavonoids produced in response to cyst nematode infection of Arabidopsis thaliana. *Nematology*, *9*, 671–677.

Jones, J., Gheysen, G. and Fenoll, C. (2011). *Genomics and Molecular Genetics of Plant-Nematode Interactions*. Springer.

Kalaiselvam, I. and Devaraj, A. (2011). Effect Of Root Exudates of *Tagetes* Spp. on Egg Hatching Behavior of *Meloidogyne incognita*. *International Research Journal of Pharmacy*, *2* (10), 93–96.

Kammerhofer, N., Radakovic, Z ., Regis, M. A. J., Dobrev, P., Vankova, R., Grundler, F. M. W., Siddique, S., Hofmann, J., and Wieczorek, K. . (2015). 2015. Role of stress-related hormones in plant defense during early infection of the cyst nematode *Heterodera schachtii* in *Arabidopsis*. *New Phytologist*, *207*, 778–789.

Kaplan, I., Halitschke, R., Kessler, A., Rehill, B. J., Sardanelli, S., and Denno, R. F. (2008). Physiological integration of roots and shoots in plant defense strategies links above- and belowground herbivory. *Ecology Letters*, *11*, 841–851.

Kaplan, I., Sardanelli, S., and Denno, R. F. (2009). Field evidence for indirect interactions between foliar-feeding insect and root-feeding nematode communities on *Nicotiana tabacum*. *Ecological Entomology*, *34*, 262–270.

Kaplan, I., Sardanelli, S., Rehill, B. J., and Denno, R. F. (2011). Toward a mechanistic understanding of competition in vascular-feeding herbivores: an empirical test of the sink competition hypothesis. *Oecologia*, *166*, 627–636.

Kaplan, I., Halitschke, R., Kessler, A., Sardanelli, S., and Denno, R. F. (2008). Constitutive and induced defenses to herbivory in above- and belowground plant tissues. *Ecology*, *89* (2), 392–406.

Karssen, G. and Moens, M. (2006). Root-knot Nematodes. In M. Perry, R.N. and Moens (Ed.), *Plant nematology* (pp. 60–90). CABI Publishing.

Kerry, B. R. (2000). Rhizoshphere interactions and the exploitation of microbial agents for the biological control of plant-parasitic nematodes. *Annual Review of Phytopathology*, *38*, 423–441.

Khan, W. M. (Ed.). (1993). *Nematode interactions*. London: Chapman and Hall.

Khan, W. M. (Ed.). (1993). *Nematode interactions*. London: Chapman & Hall.

Khanna, K., Jamwal, V. L., Sharma, A., Gandhi, S. G., Ohri, P., Bhardwaj, R., Al-Huqail, A. A., Siddiqui, M. H., Marraiki, N., and Ahmad, P. (2019). Evaluation of the role of rhizobacteria in controlling root-knot nematode (RKN) infection in *Lycopersicon esculentum* plants by modulation in the secondary metabolite profiles. *AoB PLANTS*, *11* (6).

Kihika, R., Murungi, L. K., Coyne, D., Ng'ang'a, M., Hassanali, A., Teal, P. E. A., and Torto, B. (2017). Parasitic nematode *Meloidogyne incognita* interactions with different *Capsicum annum* cultivars reveal the chemical constituents modulating root herbivory. *Scientific Reports*, *7*, 2903.

Kihika, R., Tchouassi, D. P., Ng'ang'a, M. M., Hall, D. R., Beck, J. J., and Torto, B. (2020). Compounds associated with infection by the root-knot nematode, *Meloidogyne javanica* , influence the ability of infective juveniles to recognize host plants. *Journal of Agricultural and Food Chemistry*, *68*, (34), 9100-9109.

Kim, T. Y., Jang, J. Y., Jeon, S. J., Lee, H. W., Bae, C.-H., Yeo, J. H., Lee, H. B., Kim, I. S., Park, H. W., and Kim, J.-C. (2016). Nematicidal activity of kojic acid produced by *Aspergillus oryzae* against *Meloidogyne incognita*. *Journal of Microbiology and Biotechnology*, *26* (8).

Kiriga, A. W., Haukeland, S., Kariuki, G. M., Coyne, D. L., and Beek, N. V. (2018). Effect of *Trichoderma* spp. and *Purpureocillium lilacinum* on *Meloidogyne javanica* in commercial pineapple production in Kenya. *Biological Control*, *119*, 27–32.

Kirwa, H. K., Murungi, L. K., Beck, J. J., and Torto, B. (2018). Elicitation of differential responses in the root-knot nematode *Meloidogyne incognita* to tomato root exudate cytokinin, flavonoids, and alkaloids. *Journal of Agricultural and Food Chemistry*, *66* (43), 11291–11300.

Klessig, D, F., Durner, J., Noad, R., Navarre, D. A., Wendehenne, D., Kumar, D., Zhou, J. M., Shah, J., Zhang, S. and Kachroo, P. (2000). Nitric oxide and salicylic acid signaling in plant defense. *Proceedings of the National Academy of Sciences*, *97*, 8849–8855.

Krueger, R., Dover, K. E., Mcsorley, R., and Wang, K. (2007). Marigolds (*Tagetes* spp .) for

nematode management 1. *Crop Research*, 1–8.

Kuang, M., Liu, T., Wu, H., Lan, H., Wen, Y., Wu, H., and Li, X. (2020). Constituents leached by tomato seeds regulate the behavior of root-knot nematodes and their antifungal effects against seed-borne fungi. *Journal of Agricultural and Food Chemistry*, *68* (34), 9061-9069.

Kumari, C., Dutta, T. K., Banakar, P., and Rao, U. (2016). Comparing the defence-related gene expression changes upon root-knot nematode attack in susceptible versus resistant cultivars of rice. *Scientific Reports*, *6*, 22846.

Kyndt, T., Nahar, K., Haegeman, A., De Vleesschauwer, D., Hofte, M., and Gheysen, G. (2012). Comparing systemic defence-related gene expression changes upon migratory and sedentary nematode attack in rice. *Plant Biology*, *14*, 73–82.

Lamovseki, J., Urek, G., and Trdan, S. (2013). Biological Control of Root-knot nematodes (*Meloidogyne* spp.): microbes against the pests. *Acta Agriculturae Slovenica*, *101* (2), 263–275.

Laznik, Ž., and Trdan, S. (2013). An investigation on the chemotactic responses of different entomopathogenic nematode strains to mechanically damaged maize root volatile compounds. *Experimental Parasitology*, *134*(3), 349–355.

Leelarasamee, N., Zhang, L., and Gleason, C. (2018). The root-knot nematode effector MiPFN3 disrupts plant actin filaments and promotes parasitism. *PLOS Pathogens*, *14*(3), e1006947.

Lenth, R. (2018). *Emmeans: Estimated Marginal Means, Aka Least-Squares Means.* R Package Version 1.2.2.

Li, R., Zhou, Y., Wu, Z. and Ding, L. (2006). ESI-QqTOF-MS/MS and APCI-IT-MS/MS analysis of steroid saponins from the rhizomes of *Dioscorea panthacia*. *Journal of Mass Spectrometry*, *41*, 1–22.

Li, X.-G., Zhang, T.-I., Wang, X.-X., Hua, K., Zhao, L., and Han, Z.-M. (2013). The composition of root exudates from two different resistant peanut cultivars and their effects on the growth of soil-borne pathogen. *International Journal of Biological Sciences*, *9*, 164.

Li, Y., Li, J., Qian, B., Cheng, L., Xu, S., and Wang, R. (2018). De Novo Biosynthesis of p-Coumaric Acid in *E. coli* with a trans-Cinnamic Acid 4-Hydroxylase from the Amaryllidaceae Plant *Lycoris aurea*. *Molecules*, *23*, 3185.

Lilley, C.J., Kyndt, T., Gheysen, G. (2011). Nematode Resistant GM Crops in Indusrtrialised and Developing Countries. In C. Jones, J., Gheysen, G. Fenoll (Ed.), *Genomics and Molecular Genetics of Plant-Nematode Interactions* (pp. 347–367). Springer New York.

Ling, J., Mao, Z., Zhai, M., Zeng, F., Yang, Y., and Xie, B. (2017). Transcriptome profiling of *Cucumis metuliferus* infected by *Meloidogyne incognita* provides new insights into putative defense regulatory network in Cucurbitaceae. *Scientific Reports*, *7*, 3544.

Liu, N., Yang, C., Zhang, Z., Tian, Y., XU, F., and Chen, Y. (2008). Simultaneous quantification of sodium, salicylic acid, cinnarizine and vitamin B1 in human plasma by LC tandem MS detection. *Chromatographia*, *67*, 583–590.

Luc, M., Sikora, R.A. and Bridge, J. (2005). Plant parasitic nematodes in subtropical and tropical agriculture. In J. Luc, M., Sikora, R.A. and Bridge (Ed.), *Plant parasitic nematodes in subtropical and tropical agriculture* (2nd ed.). CABI Publishing.

Masamune, T., Anetai, M., Takasugi, M., and Katsui, N. (1982). Isolation of a natural hatching stimulus, glycinoeclepin A, for the soybean cyst nematode. *Nature*, *297*, 495–496.

Mateille, T., Cadet, P., and Fargette, M. (2007). Control and management of plant parasitic nematode communities in a soil conversation approach. Integrated Management and Biocontrol of Vegetable and Grain Crops Nematodes, 434: 71–89.

McBride, R.G., Mikkelsen, R. L., and Barker, K. R. (2000). The role of low molecular weight organic acids from decomposing rye in inhibiting root-knot nematode populations in soil. *Applied Soil Ecology*, *15*, 243–251.

Migunova, V. D. and Sasanelli, N. (2021). Bacteria as biocontrol tool against phytoparasitic nematodes. *Plants*, *10*, 389.

Mitkowski, N. A. and Abawi, G. S. (2003). Root-knot nematodes. *The Plant Health Instructor*, 1–9.

Murungi, L. K., Kirwa, H., Coyne, D., Teal, P. E. A., Beck, J. J., and Torto, B. (2018). Identification of key root volatiles signalling preference of tomato over spinach by the root-knot nematode *Meloidogyne incognita*. *Journal of Agricultural and Food Chemistry*, *66*, 7328–7336.

Mwamba, S., Kihika-Opanda, R., Murungi, L. K., Losenge, T., Beck, J. J., and Torto, B. (2021). Identification of repellents from four non-host asteraceae plants for the root-knot nematode, *Meloidogyne incognita*. *Journal of Agricultural and Food Chemistry*, *69*, 15145–15156.

Mwangi, M. W., Kimenju, J. W., Narla, R. D., Muiru, W. M., and Kariuki, G. M. (2017). Evaluation of selected tomato cultivars reaction to infestation with *Meloidogyne javanica* in greenhouse conditions. *International Journal of Agronomy and Agricultural Research*, *11*, 17–25.

Nahar, K., Kyndt, T., De Vleesschauwer, D., Hofte, M., and Gheysen, G. (2011). The jasmonate pathway is a key player in systemically induced defense against root-knot nematodes in rice. *Plant Physiology*, *157*, 305–316.

National Institutes of Standards and Technology. (2008). *NIST/EPA/NIH mass spectral library*. http://www.nist.gov.

Nchore, S. B., Waceke, J. W., and Kariuki, G. M. (2012). Efficacy of selected agroindustrial wastes in managing root-knot nematodes on black nightshade in Kenya. *ISRN Agronomy*.

Nicol, J. M., Turner, S. J., Coyne, D. L., Nijs, L. Den, and Hockland, S. (2011). Current Nematode Threats to World Agriculture. In Jones, C., Gheysen, J., Fenoll G. (Ed.), Genomics and Molecular Genetics of Plant-Nematode Interactions (pp. 21–45). Springer.

Njuguna, P. K., Murungi, L. K., Fombong, A., Teal, P. E. A., Beck, J. J., and Torto, B. (2018). Cucumber and Tomato Volatiles: Influence on Attraction in the Melon Fly *Zeugodacus cucurbitate* (Diptera: Tephritidae). *Journal of Agricultural and Food Chemistry*, *66*(32), 8504–8513.

Ochola, J. (2021). *Elucidation of physio-chemical mechanism associated with banana paper in the management of potato cyst nematodes*. MSc Thesis, Kenyatta University.

Ochola, J., Cortada, L., Ng'ang'a, M., Hassanali, A., Coyne, D., and Torto, B. (2020a). Mediation of potato–potato cyst nematode, *G. rostochiensis* interaction by specific root exudate compounds. *Frontiers in Plant Science*, *11*, 649.

Ochola, J., Coyne, D., Cortada, L., Haukeland, S., Ng'ang'a, M., Hassanali, A., Opperman, C., and Torto, B. (2020b). Cyst nematode bio‐communication with plants: implications for novel management approaches. *Pest Management Science*, ps.6105.

Olson, D. M., Davis, R. F., Wackers, F. L., Rains, G. C., and Potter, T. (2008). Plant-herbivore-carnivore interactions in cotton, *Gossypium hirsutum*: linking belowground and aboveground. *Journal of Chemical Ecologyl Ecology*, *34*, 1341–1348.

Onkendi, E. and Moleleki, L. (2013). Detection of *Meloidogyne enterolobii* in potatoes in South Africa and phylogenetic analysis based on intergenic region and the mitochondrial DNA sequences. *European Journal of Plant Pathology*, *136* (1), 1–5.

Onkendi, E. M., Kariuki, G. M., Marais, M., and Moleleki, L. N. (2014). The threat of root-knot nematodes (*Meloidogyne* spp.) in Africa: A review. *Plant Pathology*, *63* (4), 727–737.

Perry, R.N., Moens, M., and Starr, J. L. (2009). *Root Knot Nematodes*. (J. L. Perry, R.N., Moens, M., and Starr, Ed.). CABI International.

Pierre, A., Castagnone-Sereno,P., Rosso, M-N J. de Almeider,. E. and Bruno, F. (2009). Invasion, Feeding and Development. In Perry, R.N., Moens, M., and Starr, J. L. (Ed.), *Root-knot Nematodes* (pp. 163–176). CABI Publishing.

Portillo, M., Cabrera, J., Lindsey, K ., Topping, J., Andres, M. F., Emiliozzi, M., Oliveros, J. C., Garcia-Casado, G., Salano, R., Koltai, H., Resnick, N., Fenoll, C., and Escobar, C. (2013). Distinct and conserved transcriptomic changes during nematode-induced giant cell development in tomato compared with *Arabidopsis*: a functional role for gene repression. *New Phytologist*, *197*, 1276–1290.

Qureshi, S.A., Ruqqia, Sultan, V., Ara, J. and Ehteshamul-Haque, S. (2012). Nematicidal potential of culture filtrates of soil fungi associated with rhizosphere and rhizoplane of cultivated

and wild plants. *Pakistan Journal of Botany*, *44* (3), 1041–1046.

Rani, C. I., Veeraragavathathan, D., and Sanjjutha, S. (2008). Analysis of Biochemical basis of root-knot nematode (*Meloidogyne incognita*) resistance in tomato (*Lycopersicon esculentum* Mill.). *Research Journal of Agriculture and Biological Sciences*, *4*, 866–870.

Rasmann, S., Köllner, T. G., Degenhardt, J., Hiltpold, I., Toepfer, S., Kuhlmann, U., … Turlings, T. (2005). Recruitment of entomopathogenic nematodes by insect-damaged maize roots. *Nature*, *434*(7034), 732–737.

Rawdan, M. A., Ahu-Elamayem, M. M., Farrag, S. A. A. and Ahmed, N. S. (2017). Comparative suppressive effect of some organic acids against *Meloidogyne incognita* infecting tomato. *Pakistan Journal of Nematology*, *35*, 197–208.

Riegel, C. and Noe, J. (2000). Chicken litter soil amendment effects on soil microbes and *Meloidogyne incognita* on cotton. *Plant Disease*, *33*, 1275–1281.

Rudrappa, T., Czymmek, K. J., Pare, P. W., and Bais, H. P. (2008). Root-secreted malic acid recruits beneficial soil microbes. *Plant Physiology*, *148*, 1547–1556.

Russin, J. S., Layton, M. B., Boethel, D. J., Mcgawley, E. C., Snow, J. P., and Berggren, G. T. (1989). Development of *Heterodera glycines* on soybean damaged by soybean looper and stem canker. *Journal of Nematology*, *21*, 108–114.

Russin, J. S., Mcgawley, E. C., and Boethel, D. J. (1993). Population development of *Meloidogyne incognita* on soybean defoliated by Pseu- doplusia includens. *Journal of Nematology*, *25*, 50–54.

Schenk, H. Driessen, R. A. J., De Gelder, R., Goubitz, K., Nie-Boer, H., Bruggemann-Rotgans, I. E. M., and Dierpenhorst, P. (1999). Elucidation of the structure of Solanoeclepin A, a natural hatching factor of potato and tomato cyst nematodes, by single-crystal x-ray diffraction. *Croatia Chemica Acta*, *72*, 593–606.

Schneider, S.M., and Hanson, B. D. (2009). *Effects of Fumigant Alternatives to Methyl Bromide on Pest Control in Open Field Nursery Production of Perennial Fruit and Nut Plants* (Vol. 0353, Issue 19).

Schneider, S.M., Ajwa, H. and Trout, T. J. (2006). Chemical alternatives to methyl bromide for nematode control under vineyard replant conditions. *American Journal of Enology and Viticulture*, *57* (2), 183–193.

Schneider, S.M., Rosskopf, E.N., Leesch, J.G., Chellemi, D.O., Bull, C.T., and Mazzola, M. (2003). United States Department of Agriculture-Agricultural Research Service research on alternatives to methyl bromide: pre-plant and post-harvest. *Pest Management Science*, *59* (6–7), 814–826.

Seo, Y., and K. Y. H. (2014). Control of *Meloidogyne incognita* using mixtures of organic acids.

The Plant Pathology Journal, 30, 450–455.

Seo, H. J., Park, A. R., Kim, S., Yeon, J., Yu, N. H., Ha, S., Chang, J. Y., Park, H. W., and Kim, J.-C. (2019). Biological control of root-knot nematodes by organic acid-producing *Lactobacillus brevis* WiKim0069 isolated from Kimchi. *The Plant Pathology Journal*, *35* (6).

Shazaukat, S. S., Siddiqui, I. A., Ali, N. I., Ali, S. A., and Khan, G. H. (2003). Nematicidal and allelopathic responses of *Lantana camara* root extract. *Phytopathol. Mediterr.*, *42*, 71−78.

Shukla, N., Yadav, R., Kaur, P., Rasmussen, S., Goel, S., Agarwal, M., Jagannath, A., Gupta, R., and Kumar, A. (2018). Transcriptome analysis of root-knot nematode (*Meloidogyne incognita*)-infected tomato (*Solanum lycopersicum*) roots reveals complex gene expression profiles and metabolic networks of both host and nematode during susceptible and resistance responses. *Molecular Plant Pathology*, *19*, 615–633.

Siddiqui, Z. A., and Futai, K. (2009). Biocontrol of *Meloidogyne incognita* on tomato using antagonistic fungi, plant-growth-promoting rhizobacteria and cattle manure. *Pest Management Science*, *65*, 943–948.

Sikora, R. A., Coyne, D. L., Hallman, J., and Timper, P. (2018). *Plant Parasitic Nematodes in Subtropical and Tropical Agriculture.* (3rd ed.). Wallingford, UK., CABI.

Silva, D. B., Weldegergis, B. T., Van Loon, J. J. A., and Bueno, V. H. P. (2017). Qualitative and quantitative differences in herbivore-induced plant volatile blends from tomato plants infested by either *Tuta absoluta* or *Bemisia tabaci*. *Journal of Chemical Ecology*, *43*(1), 53–65.

Singewar, K., Fladung, M. and Robischon, M. (2021). Methyl salicylate as a signaling compound that contributes to forest ecosystem stability. *Trees*, *35*, 1755–1769.

Starr, J.L., Bridge, J., and Cook, R. (2002). Resistance to plant-parasitic nematodes: History, current use and future potential. In R. Starr, J.L., Bridge, J., Cook (Ed.), *Plant Resistance to Parasitic Nematodes* (pp. 1–22). CAB International.

Szakasits, D., Heinen, P., Wieczorek, K., Hofmann, J., Wagner, F., Kreil , D. P., Sykacek, P., Grundler, F. M. W., and Bohlmann, H. . (2009). The transcriptome of syncytia induced by the cyst nematode *Heterodera schachtii* in *Arabidopsis roots*. *The Plant Journal*, *57*, 771–784.

Taba, S., A. Ajitomi, Y. Shimabukuro, M. Yonaha, A. Takara, Y. Nagamatsu, and Moromizato, Z. (2012). Nematicidal activity of *Bidens pilosa* var. radiata boiled extracts on plant-parasitic nematodes and stability of the activity. *Journal of. Weed Science and Technology.*, *57*, 1–6.

Taba, S., S. Juri, and Moromizato, Z. (2007). Nematicidal activity of Okinawa Island plants on the root-knot nematode, *Meloidogyne incognita* (Kofoid and White) Chitwood. *Plant Soil*, *303*, 207–216.

Taba, S., Y. Shimabukuro, A. Ajitomi, and Moromizato, Z. (2010). The effects of boiled extracts of *Bidens pilosa* L. var. radiata Scherff. in controlling the root-knot nematode, *Meloidogyne*

incognita (Kofoid and White) Chitwood, and on soil microflora in differing soils. *Soil Microorg., 64*, 95–100.

Taba, S., Ashikaga, K., Oohama, T., Ajitomi, A., Kiyuna, C., Kinjo, M., and Sekine, K.-T. (2020). *Bidens pilosa* extract effects on pine wilt: causal agents and their natural enemies. *Forest Science, 66* (3). Page..

Taylor, A.L. and Sasser, J. N. (1978). *Biology, Identifiction and Control of Root-Knot nematodes (Meloidogyne spp)*. Department of Plant Pathology, North Carolina State University and US Agency for International Development

Team R. C. (2021). *R: A language and environment for statistical computing* (2.15.1). R Foundation for Statistical Computing. http://www.r-project.org/.

Thies, J.A., Dickson, D.W. and Fery, R. L. (2008). Stability of resistance to root-knot nematodes in "Charleston Belle" and "Carolina Wonder" bell peppers in a sub-tropical environment. *HortScience, 43*, 188–190.

Tiwari, S., Youngman, R. R., Lewis, E. E., and Eisenback, J. D. (2009). European cornborer (Lepidoptera: Crambidae) stalk tunneling on root-knot nematode(Tylenchida:Heteroderidae) fitness on corn. *Journal of Economic Entomolgy*, *102*, 602–609.

Torto, B., Kirwa, H., Kihika, R., and Murungi, L. K. (2018). Strategies for the manipulation of root-knot nematode behavior with natural products in small scale farming systems. In *Roles of Natural Products for Biorational Pesticides in Agriculture* (Vol. 1294, pp. 115–126). American Chemical Society.

Tsay, T. T., Wu, S. T., and Lin, Y. Y. (2004). Evaluation of Asteraceae Plants for Control of Meloidogyne incognita. Journal of Nematology, 36: 36–41.

Turlings, T. C. J., Hiltpold, I., and Rasmann, S. (2012). The importance of root-produced volatiles as foraging cues for entomopathogenic nematodes. *Plant and Soil*, *358*(1–2), 51–60.

Van Tol, R. W. H. M., Van Der Sommen, A. T. C., Boff, M.I.C. Van Bezooijen, J., Sabelis, M. W., and Smits, P. H. (2001). Plants protect their roots by alerting the enemies of grubs. *Ecology Letters*, *4*, 292–294.

Webster, J. M. (Ed.). (1972). Nematodes and biological control. In *Economic Nematology* (pp. 469–496). Academic Press Inc.London and New York.

Wesemael, W. M. L., Taning, L. M., Viaene, N., and Moens, M. (2014). Life cycle and damage of the root-knot nematode *Meloidogyne minor* on potato, *Solanum tuberosum*. *Nematology*, *16* (2), 185–192.

Willet, D.S., Alborn, H.T., Duncan, L.W., and Stelinski, L. L. (2015). Social networks of educated nematodes. *Nature Scientific Reports*, *5*, 14338.

Wilson, M. J., Ehlers, R., and Glazer, I. (2012). Entomopathogenic nematode foraging strategies is *Steinernema carpocapsae* really an ambush forager? *Nematology*, *14*, 389–394.

Wondafrash, M., Dam, N. M. Van, Tytgat, T. O. G., Poelman, E., Erb, M., and Kaplan, I. (2013). Plant systemic induced responses mediate interactions between root parasitic nematodes and aboveground herbivorous insects. *Frontiers in Plant Science*, *4*(87).

Wuyts, N., Lognay, G., Swennen, R., and De Waele, D. (2006). Nematode infection and reproduction in transgenic and mutant *Arabidopsis* and tobacco with an altered phenylpropanoid metabolism. *Journal of Experimental Botany*, *57*, 2825–2835.

Wuyts, N., Swennen, R., and De Waele, D. (2006). Effects of plant phenylpropanoid pathway products and selected terpenoids and alkaloids on the behaviour of the plant-parasitic nematodes *Radopholus similis, Pratylenchus penetrans* and *Meloidogyne incognita*. *Nematology*, *8* (1), 89–101.

Zebelo, S., Piorkowski, J., Disi, J., and Fadamiro, H. (2014). Secretions from the ventral eversible gland of *Spodoptera exigua* caterpillars activate defense-related genes and induce emission of volatile organic compounds in tomato, *Solanum lycopersicum*. *BMC Plant Biology*, *14* (1).

Zhang, P.-J., Broekgaarden, C., Zheng, S.-J., Snoeren, T. A. L., van Loon, J. J. A., Gols, R., and Dicke, M. (2013). Jasmonate and ethylene signaling mediate whitefly-induced interference with indirect plant defense in *Arabidopsis thaliana*. *New Phytologist*, *197* (4), 1291–1299.

Zhang, P. J., Zheng, S. J., Van Loon, J. J. A., Boland, W., David, A., Mumm, R., and Dicke, M. (2009). Whiteflies interfere with indirect plant defense against spider mites in Lima bean. *Proceedings of the National Academy of Sciences of the United States of America*, *106* (50), 21202–21207.

APPENDICES

Appendix I: Table of macro- and micro-nutrients used in the nutrient solution

Macronutrients	**Concentration of stock solution (g/L)**
*Calcium nitrate tetrahydrate ($Ca(NO_3)_2.4H_2O$)	653
*Magnesium sulfate heptahydrate ($MgSO_4.7H_2O$)	399
**Potassium nitrate (KNO_3)	184
*Ammonium phosphate dibasic ($NH_4H_2PO_4$)	108
*Iiron (II) sulfate heptahydrate ($FeSO_4.7H_2O$)	10 g containing 72 mL of 500 mM ethylenediaminetetraacetic acid (pH 8.0)
***Micronutrients**	
Manganese (II) chloride tetrahydrate ($MnCl_2.4H_2O$)	1.81
Copper (II) sulfate pentahydrate ($CuSO_4.5H_2O$)	0.1
Zinc sulfate heptahydrate ($ZnSO_4.7H_2O$)	0.22
Boric acid (H_3BO_3)	2.86
Molybdic acid ($H_2MoO_4.H_2O$)	0.02

Amounts used to formulate the watering solution contained *$Ca(NO_3)_2$, 25 mL; *$MgSO_4$, 25 mL; **KNO_3, 75 mL; *$NH_4H_2PO_4$, 25 mL; *Fe/EDTA, 25 mL and *micronutrients, 25 mL mixed with distilled water to constitute a final volume of 50 L.

Appendix II: Mass spectrum showing the ESI fragmentation pattern of ascorbic acid

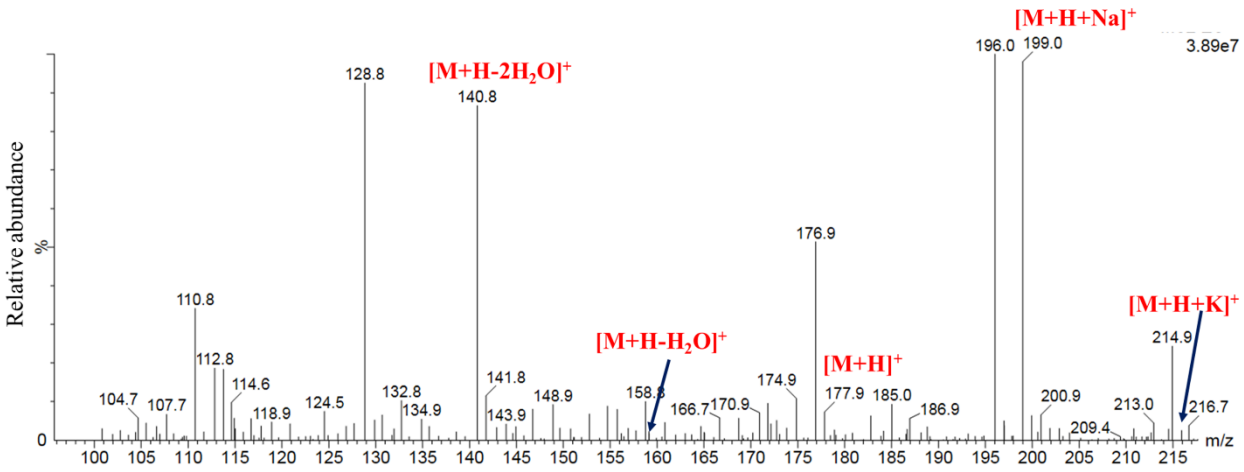

Appendix III: Mass spectrum showing the ESI fragmentation pattern of malic acid

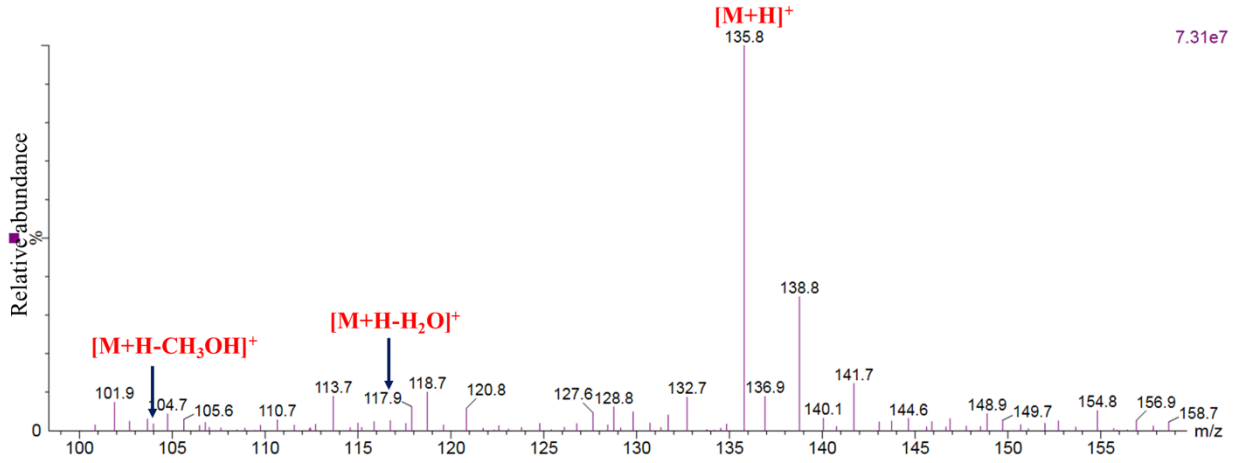

Appendix IV: Mass spectrum showing the ESI fragmentation pattern of nicotinic acid

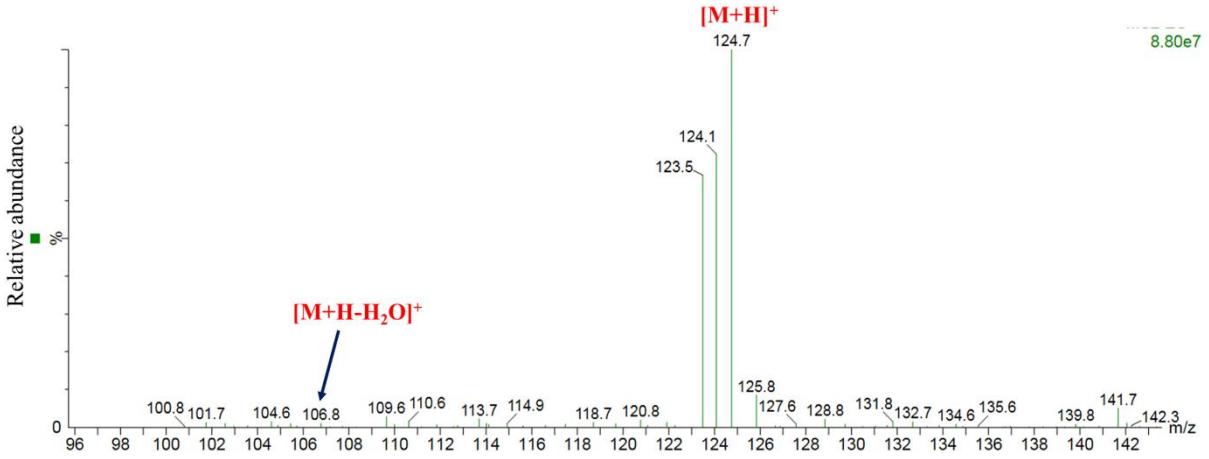

Appendix V: Mass spectrum showing the ESI fragmentation pattern of tyrosine

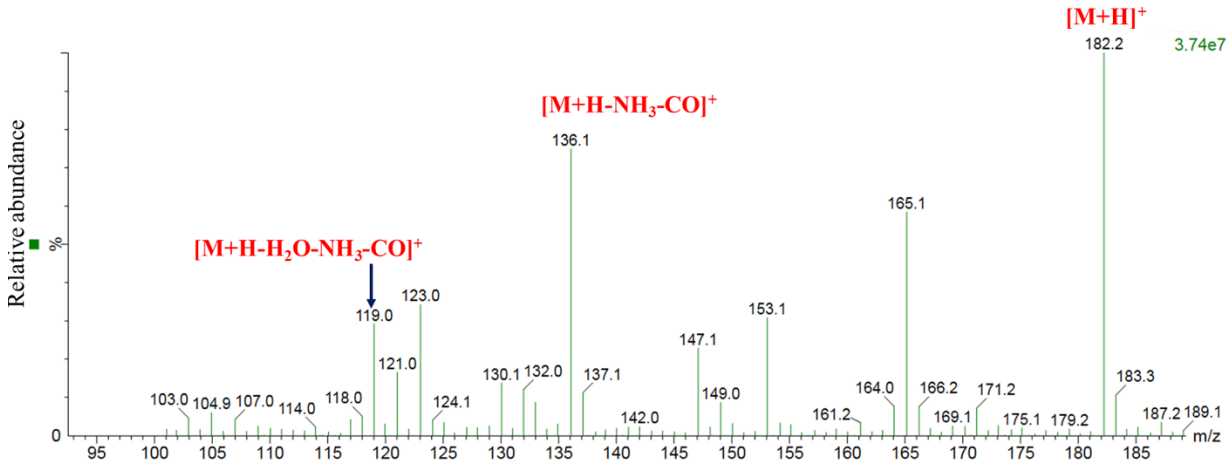

Appendix VI: Mass spectrum showing the ESI fragmentation pattern of phenylalanine

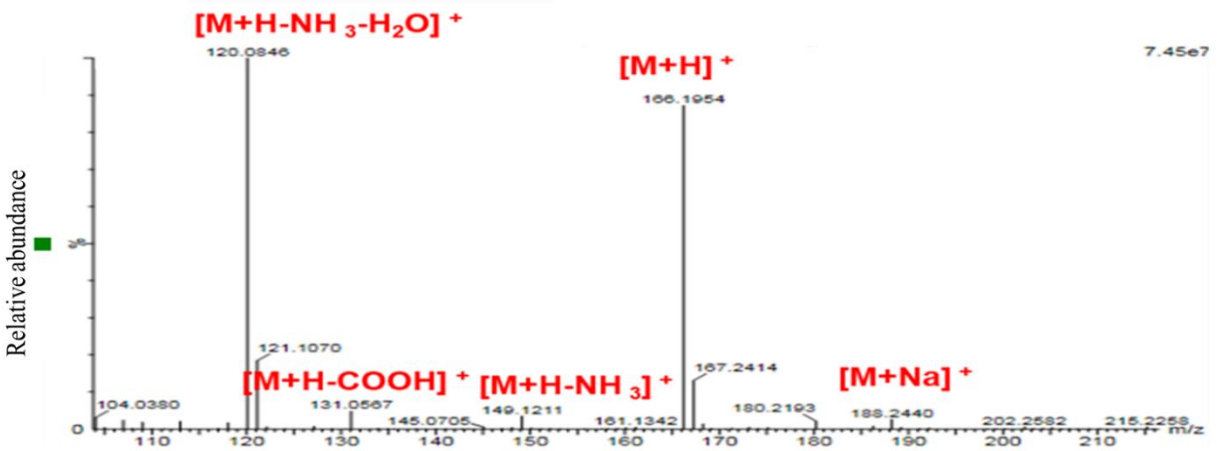

Appendix VII: Mass spectrum showing the ESI fragmentation pattern of zeatin

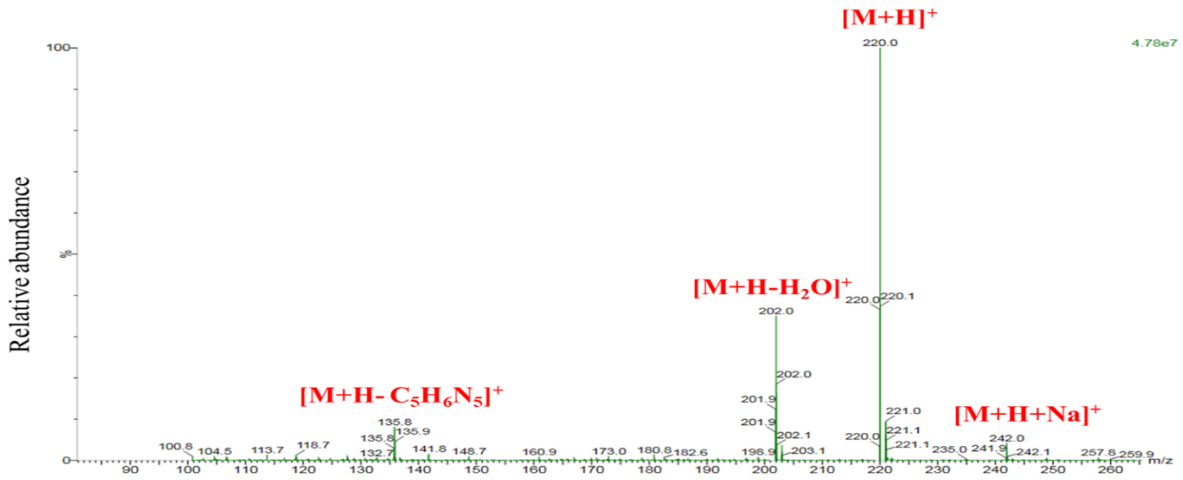

Appendix VIII: Mass spectrum showing the ESI fragmentation pattern of diosgenin 3-O-beta-D-glucoside

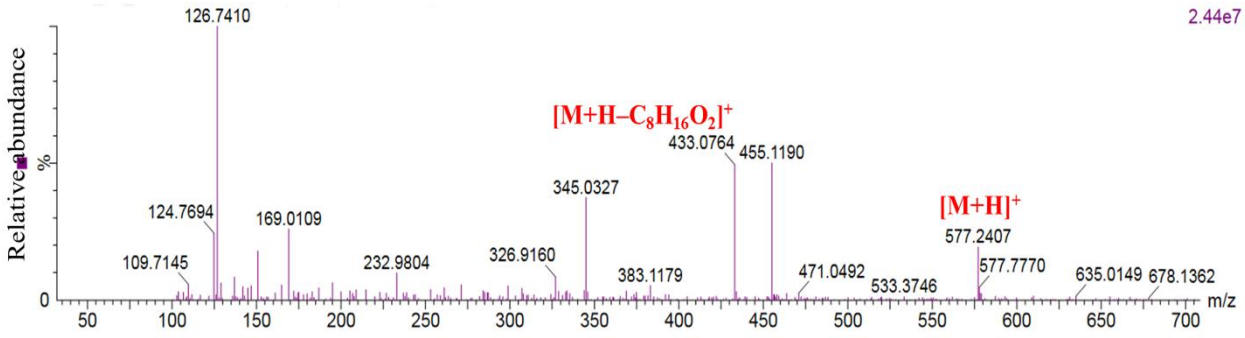

Appendix IX: Mass spectrum showing the ESI fragmentation pattern of *p*-coumaric acid

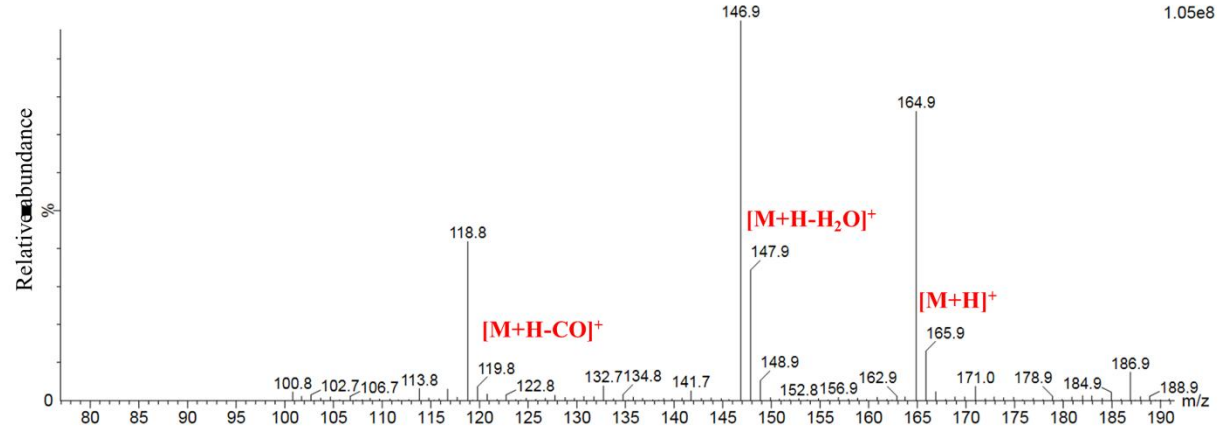

Appendix X: Mass spectrum showing the ESI fragmentation pattern of 2-hydroxybenzoic acid

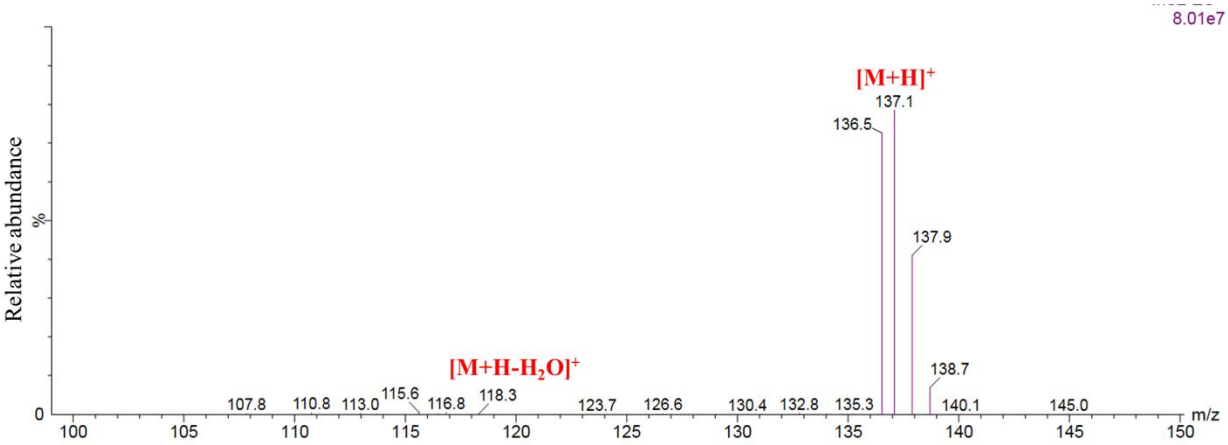

Appendix XI: Mass spectrum showing the ESI fragmentation pattern of dehydrotomatine

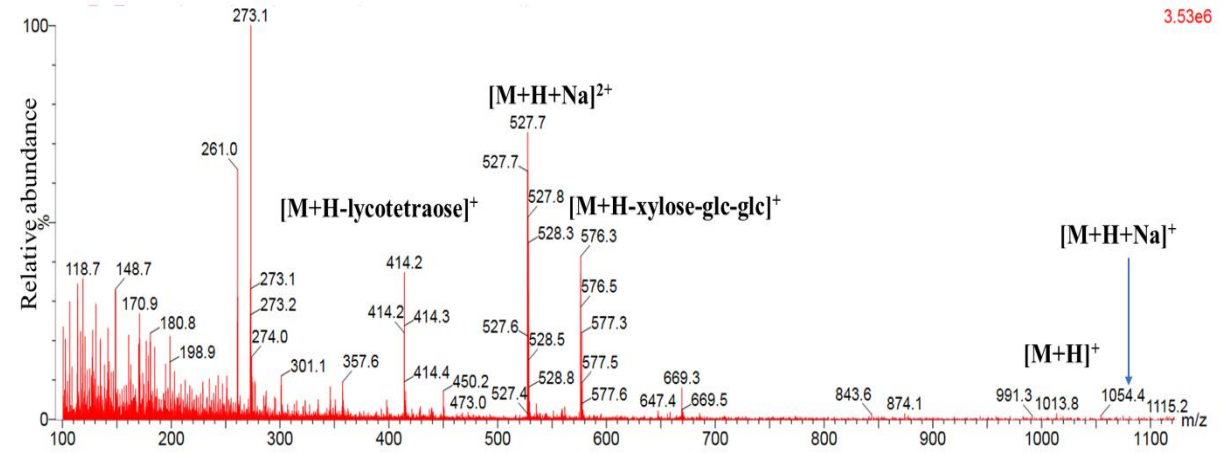

Appendix XII: Mass spectrum showing the ESI fragmentation pattern of tomatine

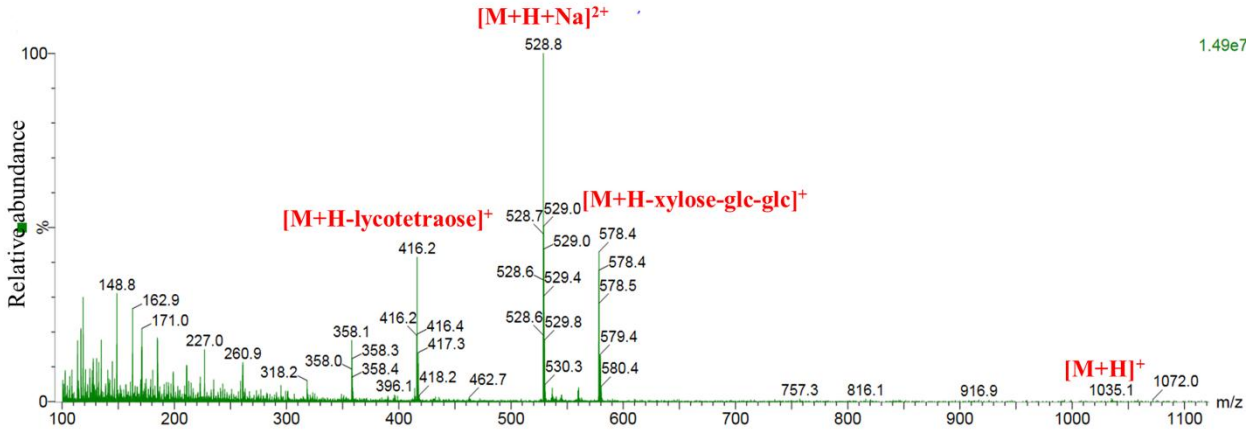

Appendix XIII: Mass spectrum showing the ESI fragmentation pattern of kaempferol

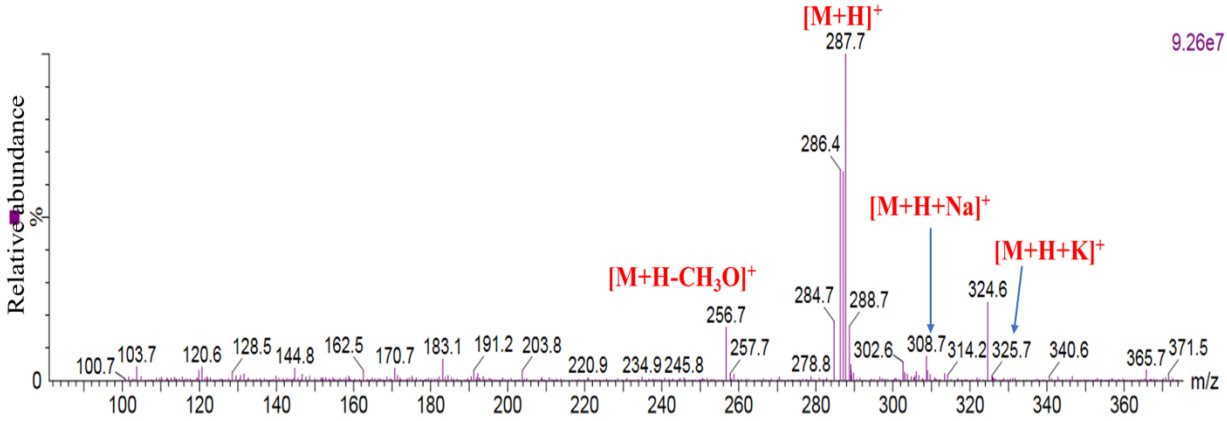

Appendix XIV: Mass spectrum showing the ESI fragmentation pattern of tomatidine

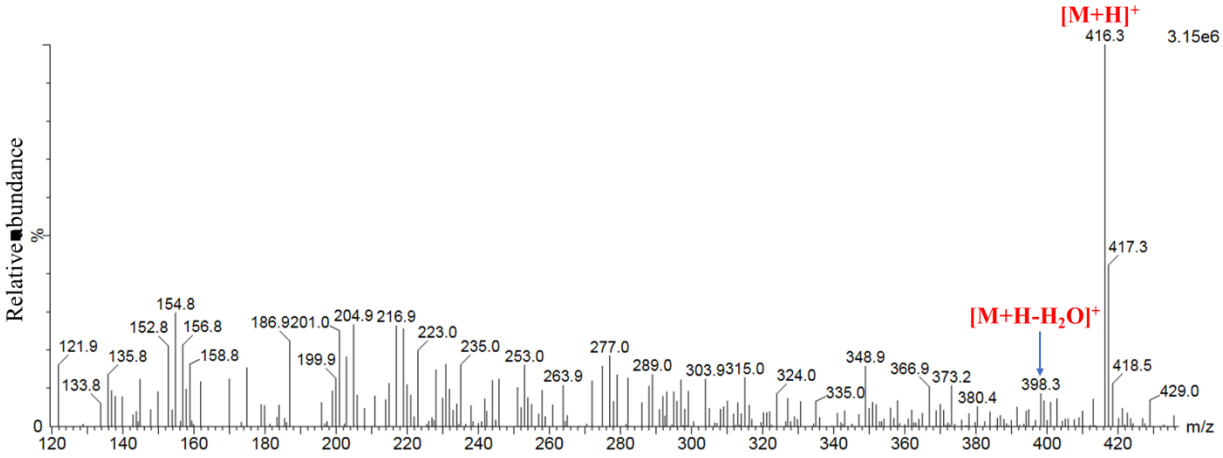

Appendix XV: Mass spectrum showing the ESI fragmentation pattern of solasodine